

# **NUCLEAR RESPONSE IN ELECTROMAGNETIC INTERACTIONS WITH COMPLEX NUCLEI**

**S. BOFFI, C. GIUSTI and F.D. PACATI**

*Dipartimento di Fisica Nucleare e Teorica, Università di Pavia, Pavia, Italy*

*Istituto Nazionale di Fisica Nucleare, Sezione di Pavia, Pavia, Italy*



**NORTH-HOLLAND**

## Nuclear response in electromagnetic interactions with complex nuclei

S. Boffi, C. Giusti and F.D. Pacati

Dipartimento di Fisica Nucleare e Teorica, Università di Pavia, Pavia, Italy  
Istituto Nazionale di Fisica Nucleare, Sezione di Pavia, Pavia, Italy

Received August 1992; editor: G.E. Brown

### Contents:

|  |    |   |    |
|--|----|---|----|
| 1. Introduction                                      | 3  | 6. The hadron tensor in semi-inclusive inelastic scattering | 47 |
| 2. One-photon exchange approximation                 | 4  | 6.1. The hadron tensor in $(e, e'N)$ reactions              | 50 |
| 3. The lepton tensor                                 | 9  | 6.2. The spectral density                                   | 52 |
| 4. Elastic scattering and form factors               | 13 | 6.3. Nucleon and electron distortion                        | 55 |
| 4.1. Scalar particle                                 | 14 | 6.4. Comparison with experiment                             | 58 |
| 4.2. Dirac point-like particle                       | 17 | 6.5. Structure functions                                    | 63 |
| 4.3. Dirac particle with an internal structure       | 18 | 6.6. Inelastic scattering above threshold for               |    |
| 4.4. The electromagnetic form factors of the nucleon | 21 | two-particle emission                                       | 67 |
| 4.5. Multipole decomposition of the current          |    | 6.7. $y$ -scaling   | 68 |
| and the neutron form factor                          | 23 | 6.8. Lepton–nucleus deep inelastic scattering               | 71 |
| 5. The hadron tensor in inelastic scattering         | 26 | 7. Spin observables   | 75 |
| 5.1. The nuclear current                             | 29 | 7.1. Electron polarization                                  | 76 |
| 5.2. Nuclear response in inclusive inelastic         |    | 7.2. Hadron tensor with polarized particles                 | 78 |
| scattering   | 35 | 7.3. Target polarization                                    | 81 |
| 5.3. The Coulomb sum rule                            | 41 | 7.4. Nucleon recoil polarization                            | 85 |
| 5.4. Deep inelastic scattering                       | 43 | 7.5. Complete determination of the scattering               |    |
|  |    | amplitudes  | 90 |
|  |    | 8. Final discussion   | 92 |
|  |    | References  | 94 |

### Abstract:

The response of nucleons and complex nuclei to an external electromagnetic probe at intermediate and high energy is illustrated by considering both inclusive and semi-inclusive electron scattering. Gauge invariance and current conservation allow one to define form factors for elastic scattering and structure functions for inelastic scattering which contain the relevant information on the structure and dynamics of the target hadron system under investigation. They are derived and discussed in some specific examples, also taking into account polarization observables.

## 1. Introduction

In the framework of intermediate energy nuclear physics the key element for understanding the structure and dynamics of hadronic matter is its response to an external probe as a function of energy and momentum transfer ( $\omega, \mathbf{q}$ ). The traditional picture of an atomic nucleus consisting of strongly interacting nucleons, which is successful at low ( $\omega, \mathbf{q}$ ), must be implemented by also considering new degrees of freedom ultimately related to the composite structure of nucleons. The definition and the relevance of such degrees of freedom in the nuclear many-body theory is intimately related to the explored portion of the  $(\omega, \mathbf{q})$ -plane and to the possibility of disentangling the hadron response in a clear way.

More than thirty years of experimentation have proved that electron scattering is the best tool for investigating hadron systems such as atomic nuclei and their constituents. The electromagnetic interaction is known from quantum electrodynamics (QED) and is weak compared to the strength of the interaction between hadrons. Thus electron scattering is adequately treated assuming the validity of the Born approximation, i.e., the one-photon exchange mechanism between electron and target. This simplifies the form of the cross section, which becomes a contraction between two tensors: the lepton tensor, describing the electron and entirely determined by QED, and the hadron tensor, describing the transition of the target system induced by the electron. It is therefore possible in principle to access the relevant information about the hadron structure contained in the target response to the electromagnetic probe. In addition, the virtual photon, like the real one, has a mean free path much larger than the target dimensions, thus exploring the whole target volume. This contrasts with hadron probes, which are absorbed at the target surface.

With respect to real photon absorption, electron scattering allows independent variation of energy and momentum transfer as well as of the (longitudinal and transverse) polarization of the exchanged virtual photon. This large flexibility of the electron probe is reflected in the cross section, where a correspondingly large number of structure functions appear, related to the different ways the target can absorb the virtual photon. Thus separation of the longitudinal and transverse components of the transition matrix elements is in principle possible, with detailed information on the target dynamics.

However, the full exploration of all these potentialities is limited by the smallness of the involved cross sections (proportional to  $\alpha^2$ , where  $\alpha = e^2/4\pi = 1/137$  is the fine structure constant). Thus coincidence experiments, necessary to detect specific final states, require high duty cycle and high electron currents. Measurements of polarization observables, absolutely required for a complete determination of the transition amplitudes, imply sophisticated techniques in preparing polarized targets and/or in detecting recoiling polarized particles. It is not a surprise, therefore, that such a program is only starting now with the advent of continuous wave electron beams such as those available at NIKHEF, Mainz, MIT-BATES and Saskatoon, while on the theoretical side the basic formalism of electron scattering goes back to the earlier days of quantum mechanics.

Excellent books [1–5] and review papers [6–12] exist on the subject of electron scattering off nuclei. The demand for a renewed review of the field comes from the increased interest of young people involved in experimentation with electrons in the next few years with the commissioning of the new laboratory at CEBAF. Thus for pedagogical reasons the basic formalism is here presented again. Much emphasis is put on the derivation of the general formulae and the validity of the

approximations involved. A variety of applications of intermediate and high energy electron scattering off nucleons and complex nuclei is discussed with a rich, though not exhaustive, list of references.

In section 2 the one-photon exchange approximation is described in terms of the Møller potential. In section 3 the lepton tensor is defined and calculated; the connection between different existing conventions is also established. Section 4 concerns elastic scattering in order to illustrate the notion of form factor with several examples. In particular the nucleon form factors are briefly discussed. The remaining sections are dedicated to the construction of the hadron tensor in different situations, i.e. inclusive ( $e, e'$ ) reactions (section 5), semi-inclusive reactions with unpolarized particles (section 6), reactions where polarization observables are considered (section 7). Here the notion of structure function (or response) plays a major role and is discussed in some examples. Some effort has also been made to show the connection between different notations and derivations of the hadron response.

## 2. One-photon exchange approximation

An incident electron with mass  $m_e$ , charge  $e (< 0)$ , initial four-momentum  $k \equiv k^\mu = (E, \mathbf{k})$  and spin  $s$  is scattered to a final four-momentum  $k'^\mu = (E', \mathbf{k}')$  thus transferring the four-momentum  $q^\mu = k^\mu - k'^\mu \equiv (\omega, \mathbf{q})$  to the target. In the following the notations of ref. [1] will be used so that for space-like momentum transfer one has

$$q_\mu^2 \equiv q_\mu q^\mu \equiv q \cdot q = \omega^2 - |\mathbf{q}|^2 \leq 0. \quad (2.1)$$

One also defines

$$Q^2 = -q_\mu^2 \geq 0. \quad (2.2)$$

The electron wave function  $\Psi$  corresponding to positive energy,

$$\Psi = \sqrt{m_e/E} u(k, s) e^{-ik \cdot x}, \quad (2.3)$$

is given in terms of normalized spinors,

$$\bar{u}(k, s) u(k, s) = 1, \quad (2.4)$$

satisfying the Dirac equation for the free particle,

$$(\not{k} - m_e) u(k, s) = 0, \quad (2.5)$$

where  $\not{k} \equiv \gamma \cdot k$  is the Feynman notation of the four-product of a vector  $k$  with the Dirac  $\gamma$ -matrices. In the rest frame of the electron,  $k^\mu = (m_e, 0)$  and  $s^\mu = (0, \mathbf{s})$  with  $s^2 = 1$ . Thus the properties

$$s \cdot s = -1, \quad s \cdot k = 0, \quad (2.6)$$

hold in any frame.

At high energy the transverse polarization is suppressed with respect to the longitudinal one by a factor  $m_e/E$ . Therefore only longitudinal polarization can be obtained in practice at high energy. The corresponding spin is

$$s^\mu = h(|\mathbf{k}|/m_e, (E/m_e)\hat{\mathbf{u}}_L), \quad (2.7)$$

where  $\hat{\mathbf{u}}_L$  is a unit vector in the direction of  $\mathbf{k}$  and  $h = +1 (-1)$  is the electron helicity for the spin parallel (antiparallel) to the momentum. Consequently, one deals with right- or left-handed electrons, respectively. The state with definite helicity is projected out by means of the helicity projection operator  $\frac{1}{2}(1 + h\gamma^5)$ .

The energy regime of interest here is the ultrarelativistic limit where the electron mass  $m_e$  can be neglected, i.e.,

$$E = \sqrt{|\mathbf{k}|^2 + m_e^2} \simeq |\mathbf{k}|. \quad (2.8)$$

Then

$$Q^2 = -2m_e^2 + 2\mathbf{k} \cdot \mathbf{k}' \simeq 2\mathbf{k} \cdot \mathbf{k}' = 4EE' \sin^2 \frac{1}{2}\theta, \quad (2.9)$$

where  $\theta$  is the scattering angle of the electron in the laboratory.

In the ultrarelativistic limit the electron spin is aligned with its momentum:

$$s^\mu = \hbar k^\mu/m_e. \quad (2.10)$$

In the one-photon exchange approximation the scattering matrix of the process depicted in fig. 1 is given by

$$S_{fi} = -i \int d^{(4)}x H_I(x), \quad (2.11)$$

where the interaction Hamiltonian density,

$$H_I(x) = e_T A_\mu(x) J^\mu(x), \quad (2.12)$$

is written in terms of the four-current  $J_\mu(x)$  of the target with charge  $e_T$  and the Møller potential  $A_\mu(x)$  generated by the electron four-current [13],

$$j_\mu(x) = \frac{m_e}{\sqrt{EE'}} e^{i(k' - k) \cdot x} \bar{u}_f \gamma_\mu u_i. \quad (2.13)$$

The Møller potential thus satisfies a Klein–Gordon equation with a source term given by  $j_\mu(x)$ , i.e.,

$$\square A_\mu(x) = ej_\mu(x), \quad (2.14)$$

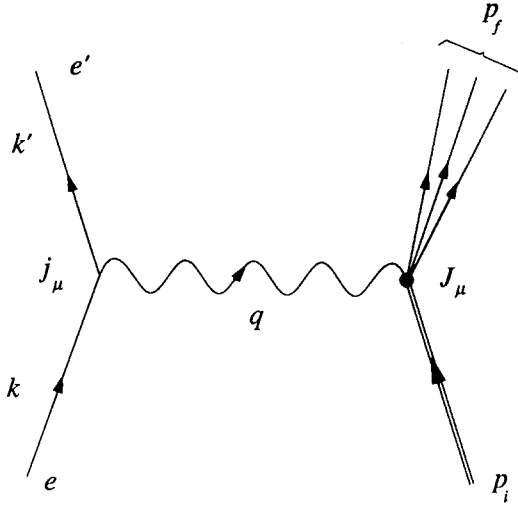


Fig. 1. One-photon exchange diagram for electron scattering.

whose solution

$$A_\mu(x) = e \int d^{(4)}y D(x - y) j_\mu(y), \quad (2.15)$$

is obtained in terms of the Green's function  $D(x - y)$  obeying the following equation:

$$\square D(x - y) = \delta^{(4)}(x - y). \quad (2.16)$$

The explicit expression of the Møller potential can be found by Fourier transforming  $D(x - y)$ ,

$$D(x - y) = \frac{1}{(2\pi)^4} \int d^{(4)}p e^{ip \cdot (x - y)} D(p), \quad (2.17)$$

where by eq. (2.16)

$$D(p) = -1/p_\mu^2. \quad (2.18)$$

Then

$$\begin{aligned} A_\mu(x) &= e \int d^{(4)}y \frac{1}{(2\pi)^4} \int d^{(4)}p e^{ip \cdot (x - y)} \left( -\frac{1}{p_\nu^2} \right) j_\mu(y) \\ &= -\frac{1}{(k'_\nu - k_\nu)^2} \frac{em_e}{\sqrt{EE'}} \bar{u}_f \gamma_\mu u_i e^{i(k' - k) \cdot x}, \end{aligned}$$

i.e.,

$$A_\mu(x) = a_\mu e^{-iq \cdot x}, \quad (2.19)$$

$$a_\mu = -\frac{1}{q_v^2} \frac{em_e}{\sqrt{EE'}} \bar{u}_f \gamma_\mu u_i \equiv e \frac{1}{Q^2} j_\mu. \quad (2.20)$$

The electron spinors satisfy the free Dirac equation. As a consequence, the electron current is conserved,

$$q_\mu j^\mu = 0, \quad (2.21)$$

and the Møller potential is defined in the Lorentz gauge:

$$\partial_\mu A^\mu(x) = 0. \quad (2.22)$$

Also the target current must be conserved, i.e.,

$$\partial_\mu J^\mu(x) = 0, \quad (2.23)$$

$$q_\mu J^\mu = 0. \quad (2.24)$$

If one defines the time and space components of the currents in terms of the charge and the (three-vector) current density as follows:

$$j_\mu \equiv (j_0, \mathbf{j}), \quad J_\mu \equiv (\rho, \mathbf{J}), \quad (2.25)$$

eqs. (2.21) and (2.24) can equivalently be written as

$$\omega j_0 - \mathbf{q} \cdot \mathbf{j} = 0, \quad (2.26)$$

$$\omega \rho - \mathbf{q} \cdot \mathbf{J} = 0. \quad (2.27)$$

Separating the longitudinal (L) and transverse (T) components of the current with respect to the momentum transfer  $\mathbf{q}$ ,

$$\mathbf{j} = \mathbf{j}_L + \mathbf{j}_T, \quad \mathbf{j}_T \cdot \mathbf{q} = 0, \quad (2.28)$$

$$\mathbf{J} = \mathbf{J}_L + \mathbf{J}_T, \quad \mathbf{J}_T \cdot \mathbf{q} = 0, \quad (2.29)$$

eqs. (2.26) and (2.27) give a constraint between the longitudinal component of the current and the charge:

$$\mathbf{j}_L = (\omega/|\mathbf{q}|) j_0 \hat{\mathbf{q}}, \quad (2.30)$$

$$\mathbf{J}_L = (\omega/|\mathbf{q}|) \rho \hat{\mathbf{q}}. \quad (2.31)$$

These relations are a consequence of gauge invariance and current conservation; as such they must be guaranteed by any model calculation. In contrast, the transverse target current is completely free.

The target current  $J_\mu(x)$  is the matrix element of the four-current density operator  $\hat{J}_\mu(x)$  between the initial ( $|\Psi_i\rangle$ ) and the final ( $|\Psi_f\rangle$ ) state of the target. Due to Lorentz invariance one can write

$$J_\mu(x) = \langle \Psi_f | \hat{J}_\mu(x) | \Psi_i \rangle = e^{i(p_f - p_i) \cdot x} \langle \Psi_f | \hat{J}_\mu(0) | \Psi_i \rangle \equiv e^{i(p_f - p_i) \cdot x} J_\mu. \quad (2.32)$$

Therefore

$$\int d^{(4)}x J_\mu(x) e^{-iq \cdot x} = (2\pi)^4 \delta^{(4)}(p_f - p_i - q) J_\mu, \quad (2.33)$$

and the scattering matrix (2.11) becomes

$$S_{fi} = -ie_T \int d^{(4)}x A_\mu(x) J^\mu(x) = -iee_T j_\mu \frac{1}{Q^2} J^\mu (2\pi)^4 \delta^{(4)}(p_f - p_i - q). \quad (2.34)$$

Due to gauge invariance and current conservation the product  $j_\mu J^\mu$  is rewritten as

$$j_\mu J^\mu = j_0 \rho - \mathbf{j} \cdot \mathbf{J} = (1 - \omega^2/|q|^2) j_0 \rho - \mathbf{j}_T \cdot \mathbf{J}_T,$$

i.e.,

$$j_\mu J^\mu = (Q^2/|q|^2) j_0 \rho - \mathbf{j}_T \cdot \mathbf{J}_T. \quad (2.35)$$

Alternatively, one could express the charge product in terms of the longitudinal components of the electron and target currents. Here expression (2.35) is preferred because the charge distribution of the target is usually better known from experiment. In any case the product  $j_\mu J^\mu$  is split into the sum of one longitudinal (charge) and two transverse pieces, whose contributions to the cross section cause different types of target response.

Incidentally, it should be noted that the reduction (2.35) is obtained in the laboratory frame and is not frame independent. When  $J^\mu$  is evaluated in the CM frame an extra factor  $(W/M_T)$ , where  $W$  is the invariant mass of the final hadron system and  $M_T$  is the target mass, must accompany  $j_0 \rho$  as a result of the transformation to the laboratory frame [14]. The corresponding correction in the cross section is of the order  $(Q^2/M_T^2)$  and is important only for very light nuclei and high  $Q^2$ . As we are here mainly interested in electron scattering off complex nuclei, this correction will be ignored.

The result (2.35) is also in agreement with the fact that the exchanged virtual photon has both transverse and longitudinal polarization. This is better shown as follows. By current conservation the scattering matrix (2.34) can also be written as

$$S_{fi} = -iee_T j_\mu \frac{\tilde{g}^{\mu\nu}}{Q^2} J_\nu (2\pi)^4 \delta^{(4)}(p_f - p_i - q), \quad (2.36)$$

$$\tilde{g}^{\mu\nu} = g^{\mu\nu} - q^\mu q^\nu / q_\lambda^2. \quad (2.37)$$

In analogy with the case of real photons, to describe the polarization of the virtual photon it is useful to introduce unit four-vectors  $\varepsilon_\lambda^\mu$ , with  $\lambda = 0$  for longitudinal polarization and  $\lambda = \pm 1$  for the two transverse polarizations. The photon polarization vectors  $\varepsilon_\lambda^\mu$  have the following properties:

$$q_\mu \varepsilon_\lambda^\mu = 0, \quad g_{\mu\nu} \varepsilon_\lambda^{\mu*} \varepsilon_{\lambda'}^\nu = (-)^\lambda \delta_{\lambda\lambda'}, \quad (2.38)$$

$$\tilde{g}^{\mu\nu} = \sum_\lambda (-)^\lambda \varepsilon_\lambda^{\mu*} \varepsilon_\lambda^\nu, \quad (2.39)$$

and satisfy the reflection symmetry

$$\varepsilon_\lambda^{\mu*} = (-)^\lambda \varepsilon_{-\lambda}^\mu. \quad (2.40)$$

In the laboratory frame of reference with the  $z$ -axis along  $\mathbf{q}$ ,

$$q^\mu = (\omega, 0, 0, |\mathbf{q}|), \quad (2.41)$$

one has

$$\varepsilon_{\pm 1}^\mu = \mp (1/\sqrt{2})(0, 1, \pm i, 0), \quad \varepsilon_0^\mu = (|\mathbf{q}|/Q, 0, 0, \omega/Q). \quad (2.42)$$

Equations (2.42) are the explicit covariant generalization to virtual photons of the definition of unit polarization vectors for real photons, where

$$\varepsilon^\mu = (0, \varepsilon_x, \varepsilon_y, 0), \quad |\varepsilon_x|^2 + |\varepsilon_y|^2 = 1. \quad (2.43)$$

In terms of the polarization vectors one defines covariant electron and target currents,

$$j_\lambda = j_\mu \varepsilon_\lambda^{\mu*}, \quad J_\lambda = (-)^\lambda J_\mu \varepsilon_\lambda^\mu, \quad (2.44)$$

respectively, which can be separately calculated in any frame of reference. Then the scattering matrix (2.36) reads

$$S_{fi} = -iee_T \sum_\lambda j_\lambda \frac{1}{Q^2} J_\lambda (2\pi)^4 \delta^{(4)}(p_f - p_i - q). \quad (2.45)$$

### 3. The lepton tensor

As an intermediate step in the calculation of the scattering cross section one has to perform an average over the unobserved initial states and a sum over the undetected final states. The resulting leptonic contribution is derived and discussed in this section. If the electron is in a pure helicity state, the electron current can be written as

$$j^\mu = (m_e/\sqrt{EE'}) \bar{u}_f \gamma^\mu \frac{1}{2}(1 + h\gamma^5) u_i. \quad (3.1)$$

The contribution of the electron current to the cross section is given by

$$\sum_{\text{spin}} (j_\mu \varepsilon_\lambda^{\mu*}) (j_\nu \varepsilon_{\lambda'}^{\nu*})^* \equiv \frac{1}{4EE'} L_{\lambda\lambda'} = \sum_{\text{spin}} \frac{m_e^2}{EE'} \bar{u}_f \not{\epsilon}_{\lambda}^* \frac{1}{2}(1 + h\gamma^5) u_i \bar{u}_i \not{\epsilon}_{\lambda'} u_f , \quad (3.2)$$

which also defines the lepton tensor  $L_{\lambda\lambda'}$ .

With the aid of the projection operators

$$\sum_{\text{spin}} u_i \bar{u}_i = \frac{\not{k} + m_e}{2m_e}, \quad \sum_{\text{spin}} u_f \bar{u}_f = \frac{\not{k}' + m_e}{2m_e} , \quad (3.3)$$

summation over spins is converted into the trace of a product of Dirac  $\gamma$ -matrices. Thus  $L_{\lambda\lambda'}$  becomes

$$L_{\lambda\lambda'} = \text{Tr}[(\not{k}' + m_e) \not{\epsilon}_{\lambda}^* \frac{1}{2}(1 + h\gamma^5)(\not{k} + m_e) \not{\epsilon}_{\lambda'}] . \quad (3.4)$$

In the present ultrarelativistic limit ( $m_e \simeq 0$ ), making use of the trace theorems on the  $\gamma$ -matrices (see, e.g., appendix A of ref. [1]) one obtains

$$L_{\lambda\lambda'} = 2[k' \cdot \varepsilon_\lambda^* k \cdot \varepsilon_{\lambda'} + k \cdot \varepsilon_\lambda^* k' \cdot \varepsilon_{\lambda'} - k \cdot k' \varepsilon_\lambda^* \varepsilon_{\lambda'}] + 2ih\varepsilon_{\mu\nu\alpha\beta} \varepsilon_\lambda^* \varepsilon_{\lambda'}^\nu k^\alpha k'^\beta \equiv L_{\lambda\lambda'}^0 + hL_{\lambda\lambda'}^h . \quad (3.5)$$

In eq. (3.5)  $\varepsilon_{\mu\nu\alpha\beta}$  is the totally antisymmetric tensor with  $\varepsilon_{0123} = +1$  and the lepton tensor is separated into helicity independent and dependent terms,  $L_{\lambda\lambda'}^0$  and  $L_{\lambda\lambda'}^h$ , respectively. Thus  $L_{\lambda\lambda'}^0$  is parity conserving and  $L_{\lambda\lambda'}^h$  is parity violating.

If the initial helicity is unobserved, a summation over  $h$  must be performed in eq. (3.2) as well. In this case the term containing  $h$  is averaged to zero and only  $L_{\lambda\lambda'}^0$  survives in  $L_{\lambda\lambda'}$ .

The lepton tensor is hermitian,

$$L_{\lambda\lambda'} = L_{\lambda'\lambda}^* , \quad (3.6)$$

and from the reflection symmetry (2.40) it follows that

$$L_{-\lambda-\lambda'}^0 = (-)^{\lambda-\lambda'} L_{\lambda\lambda'}^{0*}, \quad L_{-\lambda-\lambda'}^h = (-)^{1+\lambda-\lambda'} L_{\lambda\lambda'}^{h*} . \quad (3.7)$$

The general structure of the lepton tensor is given in table 1. The six independent elements of the lepton tensor can be readily evaluated in the laboratory frame using the explicit forms of the polarization vectors given in eqs. (2.42). One can factor out a common factor [14]

$$L_{\lambda\lambda'}^0 = 2\beta l_{\lambda\lambda'}^0, \quad L_{\lambda\lambda'}^h = 2\beta l_{\lambda\lambda'}^h , \quad (3.8)$$

$$\beta = 2EE' \cos^2 \frac{1}{2}\theta . \quad (3.9)$$

In table 2 the coefficients  $l_{\lambda\lambda'}^0, l_{\lambda\lambda'}^h$ , calculated in the frame of reference of fig. 2, are given and connected with other quantities of common use [15–17]. In particular, the coefficients  $\rho_{\lambda\lambda'}$  are those of ref. [16] divided by  $\beta$  and the coefficients  $v_i$  are those of ref. [17].

Table 1  
General structure of the lepton tensor  $L_{\lambda\lambda'} = L_{\lambda\lambda'}^0 + hL_{\lambda\lambda'}^h$

|   |   |
|---|---|
| $L_{00}^0$  | $L_{00}^h = 0$                                      |
| $L_{01}^0 = L_{10}^{0*} = -L_{0-1}^{0*} = -L_{-10}^0$ | $L_{01}^h = L_{10}^{h*} = L_{0-1}^{h*} = L_{-10}^h$ |
| $L_{11}^0 = L_{-1-1}^{0*}$                            | $L_{11}^h = -L_{-1-1}^{h*}$                         |
| $L_{1-1}^0 = L_{-11}^{0*}$                            | $L_{1-1}^h = L_{-11}^{h*} = 0$                      |

Table 2  
Independent components of the lepton tensor

|   |   |  |
|---|---|--|
| $\rho_{00}^0 = Q^2/ \mathbf{q} ^2$  | $\rho_{00} = (Q^2/ \mathbf{q} ^2) l_{00}^0$ | $v_L = (Q^2/ \mathbf{q} ^2) l_{00}^0$  |
| $\rho_{11}^0 = Q^2/2 \mathbf{q} ^2 + \tan^2 \frac{1}{2}\theta$                                    | $\rho_{11} = l_{11}^0$                      | $v_T = l_{11}^0$                       |
| $\rho_{01}^0 = (1/\sqrt{2})(Q/ \mathbf{q} )(Q^2/ \mathbf{q} ^2 + \tan^2 \frac{1}{2}\theta)^{1/2}$ | $\rho_{01} = (Q/ \mathbf{q} ) l_{01}^0$     | $v_{TL} = -(Q/ \mathbf{q} ) l_{01}^0$  |
| $\rho_{1-1}^0 = -Q^2/2 \mathbf{q} ^2$   | $\rho_{1-1} = l_{1-1}^0$                    | $v_{TT} = l_{1-1}^0$                   |
| $\rho_{01}' = (1/\sqrt{2})(Q/ \mathbf{q} ) \tan \frac{1}{2}\theta$                                | $\rho_{01}' = (Q/ \mathbf{q} ) l_{01}^h$    | $v'_{TL} = -(Q/ \mathbf{q} ) l_{01}^h$ |
| $\rho_{11}' = \tan \frac{1}{2}\theta(Q^2/ \mathbf{q} ^2 + \tan^2 \frac{1}{2}\theta)^{1/2}$        | $\rho_{11}' = l_{11}^h$                     | $v'_T = l_{11}^h$                      |

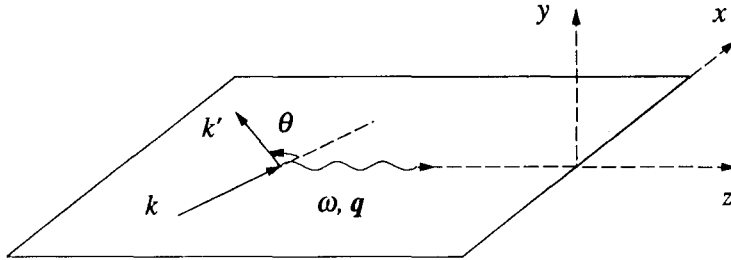


Fig. 2. Reference frame for electron scattering.

The lepton tensor can also be defined in a cartesian basis [7], i.e.,

$$\sum_{\text{spin}} j_\mu j_\nu^* = \frac{1}{4EE} L_{\mu\nu}, \quad (3.10)$$

$$\begin{aligned} L_{\mu\nu} &= L_{\mu\nu}^0 + hL_{\mu\nu}^h = \text{Tr}[(\not{k}' + m_e)\gamma_\mu \not{\gamma}_2 (1 + h\not{\gamma}^5)(\not{k} + m_e)\gamma_\nu] \\ &\simeq 2(k'_\mu k_\nu + k_\mu k'_\nu - g_{\mu\nu}k \cdot k') + 2i\hbar\epsilon_{\mu\nu\alpha\beta}k^\alpha k'^\beta. \end{aligned} \quad (3.11)$$

In this case  $L_{\mu\nu}^0$  is symmetric and  $L_{\mu\nu}^h$  antisymmetric in the Lorentz indices.

The form of the lepton tensor turns out to be quite general and useful for many different processes everywhere a lepton interacts with a hadron exchanging a vector boson. In table 3 the association of the specific variables entering the lepton tensor is given for a variety of such processes [10].

Table 3  
 $L_{\mu\nu} = 2(k'_\mu k_\nu + k_\mu k'_\nu - g_{\mu\nu} k \cdot k') + 2i\xi \epsilon_{\mu\nu\alpha\beta} k^\alpha k'^\beta$

| Process                         | $k$            | $k'$            | $q$       | $\xi$ |
|---------------------------------|----------------|-----------------|-----------|-------|
| $\beta^-$ -decay                | $e^-$          | $\bar{v}_e$     | $-k - k'$ | —     |
| $\beta^+$ -decay                | $e^+$          | $v_e$           | $-k - k'$ | +     |
| $(\ell^-, v_\ell)$              | $\ell^-$       | $v_\ell$        | $k - k'$  | +     |
| $(v_\ell, \ell^-)$              | $v_\ell$       | $\ell^-$        | $k - k'$  | +     |
| $(\bar{v}_\ell, \ell^+)$        | $\bar{v}_\ell$ | $\ell^+$        | $k - k'$  | —     |
| $(v_\ell, v'_\ell)$             | $v_\ell$       | $v'_\ell$       | $k - k'$  | +     |
| $(\bar{v}_\ell, \bar{v}'_\ell)$ | $\bar{v}_\ell$ | $\bar{v}'_\ell$ | $k - k'$  | —     |
| $(\ell^-, \ell^-)$              | $\ell^-$       | $\ell^-$        | $k - k'$  | $h$   |

Introducing the four-vector  $K^\mu = \frac{1}{2}(k^\mu + k'^\mu)$ ,  $L_{\mu\nu}^0$  can also be rewritten as

$$L_{\mu\nu}^0 = 4K_\mu K_\nu - q_\mu q_\nu - Q^2 g_{\mu\nu}. \quad (3.12)$$

In the lepton Breit frame [3], where the lepton scatters backwards with no energy loss, i.e.,  $k' = -k$ ,  $q_\mu \equiv (0, 2\mathbf{k})$ , unpolarized relativistic electrons emit transverse polarized (virtual) photons. As a relativistic electron preserves its helicity, the virtual photon is an equal incoherent mixture of  $+1$  and  $-1$  helicity states. In this frame,  $Q^2 = 4|\mathbf{k}|^2$  and from eq. (3.12) the only surviving elements of  $L_{\mu\nu}^0$  are  $L_{xx}^0 = L_{yy}^0 = Q^2$ . It is useful to define a matrix  $\rho_{\mu\nu}^B$  as follows:

$$L_{\mu\nu}^0 = 2Q^2 \rho_{\mu\nu}^B. \quad (3.13)$$

Thus  $\rho_{\mu\nu}^B$  is the density matrix of the virtual photon polarization, and the only nonvanishing components are  $\rho_{xx}^B = \rho_{yy}^B = \frac{1}{2}$ .

Transforming to the laboratory frame, with the  $z$ -axis along  $\mathbf{q}$ , one similarly defines

$$L_{\mu\nu} = 2Q^2 \frac{1}{1-\varepsilon} \rho_{\mu\nu}, \quad (3.14)$$

$$\varepsilon = [1 + 2(|\mathbf{q}|^2/Q^2)\tan^2 \frac{1}{2}\theta]^{-1}. \quad (3.15)$$

In the lepton Breit frame,  $\varepsilon = 0$ . In general  $\varepsilon$  is a measure of the transverse linear polarization of the virtual photon, as will become apparent when the density matrix  $\rho_{\mu\nu}$  is exhibited explicitly. To do that it is convenient to include the current conservation factor  $Q^2/|\mathbf{q}|^2$  in the lepton tensor and ignore it in the hadron tensor when writing the amplitude  $S_{fi}$  in terms of the currents. In this way  $\rho_{\mu\nu}$  can be reduced to a  $3 \times 3$  matrix  $\rho_{ab}$ , with  $a, b = 0, x, y$ , if one eliminates the (longitudinal)

*z*-component of the lepton current taking advantage of eq. (2.35). Then [7, 16]

$$\rho_{ab} = \begin{vmatrix} \varepsilon_L & (1/\sqrt{2})\sqrt{\varepsilon_L(1+\varepsilon)} & -ih(1/\sqrt{2})\sqrt{\varepsilon_L(1-\varepsilon)} \\ (1/\sqrt{2})\sqrt{\varepsilon_L(1+\varepsilon)} & \frac{1}{2}(1+\varepsilon) & -ih\frac{1}{2}\sqrt{1-\varepsilon^2} \\ ih(1/\sqrt{2})\sqrt{\varepsilon_L(1-\varepsilon)} & ih\frac{1}{2}\sqrt{1-\varepsilon^2} & \frac{1}{2}(1-\varepsilon) \end{vmatrix}, \quad (3.16)$$

$$\varepsilon_L = (Q^2/|\mathbf{q}|^2)\varepsilon. \quad (3.17)$$

In the case of real photons propagating along the *z*-axis  $\rho_{ab}$  has only *x*, *y* components, and for a partially linearly polarized beam of relative strength  $(1+\varepsilon')$  in the *x*-direction to  $(1-\varepsilon')$  in the *y*-direction, one has

$$\rho_{ab} = \begin{vmatrix} 0 & 0 & 0 \\ 0 & \frac{1}{2}(1+\varepsilon') & 0 \\ 0 & 0 & \frac{1}{2}(1-\varepsilon') \end{vmatrix}. \quad (3.18)$$

The case  $\varepsilon' = 0$  corresponds to unpolarized photons. It is now obvious why  $\varepsilon$  is a measure of the transverse linear polarization of the virtual photon and  $\varepsilon_L$  defines the scalar (longitudinal) polarization.

The density matrix (3.16) shows that the virtual photon is in the pure polarization state

$$(\varepsilon_x, \varepsilon_y, \varepsilon_z) = \{(1/\sqrt{2})\sqrt{1+\varepsilon}, ih(1/\sqrt{2})\sqrt{1-\varepsilon}, -(|\mathbf{q}|/\omega)\sqrt{\varepsilon_L}\}. \quad (3.19)$$

Thus, scattering by polarized electrons is equivalent to scattering by a photon whose polarization is a superposition of a transverse elliptic component and a longitudinal component. For  $\varepsilon = 0$ , the photon is circularly polarized. This occurs for backward electron scattering, i.e.,  $\theta = \pi$ .

The six independent elements of the density matrix  $\rho_{ab}$  in eq. (3.16) correspond to the six independent elements  $L_{00}^0, L_{0x}^0, L_{xx}^0, L_{yy}^0, L_{0x}^h$  and  $L_{xy}^h$ . In a spherical basis, they correspond to the coefficients  $\rho_{\lambda\lambda'}$  in table 2 apart from a common factor and a possible change of sign (see ref. [16]).

#### 4. Elastic scattering and form factors

In this section some simple examples are given of elastic electron scattering. The purpose of that is to show some general features of the formalism which are basic guidelines for more complicated cases. An important result of elastic electron scattering is the possibility to define form factors which describe charge and magnetization distributions inside a target with internal structure. In particular the nucleon form factors will be briefly discussed because of their extensive use in the electron–nucleus interaction.

#### 4.1. Scalar particle

As a simple illustrative example to calculate cross sections let us consider elastic electron scattering off a scalar (hadron) particle with mass  $M$  and charge  $e_T$  (in units of the proton charge). The wave function for such a particle with positive energy  $E$  is

$$\Phi = (1/\sqrt{2E}) e^{-ip \cdot x} . \quad (4.1)$$

The Feynman diagram for the process is shown in fig. 3. According to the usual rules for Feynman diagrams (see, e.g., appendix B of ref. [1]) the hadron current can be expressed in terms of the only two available independent Lorentz vectors,  $P^\mu = p_i^\mu + p_f^\mu$  and  $q^\mu = p_f^\mu - p_i^\mu$ , as

$$J^\mu = \frac{1}{\sqrt{2E_i}} \frac{1}{\sqrt{2E_f}} (P^\mu F_1 + q^\mu F_2) , \quad (4.2)$$

where a priori the two form factors  $F_{1,2}$  are functions of the three available independent Lorentz scalars,  $Q^2, p_i^2, p_f^2$ :

$$F_{1,2} = F_{1,2}(Q^2, p_i^2, p_f^2) . \quad (4.3)$$

However, the free scalar particle is on shell in its initial and final states, i.e.,

$$p_i^2 = p_f^2 = M^2 . \quad (4.4)$$

Therefore, while in principle eq. (4.3) holds true for a bound particle, for a free particle as here eq. (4.3) simplifies to

$$F_{1,2} = F_{1,2}(Q^2) . \quad (4.5)$$

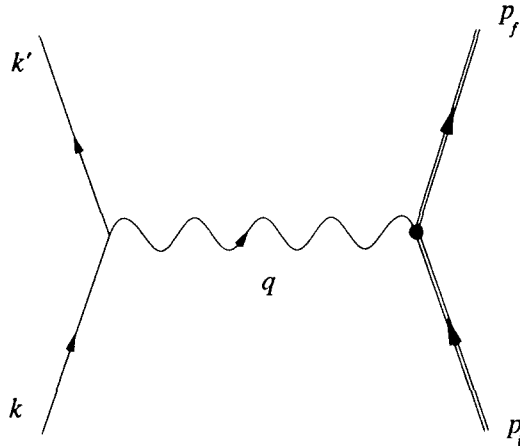


Fig. 3. One-photon exchange diagram for elastic electron scattering off a scalar particle.

Furthermore, as a consequence of current conservation, eq. (2.24), the two form factors are no longer independent of each other:

$$F_2 = -\frac{q \cdot P}{q_\mu^2} F_1 . \quad (4.6)$$

In particular, on shell  $F_2 = 0$ . Defining the gauge invariant vector

$$\tilde{P}^\mu = P^\mu - \frac{q \cdot P}{q_v^2} q^\mu , \quad (4.7)$$

the hadron current becomes

$$J^\mu = \frac{1}{2\sqrt{E_i E_f}} \tilde{P}^\mu F_1(Q^2) , \quad (4.8)$$

which is automatically conserved even when going off shell.

The cross section for the elastic process is written as

$$d\sigma = \frac{1}{J_{\text{inc}}} \sum_{\text{spin}} |S_{fi}|^2 \frac{d^3 k'}{(2\pi)^3} \frac{d^3 p_f}{(2\pi)^3} , \quad (4.9)$$

where the incident flux is  $J_{\text{inc}} = 1$  with the present normalizations. The sum over electron spins involves trace evaluation along the lines described in the previous section. For unpolarized electrons one has:

$$\sum_{\text{spin}} j_\mu j_v^* J^\mu J^{v*} = \frac{1}{4EE} L_{\mu\nu}^0 J^\mu J^{v*} = \frac{1}{8EE'E_i E_f} |F_1(Q^2)|^2 [2k \cdot \tilde{P} k' \cdot \tilde{P} - \tilde{P}^2 k \cdot k'] . \quad (4.10)$$

Equation (4.10) can be evaluated in the laboratory frame, where  $p_i^\mu \equiv (M, 0)$ , with the result

$$\sum_{\text{spin}} j_\mu j_v^* J^\mu J^{v*} = \frac{M^2}{E_i E_f} |F_1(Q^2)|^2 \cos^2 \frac{1}{2}\theta . \quad (4.11)$$

In the cross section  $|S_{fi}|^2$  contains the square of the delta function of eq. (2.34). When one is interested in the transition probability per unit time in the normalization volume, one can show (see, e.g., p. 101 of ref. [1]) that  $[(2\pi)^4 \delta^{(4)}(p_f - p_i - q)]^2$  can be simply replaced by  $(2\pi)^4 \delta^{(4)}(p_f - p_i - q)$ . As a result eq. (4.9) becomes

$$d\sigma = \frac{4e_i^2 \alpha^2}{Q^4} 2M |F_1(Q^2)|^2 \cos^2 \frac{1}{2}\theta d^3 k' \frac{d^3 p_f}{2E_f} \delta^{(4)}(p_f - p_i - q) , \quad (4.12)$$

where  $\alpha = e^2/4\pi$  is the fine structure constant. As  $d^3k' = E'^2 dE' d\Omega$ , one finally obtains

$$\frac{d\sigma}{dE' d\Omega} = \frac{4e_T^2 \alpha^2}{Q^4} 2ME'^2 |F_1(Q^2)|^2 \cos^2 \frac{1}{2}\theta \frac{d^3 p_f}{2E_f} \delta^{(4)}(p_f - p_i - q). \quad (4.13)$$

If the final hadron is not observed one may integrate over  $p_f$ . This gives

$$\int \frac{d^3 p_f}{2E_f} \delta^{(4)}(p_f - p_i - q) = \frac{1}{2M} \delta(\omega - Q^2/2M). \quad (4.14)$$

This result is a consequence of the fact that the factor  $(M/E)[d^3p/(2\pi)^3]$  forms a Lorentz invariant volume element in momentum space, provided that  $p^\mu$  is time-like as in the present case (see, e.g., p. 112 of ref. [1]). Thus

$$\frac{d\sigma}{dE' d\Omega} = \frac{4e_T^2 \alpha^2}{Q^4} (E')^2 |F_1(Q^2)|^2 \cos^2 \frac{1}{2}\theta \delta(\omega - Q^2/2M), \quad (4.15)$$

where the energy delta function guarantees that the scattering is elastic with the correct recoil of the target hadron.

Integrating over  $dE'$  and using the identity  $\int dx \delta(f(x)) = (|df/dx|_{x=\bar{x}})^{-1}$ , with  $f(\bar{x}) = 0$ , one obtains the so-called recoil factor  $f_{\text{rec}}$ :

$$f_{\text{rec}} \equiv \int dE' \delta(\omega - Q^2/2M) = [1 + (2E/M)\sin^2 \frac{1}{2}\theta]^{-1}. \quad (4.16)$$

However, by energy conservation  $f_{\text{rec}}$  also turns out to be:

$$f_{\text{rec}}^{-1} = (1/E')(E' + Q^2/2M) = E/E'. \quad (4.17)$$

Thus the cross section for elastic electron scattering off a scalar particle is

$$\frac{d\sigma}{d\Omega} = \frac{4e_T^2 \alpha^2}{Q^4} \frac{(E')^3}{E} \cos^2 \frac{1}{2}\theta |F_1(Q^2)|^2 = \sigma_M (E'/E) e_T^2 |F_1(Q^2)|^2 = \sigma_{\text{NS}} e_T^2 |F_1(Q^2)|^2, \quad (4.18)$$

where

$$\sigma_M = \frac{4\alpha^2}{Q^4} (E')^2 \cos^2 \frac{1}{2}\theta = \frac{\alpha^2 \cos^2 \frac{1}{2}\theta}{4E^2 \sin^4 \frac{1}{2}\theta} \quad (4.19)$$

is the Mott scattering cross section which describes elastic Coulomb scattering by a point-like target, and

$$\sigma_{\text{NS}} = \sigma_M E'/E \quad (4.20)$$

includes the recoil of the same target with no structure. The Mott cross section is strongly peaked in the forward direction and varies dramatically with the electron scattering angle  $\theta$ . Deviations of the observed cross section from  $\sigma_{\text{NS}}$  determine the form factor  $F_1(Q^2)$  describing the internal structure of the (scalar) target. In fig. 4 the experimental elastic cross section of  $^{206}\text{Pb}$  is shown and compared with mean field calculations [18]. The measurements [19, 20] extend over 12 decades and allow extraction of the form factor over a large range of momenta. The ground state charge distribution has been determined according to the model independent analysis of ref. [21]. The high momentum part of the cross section is related by Fourier transform to the inner part of the charge density, whose precise knowledge clearly requires high intensity and forward scattering angles, i.e. high energy of incident electrons. The experimental density is smaller in the center of the nucleus and has less structure than the theoretical prediction. A similar result has been found for all Pb isotopes and in general for heavy and medium-heavy nuclei.

#### 4.2. Dirac point-like particle

According to quantum electrodynamics the current of a Dirac point-like particle with mass  $M$  is given in terms of its spinors as

$$J^\mu = (M/\sqrt{E_i E_f}) \bar{u}_f \gamma^\mu u_i . \quad (4.21)$$

Of course this expression has the same structure as the electron current  $j_\mu$ . Therefore if one does not observe initial and final spins of the target particle, in the cross section one has to contract the

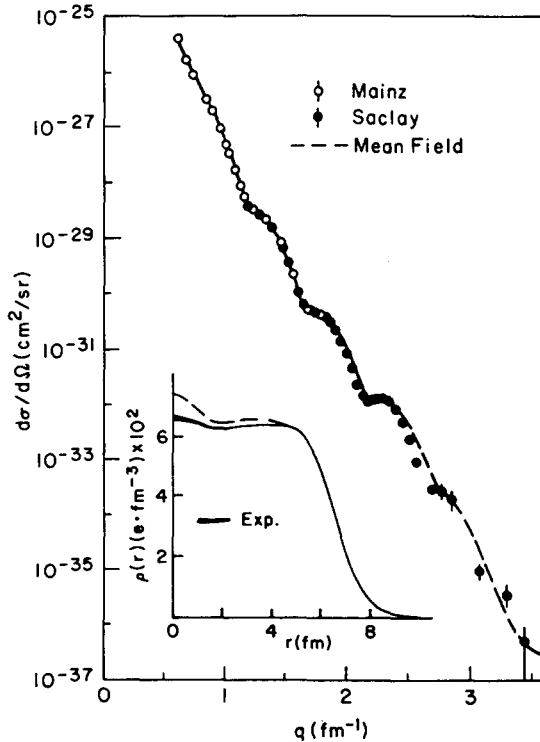


Fig. 4. Cross section for elastic scattering off  $^{206}\text{Pb}$  (from ref. [20]).

symmetric lepton tensor  $L_{\mu\nu}^0$  of the electron with an analogous symmetric tensor  $L_{\mu\nu}^{(p)}$  coming from the target current:

$$\begin{aligned} \sum_{\text{spin}} J^\mu J^{\nu*} &\equiv \frac{1}{4E_i E_f} L^{(p)\mu\nu} = \frac{1}{2} \text{Tr}[(p_f + M)\gamma^\mu(p_i + M)\gamma^\nu] \\ &= 2[p_f^\mu p_i^\nu + p_i^\nu p_f^\mu - g^{\mu\nu}(p_i \cdot p_f - M^2)] . \end{aligned} \quad (4.22)$$

The mass term appears here because one assumes that the target particle is not ultrarelativistic. Evaluating the contraction of the two tensors in the laboratory frame [ $p_i \equiv (M, 0)$ ] one obtains

$$\frac{1}{4EE'} L_{\mu\nu}^0 \frac{1}{4E_i E_f} L^{(p)\mu\nu} = \frac{M^2}{E_i E_f} \cos^2 \frac{1}{2}\theta \left( 1 + \frac{Q^2}{2M^2} \tan^2 \frac{1}{2}\theta \right) . \quad (4.23)$$

This expression differs from the corresponding one in the case of a scalar particle, eq. (4.11), in a twofold way. No form factor  $F_1$  arises because of the assumption of a point-like particle; the new term linear in  $\tan^2 \frac{1}{2}\theta$  is produced by the spin-magnetic interaction of the Dirac particle with the virtual photon exchanged by the electron.

Starting from eq. (4.9) it is now straightforward to write down the cross section for elastic electron scattering off a Dirac point-like particle along the same lines as for the scalar particle of the previous subsection [see eq. (4.15)]. One obtains

$$\frac{d\sigma}{dE' d\Omega} = \sigma_M \left( 1 + \frac{Q^2}{2M^2} \tan^2 \frac{1}{2}\theta \right) \delta(\omega - Q^2/2M) . \quad (4.24)$$

Therefore, integrating over  $dE'$  one gets

$$\frac{d\sigma}{d\Omega} = \sigma_M \frac{E'}{E} \left( 1 + \frac{Q^2}{2M^2} \tan^2 \frac{1}{2}\theta \right) = \sigma_{NS} \left( 1 + \frac{Q^2}{2M^2} \tan^2 \frac{1}{2}\theta \right) , \quad (4.25)$$

which corresponds to eq. (4.18). Equation (4.25) applies, e.g., to the case of electron-muon scattering [4], where the electron-photon and the electron-muon couplings are believed to be known exactly from quantum electrodynamics, viz. “point-like couplings”. Under the present assumptions of point-like quarks inside hadrons and with the appropriate charge inserted for the target quark, eq. (4.25) equally well applies to electron-quark scattering and is the reference cross section to study, e.g., electron-proton scattering. Any other spin- $\frac{1}{2}$  particle in fact will have an internal structure which will introduce corrections to the point-like coupling and accordingly modify the form of the scattering cross section (see section 4.3).

#### 4.3. Dirac particle with an internal structure

For a spin- $\frac{1}{2}$  particle with an unknown internal structure the current in eq. (4.21) is suitably modified by introducing appropriate form factors  $\Gamma_i$  describing its internal structure. If one

considers that there are three independent Lorentz vectors,  $p_i^\mu$ ,  $p_f^\mu$  and  $\gamma^\mu$ , the target current (4.21) now becomes

$$J^\mu = \frac{M}{\sqrt{E_i E_f}} \bar{u}_f \Gamma^\mu u_i = \frac{M}{\sqrt{E_i E_f}} \bar{u}_f (p_i^\mu \Gamma_1 + p_f^\mu \Gamma_2 + \gamma^\mu \Gamma_3) u_i , \quad (4.26)$$

where in general the three form factors  $\Gamma_i$  depend on the three scalar variables  $Q^2$ ,  $p_i^2$  and  $p_f^2$ . This is the form required, e.g., to describe a bound nucleon in the target, interacting with the virtual photon exchanged by the electron. Little is known, however, on the off-shell behaviour of the electromagnetic form factors of the nucleon. Only theoretical estimates have been given in a dispersion relation approach [22–24] and in models [25, 26] constrained by the Ward–Takahashi identity [27, 28] and also applicable to pion electroproduction [29, 30].

For a free (on-shell) particle the three form factors  $\Gamma_i$  are functions of  $Q^2$  only. However, by current conservation,

$$q_\mu \bar{u}_f \Gamma^\mu u_i = 0 , \quad (4.27)$$

they are not all independent. The spinors  $\bar{u}_f$  and  $u_i$  satisfy the free Dirac equation. Therefore, substituting in eq. (4.27) the explicit form of  $\Gamma^\mu$  from eq. (4.26) one obtains

$$\Gamma_1 = \Gamma_2 . \quad (4.28)$$

The most general form of the target current is then

$$J^\mu = \frac{M}{\sqrt{E_i E_f}} \bar{u}_f [(p_i^\mu + p_f^\mu) \Gamma_1(Q^2) + \gamma^\mu \Gamma_3(Q^2)] u_i . \quad (4.29)$$

Alternatively, one could take advantage of the Gordon decomposition of the current [1] holding for spinors that obey free Dirac equations:

$$\bar{u}_f \gamma^\mu u_i = \bar{u}_f \left( \frac{1}{2M} (p_i^\mu + p_f^\mu) + \frac{1}{2M} i\sigma^{\mu\nu} (p_{fv} - p_{iv}) \right) u_i , \quad (4.30)$$

$$\sigma^{\mu\nu} = \frac{1}{2} i(\gamma^\mu \gamma^\nu - \gamma^\nu \gamma^\mu) . \quad (4.31)$$

Inside a bracket between free spinors, the Gordon decomposition allows then the following substitution:

$$p_i^\mu + p_f^\mu \rightarrow 2M\gamma^\mu - i\sigma^{\mu\nu} q_v . \quad (4.32)$$

Thus the target current (4.29) is equivalently written as

$$J^\mu = \frac{M}{\sqrt{E_i E_f}} \bar{u}_f \left( \gamma^\mu F_1(Q^2) + i\sigma^{\mu\nu} q_v \frac{\kappa}{2M} F_2(Q^2) \right) u_i , \quad (4.33)$$

where the Dirac ( $F_1$ ) and Pauli ( $F_2$ ) form factors [31] are defined as

$$F_1(Q^2) = 2M\Gamma_1(Q^2) + \Gamma_3(Q^2), \quad \kappa F_2(Q^2) = -2M\Gamma_1(Q^2), \quad (4.34)$$

and  $\kappa$  is set equal to the anomalous part of the magnetic moment of the particle. In units of the Bohr magneton ( $\mu_B = -e\hbar/2Mc$ ), for the physical proton  $\kappa F_2(0) = \kappa_p = 1.793$  with  $F_1(0) = 1$ , while for the physical neutron  $\kappa F_2(0) = \kappa_n = -1.913$  with  $F_1(0) = 0$ . The case of a Dirac point-like particle is therefore recovered when  $F_1(Q^2) = 1$  and  $F_2(Q^2) = 0$ .

When initial and final spins are unobserved the cross section can be calculated as in previous cases adopting the trace theorems for the  $\gamma$ -matrices. The tensor originating from the target current is then obtained in a similar way as in eq. (4.22). Only, the anomalous part of the target current requires much more effort. After a lengthy but straightforward calculation one obtains

$$\begin{aligned} \frac{d\sigma}{dE'd\Omega} = \sigma_M & \left[ \left( F_1^2(Q^2) + \frac{Q^2}{4M^2} \kappa^2 F_2^2(Q^2) \right) \right. \\ & \left. + \frac{Q^2}{2M^2} [F_1(Q^2) + \kappa F_2(Q^2)]^2 \tan^2 \frac{1}{2}\theta \right] \delta(\omega - Q^2/2M). \end{aligned} \quad (4.35)$$

Therefore, integrating over  $dE'$  one has

$$\frac{d\sigma}{d\Omega} = \sigma_{NS} \left[ \left( F_1^2(Q^2) + \frac{Q^2}{4M^2} \kappa^2 F_2^2(Q^2) \right) + \frac{Q^2}{2M^2} [F_1(Q^2) + \kappa F_2(Q^2)]^2 \tan^2 \frac{1}{2}\theta \right]. \quad (4.36)$$

From an experimental point of view it is preferable to define new electromagnetic form factors which are directly related to the charge and magnetization density. These are known as the Sachs form factors [32] and are constructed in terms of the Dirac and Pauli form factors as follows:

$$G_E(Q^2) = F_1(Q^2) - \frac{Q^2}{4M^2} \kappa F_2(Q^2), \quad G_M(Q^2) = F_1(Q^2) + \kappa F_2(Q^2). \quad (4.37)$$

In fact, at  $Q^2 = 0$  the Sachs form factors  $G_E$  and  $G_M$  are normalized to the total charge  $e_T$  (in units of the proton charge) and to the total magnetic moment  $\mu$  of the particle (in units of the Bohr magneton  $\mu_B$ ), respectively. In the limit  $Q^2 \rightarrow 0$  the rms radii of the charge and magnetic moment spatial distributions are given by  $(6|dG_E/dQ^2|)^{1/2}/e_T$  and  $(6|dG_M/dQ^2|)^{1/2}/\mu$ , respectively. Obviously, the difference between  $G_E$  and  $F_1$  is of relativistic order and only shows up at high  $Q^2$ . Conversely,

$$\begin{aligned} F_1(Q^2) &= (1 + Q^2/4M^2)^{-1} [G_E(Q^2) + (Q^2/4M^2)G_M(Q^2)], \\ \kappa F_2(Q^2) &= (1 + Q^2/4M^2)^{-1} [G_M(Q^2) - G_E(Q^2)]. \end{aligned} \quad (4.38)$$

In terms of the Sachs form factors the target current (4.33) for an on-shell particle becomes [33, 34]

$$J^\mu = \frac{M}{\sqrt{E_i E_f}} \bar{u}_f [P^\mu G_E(Q^2) + (i/2M)r^\mu G_M(Q^2)] u_i , \quad (4.39)$$

$$P^\mu = p_i^\mu + p_f^\mu, \quad r^\mu = -\frac{1}{2}i(\gamma^\mu \not{p} - \not{q} \not{p} \gamma^\mu) , \quad (4.40)$$

where use has been made of the Gordon decomposition. In the form (4.39) better evidence is given to the convective part of the current involving the charge distribution described by  $G_E$  and to the magnetic part related to the magnetization density described by  $G_M$ . Correspondingly, the cross section for elastic electron scattering off a Dirac particle with internal structure is given by the Rosenbluth formula [35]

$$d\sigma/d\Omega = \sigma_{NS}[A(Q^2) + B(Q^2)\tan^2 \frac{1}{2}\theta] , \quad (4.41)$$

$$A(Q^2) = (1 + Q^2/4M^2)^{-1} [G_E^2(Q^2) + (Q^2/4M^2)G_M^2(Q^2)] , \quad (4.42)$$

$$B(Q^2) = (Q^2/2M^2)G_M^2(Q^2) . \quad (4.43)$$

Due to the explicit noninterference of  $G_E$  and  $G_M$  in the Rosenbluth formula it is experimentally possible to separate the two form factors. The contribution of the target magnetization density is enhanced at backward scattering angles where the term linear in  $\tan^2 \frac{1}{2}\theta$  dominates the cross section. Thus in a plot of the cross section versus  $\tan^2 \frac{1}{2}\theta$  one can first determine  $G_M$  from the slope  $B(Q^2)$  and then obtain  $G_E$  by subtraction from the term  $A(Q^2)$  which dominates at forward scattering angles. This procedure is known as the Rosenbluth separation.

#### 4.4. The electromagnetic form factors of the nucleon

The use of form factors to describe a composite target particle instead of referring the scattering process to its individual point-like constituents stems from insufficient knowledge about the internal structure of that particle or from difficulties in solving its dynamics. In the case of a nucleon one knows that its internal dynamics is basically governed by the coloured gluons exchanged by quarks. In the high- $Q^2$  limit, where a perturbative treatment of strong interactions is possible, quantum chromodynamics predicts the following behaviour for the nucleon form factors [36, 37]:

$$F_1 \sim \left( \frac{1}{Q^2 \log(Q^2/\Lambda_{QCD}^2)} \right)^2, \quad F_2 \sim F_1/Q^2 , \quad (4.44)$$

where  $\Lambda_{QCD}$  is the QCD cut-off momentum.

At low  $Q^2$  the available data [38–41] are in qualitative agreement with a dipole fit of the form factors, i.e. [41],

$$\begin{aligned} G_E^p(Q^2) &= (1 + Q^2/0.71)^{-2}, & G_M^p(Q^2) &= \mu_p G_E^p(Q^2) , \\ G_M^n(Q^2) &= \mu_n G_E^p(Q^2), & G_E^n(Q^2) &= (Q^2/4M^2)(1 + 5.6Q^2/4M^2)^{-1} |G_M^n(Q^2)| , \end{aligned} \quad (4.45)$$

where  $Q^2$  is in  $(\text{GeV}/c)^2$  and  $\mu_p = 1 + \kappa_p = 2.793$ ,  $\mu_n = \kappa_n = -1.913$  are the proton and neutron magnetic moments, respectively.

The dipole fit has no sound physical justification and must be considered as a mere parameterization. However, the accuracy of the data is still insufficient for using phenomenological form factors in a calculation at intermediate energies. Only  $G_M^p$  is sufficiently known up to  $Q^2 \sim 30 (\text{GeV}/c)^2$  because it is directly measured with great precision (fig. 5).  $G_E^n$  is most uncertain, because it is only known after a model dependent subtraction of all other effects in electron-deuteron scattering (see section 4.5).

From a theoretical point of view the problem arises of matching the asymptotic behaviour (4.44) with the existing information at low and intermediate energies. It is convenient to resolve proton and neutron form factors into their isotopic components by defining Dirac and Pauli isoscalar (S) and isovector (V) form factors as follows:

$$F_1 = F_1^S + \tau_3 F_1^V, \quad \kappa F_2 = \kappa^S F_2^S + \tau_3 \kappa^V F_2^V, \quad (4.46)$$

i.e.,

$$\begin{aligned} F_1^S &= \frac{1}{2}(F_1^p + F_1^n), & F_1^S(0) &= 0.5, \\ F_1^V &= \frac{1}{2}(F_1^p - F_1^n), & F_1^V(0) &= 0.5, \\ \kappa^S F_2^S &= \frac{1}{2}(\kappa_p F_2^p + \kappa_n F_2^n), & \kappa^S F_2^S(0) &= -0.060, \\ \kappa^V F_2^V &= \frac{1}{2}(\kappa_p F_2^p - \kappa_n F_2^n), & \kappa^V F_2^V(0) &= +1.853. \end{aligned} \quad (4.47)$$

At the energies of interest for nuclear physics and where meson dynamics plays the major role, effective lagrangians are necessary. Successful models for baryons have been proposed which incorporate basic QCD features [43–45].

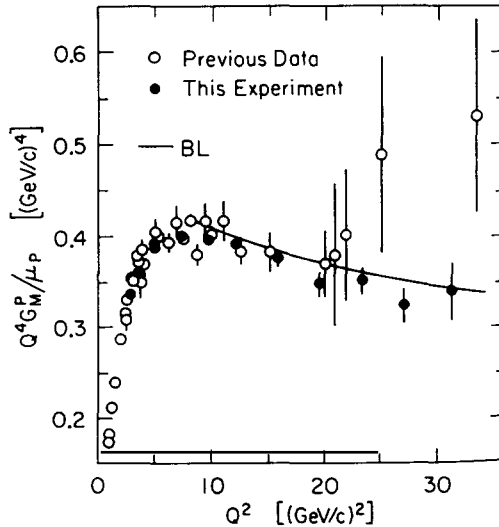


Fig. 5. Magnetic form factor of the proton (data from ref. [42], BL from ref. [37]).

Other models [46, 47] are based on an extended vector meson dominance, where besides being directly absorbed by the nucleon the physical (virtual) photon is also absorbed in a hadron state with the same quantum numbers as a photon, such as the  $\rho$ ,  $\omega$  and  $\phi$  mesons. This permits one to assume that the isoscalar and isovector form factors are products of an intrinsic common form factor times expressions appropriate to the specific channel of photon absorption by a point-like nucleon. Up to  $Q^2 \sim 1$  ( $\text{GeV}/c$ )<sup>2</sup> the results are in agreement with those derived from an effective lagrangian that extends the Skyrme soliton description of nucleons to incorporate the vector mesons  $\rho$  and  $\omega$  in a way consistent with the nonabelian anomalies of QCD and vector meson dominance [45]. In a recent review [48] the hadron form factors and their modification in the nuclear environment are considered.

#### 4.5. Multipole decomposition of the current and the neutron form factor

A multipole analysis of the electromagnetic current operator is useful when dealing with a target undergoing a transition from one state of definite angular momentum to another [6]. In eq. (2.32) it is then convenient to explicitly separate the time dependence,

$$J_\mu(x) = e^{i(E_f - E_i)t} \langle \Psi_f | \hat{J}_\mu(r) | \Psi_i \rangle, \quad (4.48)$$

and define space and time components of the four-current in momentum space,

$$J_\mu(\mathbf{q}) \equiv (\rho(\mathbf{q}), \mathbf{J}(\mathbf{q})), \quad (4.49)$$

as Fourier transforms of the charge density  $\hat{\rho}(\mathbf{r})$  and the (three-vector) current density  $\hat{\mathbf{J}}(\mathbf{r})$ :

$$\rho(\mathbf{q}) = \int d\mathbf{r} e^{i\mathbf{q} \cdot \mathbf{r}} \langle \Psi_f | \hat{\rho}(\mathbf{r}) | \Psi_i \rangle, \quad (4.50)$$

$$\mathbf{J}(\mathbf{q}) = \int d\mathbf{r} e^{i\mathbf{q} \cdot \mathbf{r}} \langle \Psi_f | \hat{\mathbf{J}}(\mathbf{r}) | \Psi_i \rangle. \quad (4.51)$$

Expanding the plane wave in eq. (4.50) in spherical harmonics gives

$$\rho(\mathbf{q}) = 4\pi \sum_{JM} i^J Y_{JM}^*(\Omega_q) \langle \Psi_f | C_{JM}(q) | \Psi_i \rangle, \quad (4.52)$$

where

$$C_{JM}(q) = \int d\mathbf{r} j_J(qr) Y_{JM}(\Omega_r) \hat{\rho}(\mathbf{r}) \quad (4.53)$$

is the Coulomb irreducible tensor operator of rank  $J$ . To treat the current density it is useful to define the orthonormal spherical basis

$$\mathbf{e}_{q0} \equiv \mathbf{e}_z = \hat{\mathbf{q}}, \quad \mathbf{e}_{q\pm 1} = \mp (1/\sqrt{2})(\mathbf{e}_x \pm i\mathbf{e}_y). \quad (4.54)$$

Then  $\mathbf{J}(\mathbf{q})$  can be expanded in terms of its spherical components as

$$\mathbf{J}(\mathbf{q}) = \sum_{\lambda=0, \pm 1} J_\lambda(\mathbf{q}) \mathbf{e}_{\mathbf{q}\lambda}^*, \quad J_\lambda(\mathbf{q}) = \mathbf{e}_{\mathbf{q}\lambda} \cdot \mathbf{J}(\mathbf{q}) . \quad (4.55)$$

Current conservation, eq. (2.31), allows us to express the longitudinal ( $\lambda = 0$ ) component in terms of the charge density. For the transverse ( $\lambda = \pm 1$ ) components, introducing the vector spherical harmonics

$$Y_{JJ}^M(\Omega) = \sum_{mm'} (J1mm' | JM) Y_{Jm}(\Omega) e_{m'} , \quad (4.56)$$

and using the identity (see, e.g., eq. (C.14) of ref. [6])

$$e_{\mathbf{q}\lambda} e^{i\mathbf{q}\cdot\mathbf{r}} = -\sqrt{2\pi} \sum_{J \geq 1} i^J \sqrt{2J+1} \{ \lambda j_J(qr) Y_{JJ}^\lambda(\Omega_r) + (1/q) \nabla \times [j_J(qr) Y_{JJ}^\lambda(\Omega_r)] \} , \quad (4.57)$$

one obtains

$$J_\lambda(\mathbf{q}) = -\sqrt{2\pi} \sum_{J \geq 1} i^J \sqrt{2J+1} \langle \Psi_f | [E_{J\lambda}(q) + \lambda M_{J\lambda}(q)] | \Psi_i \rangle , \quad (4.58)$$

where

$$E_{JM}(q) = \frac{1}{q} \int d\mathbf{r} \nabla \times [j_J(qr) Y_{JJ}^M(\Omega_r)] \cdot \hat{\mathbf{J}}(\mathbf{r}) , \quad (4.59)$$

$$M_{JM}(q) = \int d\mathbf{r} j_J(qr) Y_{JJ}^M(\Omega_r) \cdot \hat{\mathbf{J}}(\mathbf{r}) \quad (4.60)$$

are the electric and magnetic irreducible tensor operators of rank  $J$ , respectively.

Under parity operation Coulomb ( $C_J$ ) and electric ( $E_J$ ) multipoles are multiplied by  $(-)^J$  and magnetic multipoles ( $M_J$ ) by  $(-)^{J+1}$ . Thus in elastic scattering parity eliminates the odd Coulomb and electric multipoles and the even magnetic multipoles. Invariance under time reversal also eliminates the even transverse electric multipoles [6]. A further simplification occurs when the initial and final states are eigenstates of the total angular momentum: the interference between the transverse current and the charge is impossible, because the transverse current carries angular momentum  $\pm 1$  along  $\mathbf{q}$  while the Coulomb interaction carries angular momentum 0. The cross section for elastic scattering therefore contains separate contributions from even Coulomb multipoles  $C_J$  and odd magnetic multipoles  $M_J$ . It can be written as

$$d\sigma/d\Omega = \sigma_{NS} [R_L(Q^2) + (\tfrac{1}{2} + \tan^2 \tfrac{1}{2}\theta) R_T(Q^2)] , \quad (4.61)$$

which is the straightforward generalization to a target with arbitrary spin of the Rosenbluth formula (4.41), which holds for spin- $\frac{1}{2}$  particles. The longitudinal and transverse form factors,  $R_L$  and  $R_T$ , contain the separate contributions of the Coulomb and magnetic multipoles, respectively.

For spin-zero targets only  $R_L$  survives as the Fourier transform of the spherically symmetric ground state charge distribution:  $R_L = C_0$ . This was our result in section 4.1 for the scalar particle. The Coulomb quadrupole  $C_2$  appears in  $R_L$  only for target spin  $\geq 1$ . The magnetic dipole  $M_1$  arises for spin- $\frac{1}{2}$  targets and the octupole  $M_3$  only occurs for target spin  $\geq \frac{3}{2}$ . Therefore, for the nucleon only  $C_0$  contributes to  $R_L$  and  $M_1$  to  $R_T$ ;  $C_0$  and  $M_1$  give rise to the form factors  $G_E$  and  $G_M$ , respectively.

For the deuteron, which has spin 1,  $C_0$  and  $C_2$  produce the charge and the quadrupole form factors,  $G_C(Q^2)$  and  $G_Q(Q^2)$  respectively, while  $M_1$  gives the magnetic form factor,  $G_M(Q^2)$ . The corresponding elastic cross section is given by the Rosenbluth formula (4.41), where now [49]

$$A(Q^2) = G_C^2(Q^2) + \frac{8}{9}(Q^2/4M_D)^2 G_Q^2(Q^2) + \frac{2}{3}(Q^2/4M_D)G_M^2(Q^2), \quad (4.62)$$

$$B(Q^2) = \frac{4}{3}(Q^2/4M_D)(1 + Q^2/4M_D)G_M^2(Q^2), \quad (4.63)$$

$M_D$  being the deuteron mass. The magnetic structure function  $B(Q^2)$  has been measured up to  $Q^2 = 2.77(\text{GeV}/c)^2$  [50–52], while measurements of the electric structure function  $A(Q^2)$  extend to momentum transfers as large as  $6(\text{GeV}/c)^2$  [53].

The observed  $B(Q^2)$  is reasonably well described in models taking into account mesonic degrees of freedom in a coupled-channel calculation including  $\Delta\Delta$  channels [54]. An important contribution comes from the  $\rho\pi\gamma$  vertex in the exchange current during photon absorption [55]. In particular, the isoscalar current deduced from the topological properties of the Skyrme lagrangian [56], in which the  $\rho\pi\gamma$  vertex is naturally contained, is quite successful in reproducing  $B(Q^2)$ . The theoretical description of  $A(Q^2)$  suffers from uncertainties due to the effects of meson exchange currents, relativistic corrections and nucleon form factors, which are not well under control in the momentum transfer range above  $1(\text{GeV}/c)^2$ . The situation is different below  $1(\text{GeV}/c)^2$ , where a recent analysis based on very accurate data [57] has significantly improved the agreement between theory and experiment. This is an important result, because in the absence of free-neutron targets,  $A(Q^2)$  provides one of the few methods to infer the neutron electric form factor  $G_E^n(Q^2)$ , which is the least known among the four nucleon electromagnetic form factors. In this analysis the

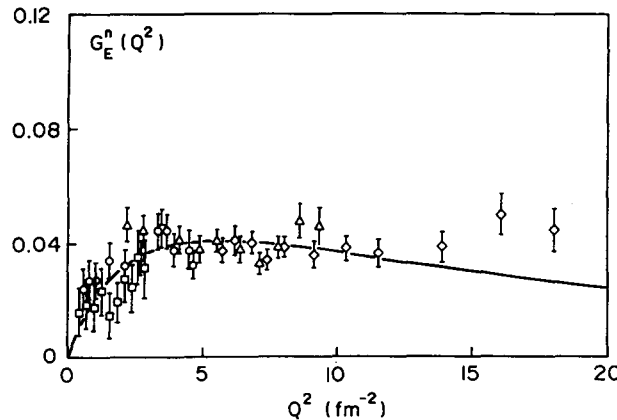


Fig. 6. Electric form factor of the neutron as analyzed in ref. [57].

model dependence of the extracted  $G_E^n(Q^2)$  is limited to a few percent, thus resulting in significantly improved information on  $G_E^n(Q^2)$ . The best fit analysis gives

$$G_E^n(Q^2) = -a\mu_n \tau G_D(Q^2)(1 + b\tau)^{-1}, \quad (4.64)$$

where  $\tau = Q^2/4M^2$  ( $M$  is the nucleon mass),  $G_D(Q^2) = (1 + Q^2/18.23)^{-2}$ , and  $Q^2$  is measured in  $\text{fm}^{-2}$  (fig. 6). The parameters  $a = 1.25 \pm 0.13$  and  $b = 18.3 \pm 3.4$  are obtained with the Paris potential, but similar values are also obtained with the Reid soft-core nucleon–nucleon interaction.

## 5. The hadron tensor in inelastic scattering

The cross section of inelastic electron scattering is obtained from the scattering matrix  $S_{fi}$ , eq. (2.34), and requires an average over the unobserved initial states and a sum over the undetected final states compatible with energy and momentum conservation. The resulting hadronic contribution is derived and discussed in this section.

As in section 3 for the leptonic contribution, it is here convenient to define the hadron tensor

$$W^{\mu\nu} \equiv \bar{\sum}_i \sum_f \int d^3 p_f \delta^{(4)}(p_f - p_i - q) J^\mu J^\nu * , \quad (5.1)$$

where the components  $J^\mu$  of the nuclear operator taken between the initial and final nuclear states, eq. (2.32), contain the relevant nuclear information entering the scattering matrix. Lorentz invariance implies that  $W^{\mu\nu}$  must be a second-rank tensor, because  $J^\mu$  is a four-vector.

When dealing with the spherical basis (2.42) as in eq. (2.45), the hadron tensor is accordingly transformed as follows:

$$W_{\lambda\lambda'} = \bar{\sum}_i \sum_f \int d^3 p_f \delta^{(4)}(p_f - p_i - q) J_\lambda J_{\lambda'}^* = (-)^{\lambda + \lambda'} W_{\mu\nu} \varepsilon_\lambda^\mu \varepsilon_{\lambda'}^\nu * . \quad (5.2)$$

Then the calculation of the cross section involves contraction of the lepton tensor with the hadron tensor. As a result of the general structure of the lepton tensor (see table 1), in general only six independent pieces occur:

$$\begin{aligned} L_{\mu\nu} W^{\mu\nu} &= \sum_{\lambda\lambda'} L_{\lambda\lambda'} W_{\lambda\lambda'} \\ &= L_{00}^0 W_{00} + L_{11}^0 (W_{11} + W_{-1-1}) + L_{01}^0 2 \operatorname{Re}(W_{01} - W_{0-1}) \\ &\quad + L_{1-1}^0 2 \operatorname{Re} W_{1-1} + h L_{01}^h 2 \operatorname{Re}(W_{01} + W_{0-1}) + h L_{11}^h (W_{11} - W_{-1-1}), \end{aligned} \quad (5.3)$$

where advantage has been taken of the hermiticity of  $W^{\mu\nu}$ .

In this section we are interested in the case of inclusive inelastic scattering, i.e. the case where only the scattered electron is detected. This will simplify expression (5.3) considerably. The most general covariant form of the hadron tensor is obtained in terms of the two independent four-vectors of the problem, i.e. the four-momentum transfer  $q^\mu$  and the four-momentum  $p^\mu$  of the target:

$$W^{\mu\nu} = W_S^{\mu\nu} + W_A^{\mu\nu}, \quad (5.4)$$

$$W_S^{\mu\nu} = W_S^{\nu\mu} = -W_1 g^{\mu\nu} + W_2 \frac{1}{M^2} p^\mu p^\nu + W_3 \frac{1}{M^2} q^\mu q^\nu + W_4 \frac{1}{M^2} (p^\mu q^\nu + q^\mu p^\nu), \quad (5.5)$$

$$W_A^{\mu\nu} = -W_A^{\nu\mu} = W'_4 \frac{1}{M^2} (p^\mu q^\nu - q^\mu p^\nu). \quad (5.6)$$

The form factors  $W_i$  are functions of the two scalars which can be formed with  $q^\mu$  and  $p^\mu$ , i.e.,  $q \cdot p$  and  $Q^2$ . Gauge invariance requires that

$$q_\mu W_S^{\mu\nu} = q_\mu W_A^{\mu\nu} = 0. \quad (5.7)$$

Thus

$$-W_1 q^\nu + W_2 \frac{1}{M^2} q \cdot p p^\nu + W_3 \frac{1}{M^2} q^2 q^\nu + W_4 \frac{1}{M^2} (q \cdot p q^\nu + q_\mu^2 p^\nu) = 0,$$

$$W'_4 \frac{1}{M^2} (q \cdot p q^\nu - q_\mu^2 p^\nu) = 0,$$

i.e.,

$$-W_1 + W_3 \frac{1}{M^2} q_\mu^2 + W_4 \frac{1}{M^2} q \cdot p = 0, \quad W_2 \frac{1}{M^2} q \cdot p + W_4 \frac{1}{M^2} q_\mu^2 = 0, \quad W'_4 = 0.$$

Therefore, the antisymmetric part of the hadron tensor vanishes identically,  $W_A^{\mu\nu} = 0$ , and only two of the four form factors in the symmetric part  $W_S^{\mu\nu}$  are independent, say  $W_1$  and  $W_2$ . Inserting

$$W_4 = -W_2 \frac{q \cdot p}{q_\mu^2}, \quad W_3 = W_2 \left( \frac{q \cdot p}{q_\mu^2} \right)^2 + W_1 M^2 \frac{1}{q_\mu^2},$$

into eq. (5.5), the hadron tensor becomes

$$W^{\mu\nu} = W_S^{\mu\nu} = -W_1 \tilde{g}^{\mu\nu} + W_2 \frac{1}{M^2} \tilde{p}^\mu \tilde{p}^\nu, \quad (5.8)$$

$$\tilde{g}^{\mu\nu} = g^{\mu\nu} - \frac{q^\mu q^\nu}{q_\lambda^2}, \quad \tilde{p}^\mu = p^\mu - \frac{q \cdot p}{q_\lambda^2} q^\mu. \quad (5.9)$$

Inserting now expression (5.8) for  $W_{\mu\nu}$  in eq. (5.2) and evaluating  $W_{\lambda\lambda'}$  in the laboratory frame, where  $p^\mu = (M, 0)$  and  $\tilde{p}_\mu \varepsilon_\lambda^\mu = p_\mu \varepsilon_\lambda^\mu$ , one obtains

$$W_{\lambda\lambda'} = \delta_{\lambda\lambda'} [(-)^{\lambda+1} W_1 + \delta_{\lambda 0} W_2 |\mathbf{q}|^2/Q^2]. \quad (5.10)$$

In eq. (5.10) the form factors  $W_{1,2}$  are now functions of  $\omega$  and  $Q^2$ . Contraction of the lepton tensor with the hadron tensor gives the cross section:

$$\frac{d\sigma}{dE' d\Omega} = \sigma_M [W_2(\omega, Q^2) + 2W_1(\omega, Q^2) \tan^2 \frac{1}{2}\theta]. \quad (5.11)$$

Alternatively, one could also separate the longitudinal and transverse contributions of the hadron current. When contracting with the symmetric lepton tensor of eq. (3.13), one has

$$L_{\mu\nu}^0 W^{\mu\nu} = \bar{\sum}_i \sum_f \delta(E_f - E_i - \omega) (4 K_\mu J^\mu K_v J^{v*} - Q^2 J_v J^{v*}), \quad (5.12)$$

where current conservation,  $q_\mu J^\mu = 0$ , has been utilized. Longitudinal (L) and transverse (T) components of  $J^\mu$  can be separated in the expressions  $K_\mu J^\mu$ , with  $q_\mu K^\mu = 0$ , as

$$K_\mu J^\mu = K_0 J_0 - \mathbf{K}_L \cdot \mathbf{J}_L - \mathbf{K}_T \cdot \mathbf{J}_T = (Q^2/|\mathbf{q}|^2) K_0 J_0 - \mathbf{K}_T \cdot \mathbf{J}_T. \quad (5.13)$$

Keeping in mind that  $\bar{\sum}_i \sum_f$  does not allow L-T interference, one finally obtains

$$L_{\mu\nu}^0 W^{\mu\nu} = \bar{\sum}_i \sum_f \delta(E_f - E_i - \omega) \times \{(Q^4/|\mathbf{q}|^4)[(E + E')^2 - |\mathbf{q}|^2] J_0 J_0^* + (4 \mathbf{K}_T \cdot \mathbf{K}_T + Q^2) \mathbf{J}_T \cdot \mathbf{J}_T^*\}. \quad (5.14)$$

Taking advantage of the ultrarelativistic limit one arrives at the following expression for the cross section:

$$\frac{d\sigma}{dE' d\Omega} = \sigma_M \{(Q^4/|\mathbf{q}|^4) R_L(\omega, Q^2) + [Q^2/2|\mathbf{q}|^2 + \tan^2 \frac{1}{2}\theta] R_T(\omega, Q^2)\}, \quad (5.15)$$

$$R_L(\omega, Q^2) = \bar{\sum}_i \sum_f \delta(E_f - E_i - \omega) J_0 J_0^*,$$

$$R_T(\omega, Q^2) = \bar{\sum}_i \sum_f \delta(E_f - E_i - \omega) \mathbf{J}_T \cdot \mathbf{J}_T^*. \quad (5.16)$$

are the longitudinal and the transverse inelastic responses, respectively. Comparison with eq. (5.11) shows that

$$R_T \equiv W_{11} + W_{-1-1} = 2W_1, \quad R_L \equiv \frac{|\mathbf{q}|^2}{Q^2} W_{00} = \frac{|\mathbf{q}|^2}{Q^2} \left( -W_1 + \frac{|\mathbf{q}|^2}{Q^2} W_2 \right). \quad (5.17)$$

Incidentally, eq. (4.61) is recovered from eq. (5.17) in the limit of elastic scattering.

It is also useful to write the cross section (5.15) as follows [3]:

$$\frac{d\sigma}{dE' d\Omega} = \frac{e^2 \pi}{2|\mathbf{q}|} \Gamma [R_T(\omega, Q^2) + 2\varepsilon_L R_L(\omega, Q^2)]. \quad (5.18)$$

In eq. (5.18) the factor

$$\Gamma = \frac{\alpha}{2\pi^2} \frac{E'}{E} \frac{|\mathbf{q}|}{Q^2} \frac{1}{1-\varepsilon} \quad (5.19)$$

can be interpreted as the flux of virtual photons [3], i.e. the number of virtual photons per scattered electron in  $dE' d\Omega$ , and the quantity  $\varepsilon_L$  is the scalar (longitudinal) polarization of the virtual photon, defined in eq. (3.18).

Equation (5.18) clearly shows that separation of the longitudinal and transverse responses can be experimentally achieved by varying the electron kinematics. In a plot of the cross section versus  $\varepsilon_L$  (or  $\varepsilon$ ) at constant  $Q^2$  and  $\omega$ , the slope gives  $R_L$  and the extrapolated intercept with the vertical axis at  $\varepsilon_L = 0$  gives  $R_T$ . Such a Rosenbluth separation is allowed by the linear dependence of the cross section upon  $\varepsilon_L$  in eq. (5.18), which is a direct consequence of two approximations, i.e. one-photon exchange and neglect of Coulomb distortion of the electron waves. Dispersive corrections due to more than one-photon exchanges, although sizeable in some particular cases, are basically small and for many purposes can be neglected [58–60]. In inclusive scattering they are of the order of 1% [58]. On the contrary, the interaction of electrons with the nuclear Coulomb field cannot be neglected. In the components of the nuclear response it introduces a dependence on all the kinematic variables of the incoming and the outgoing electrons, which, in principle, invalidates Rosenbluth separation and makes experimental determination of  $R_L$  and  $R_T$  extremely complicated. Only after experimental cross sections have been corrected for electron distortion effects, can the plane wave Born approximation (PWBA) expression (5.18) be retrieved and can the two response functions still be separated through a Rosenbluth plot. Separation procedures, making use of different kinematics, which are differently affected by Coulomb distortion, emphasize distortion effects, which generally turn out to be sizeable even for light nuclei [61–63]. Moreover, as the major effect of Coulomb distortion is a rotation of the line of the Rosenbluth plot [61–63], alignment of measured cross sections on this plot cannot be taken as a well-founded criterion to ensure the experimental validity of PWBA.

### 5.1. The nuclear current

The nuclear current is often calculated in the impulse approximation (IA). This means that it is considered as a one-body operator with each nucleon individually contributing as if it were free.

Therefore the target current is the sum of terms like the current (4.33) for the Dirac particle with internal structure discussed in section 4.3. However, the current given in eq. (4.33),

$$J^\mu = \frac{M}{\sqrt{E_i E_f}} \bar{u}_f \left( \gamma^\mu F_1(Q^2) + i\sigma^{\mu\nu} q_\nu \frac{\kappa}{2M} F_2(Q^2) \right) u_i , \quad (5.20)$$

and the one obtained in terms of the Gordon decomposition (4.30), i.e.,

$$J^\mu = \frac{M}{\sqrt{E_i E_f}} \bar{u}_f \left( \gamma^\mu [F_1(Q^2) + \kappa F_2(Q^2)] - (p_i^\mu + p_f^\mu) \frac{\kappa}{2M} F_2(Q^2) \right) u_i , \quad (5.21)$$

are equivalent only on-shell, while nucleons in the nucleus are off-shell. When going off-shell one must decide which form factors and spinors to use. The choice is not so obvious and ambiguities could arise. In particular, an off-shell extrapolation of the Rosenbluth formula for electron–nucleon scattering obtained either with the current (5.20) ( $\sigma_2^{cc}$ ) or with the current (5.21) ( $\sigma_1^{cc}$ ) has been studied in ref. [64] taking advantage of the fact that  $q^\mu$  appears explicitly in eq. (5.20), but not in eq. (5.21). The factor  $\omega$  in (5.20) was replaced in eq. (5.21) by  $\bar{\omega} = E_f - \bar{E}$ , where  $\bar{E} = (|\mathbf{p}_i|^2 + M^2)^{1/2}$ . The degree to which one is off-shell is given by the difference between  $\bar{E}$  and  $E_f - \omega = M - E_s - E_r$ , where  $E_s$  is the separation energy required to extract a nucleon from the target and  $E_r$  is the energy of the recoiling residual nucleus. Increasing either  $|\mathbf{p}_i|$  or  $E_s$  clearly brings one off-shell. As expected the ambiguities increase both with increasing initial momentum and with separation energy. However, the differences between the results obtained with  $\sigma_1^{cc}$  and  $\sigma_2^{cc}$  are small in the typical kinematic conditions of experiments that have been performed and tend to become smaller with higher electron energy.

The use of a relativistic expression of the nuclear current inside matrix elements requires that also the nuclear states are treated relativistically. In fact, some effort is presently made to describe the nucleus with relativistic wave functions, e.g. within the frame of a Dirac phenomenology [65, 66], a Dirac–Hartree method [67, 68] or of scalar–vector ( $\sigma\omega$ ) models [69]. However, the bulk of information on nuclear structure comes from nonrelativistic many-body theories. Therefore the problem arises of matching large momentum and energy transfer in electron–nucleus scattering with the nonrelativistic description of the target structure. The problem can be solved by the Foldy–Wouthuysen (FW) canonical transformation [70], which decouples the Dirac equation into two two-component equations: one reduces to the Pauli description in the nonrelativistic limit; the other one describes negative energy states. The decoupling is accomplished by removing from the equation all operators which couple the large to the small components of the wave function. Such operators are called “odd” in ref. [1]; operators which do not couple large and small components are called “even”.

One starts from the Dirac equation for a nucleon of charge  $e_N$  under the action of the Møller potential of the electron,

$$[(\not{p} - e_N F_1 A) - (e_N/4M) \kappa F_2 \sigma^{\mu\nu} F_{\mu\nu} - M] \Psi = 0 , \quad (5.22)$$

$$F_{\mu\nu} = \partial_\mu A_\nu - \partial_\nu A_\mu . \quad (5.23)$$

Equivalently, one can rewrite eq. (5.22) in a way where the odd and even operators are made explicit,

$$(i\partial/\partial t - H)\Psi = 0, \quad (5.24)$$

$$\begin{aligned} H = & -i\mathbf{a}\cdot\nabla + e_N F_1 \Phi - e_N F_1 \mathbf{a}\cdot\mathbf{A} + \frac{e_N}{2M} \kappa F_2 \beta i\mathbf{a}\cdot\mathbf{E} - \frac{e_N}{2M} \kappa F_2 \beta \boldsymbol{\sigma}\cdot\mathbf{H} + \beta M \\ & \equiv \beta M + \mathcal{O} + \mathcal{E}, \end{aligned} \quad (5.25)$$

where the odd operator  $\mathcal{O}$  is the sum of the terms containing  $\mathbf{a}$ . One has

$$\beta\mathcal{O} = -\mathcal{O}\beta, \quad \beta\mathcal{E} = \mathcal{E}\beta, \quad (5.26)$$

for the odd and even parts of the hamiltonian, respectively. In order to eliminate the odd part  $\mathcal{O}$  a unitary transformation is introduced,

$$\Psi \rightarrow \Psi' = e^{iS} \Psi, \quad H \rightarrow H' = e^{iS} H e^{-iS}. \quad (5.27)$$

According to ref. [70] the FW transformation is

$$S = -i\frac{1}{2M} \beta\mathcal{O}. \quad (5.28)$$

However, care must be paid to the fact that, in contrast with the free case of the Dirac equation, it is not possible to completely eliminate the odd operator from the hamiltonian (5.25) because it is time dependent through the fields appearing in it. The formal expansion

$$e^{iS}(H - i\partial/\partial t)e^{-iS} = H - \dot{S} + \sum_{n=1}^{\infty} \frac{i^n}{n!} [S, [S, \dots [S, H - (1/(n+1))\dot{S}] \dots]] \quad (5.29)$$

must be truncated at some order  $n$  which will correspond to a nonrelativistic expansion of the transformed hamiltonian in a power series in  $M^{-1}$ . At that order the final result will be obtained by successively applying  $n+1$  times the FW transformation. This was done through second order in ref. [71] and through fourth order in ref. [72]. In momentum space for the charge operator  $\rho^{(n)}$  one has

$$\begin{aligned} \rho^{(0)} &= F_1, \quad \rho^{(1)} = 0, \\ \rho^{(2)} &= -\frac{1}{8M^2} (F_1 + 2\kappa F_2) (\mathbf{P}^2 + i\boldsymbol{\sigma}\cdot\mathbf{P}\times\mathbf{q}), \\ \rho^{(3)} &= 0, \\ \rho^{(4)} &= \frac{1}{32M^4} (\frac{1}{24} F_1 + \kappa F_2) (\mathbf{P}^2 + \mathbf{q}^2) (\mathbf{Q}^2 + i\boldsymbol{\sigma}\cdot\mathbf{P}\times\mathbf{q}) \\ &+ \frac{17}{768M^4} F_1 (\mathbf{P}^2 + \mathbf{q}^2) (\mathbf{q}^2 + i\boldsymbol{\sigma}\cdot\mathbf{P}\times\mathbf{q}) + \frac{15}{384M^4} F_1 (\mathbf{P}\cdot\mathbf{q})^2, \end{aligned} \quad (5.30)$$

where  $\mathbf{P} = \mathbf{p}_i + \mathbf{p}_f$ . The contribution  $\rho^{(2)}$  is the so-called Darwin–Foldy term [73], which may be attributed to the Zitterbewegung. For the current operator  $\mathbf{J}^{(n)}$  one has

$$\mathbf{J}^{(0)} = 0 ,$$

$$\mathbf{J}^{(1)} = \frac{1}{2M} F_1 \mathbf{P} + \frac{1}{2M} (F_1 + \kappa F_2) i\boldsymbol{\sigma} \times \mathbf{q} ,$$

$$\mathbf{J}^{(2)} = -\frac{1}{8M^2} (F_1 + 2\kappa F_2) i\omega \boldsymbol{\sigma} \times \mathbf{P} ,$$

$$\mathbf{J}^{(3)} = -\frac{1}{16M^3} [\kappa F_2 Q^2 + F_1 (\mathbf{P}^2 + \mathbf{q}^2)] (\mathbf{P} + i\boldsymbol{\sigma} \times \mathbf{q}) - \frac{1}{16M^3} \kappa F_2 i\boldsymbol{\sigma} \cdot \mathbf{P} \mathbf{P} \times \mathbf{q} ,$$

$$\begin{aligned} \mathbf{J}^{(4)} = & \frac{1}{32M^4} \left( \frac{1}{24} F_1 + \kappa F_2 \right) i\omega \boldsymbol{\sigma} \times \mathbf{P} (\mathbf{P}^2 + \mathbf{q}^2) \\ & + \frac{17}{768M^4} F_1 \omega (\mathbf{P}^2 + \mathbf{q}^2) (\mathbf{q} + i\boldsymbol{\sigma} \times \mathbf{P}) + \frac{15}{384M^4} F_1 \omega \mathbf{P} \cdot \mathbf{q} (\mathbf{P} + i\boldsymbol{\sigma} \times \mathbf{q}) . \end{aligned} \quad (5.31)$$

The contribution  $\mathbf{J}^{(1)}$  is the well-known sum of convective and spin-magnetic currents.

The effects of the nonrelativistic approximation can be investigated [72] by comparing the Rosenbluth formula with the free electron–nucleon scattering cross section obtained with the nonrelativistic current to order  $n$ . This can be done in terms of two invariant parameters, as the two-body scattering amplitude depends on two independent combinations of the momenta involved. A suitable choice is given by  $Q^2$  and  $\kappa^2 = (k - p_i)^2$ . In elastic scattering one has  $\kappa^2 = \kappa'^2 = (k' - p_f)^2$ . In fig. 7 the curves show the percentage deviation from the Rosenbluth

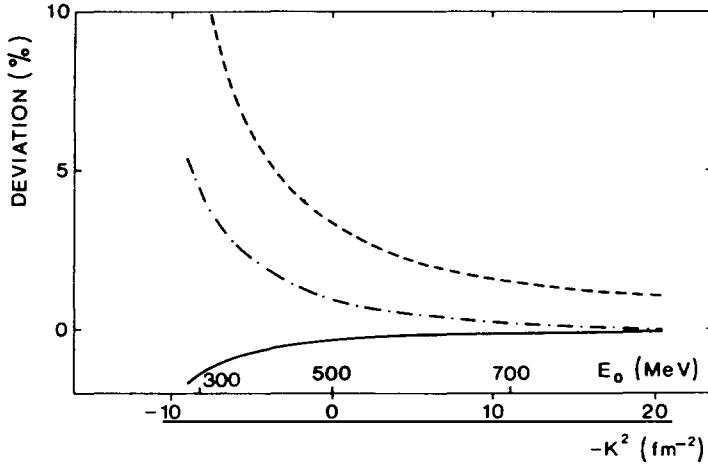


Fig. 7. The percentage deviations of the nonrelativistic free electron–proton scattering cross sections from the Rosenbluth formula versus the relative four-momentum  $\kappa^2$ , and the incident electron energy  $E_0$  with the initial proton at rest. The dashed line refers to the second-order approximation in  $Q/M$ , the dot-dashed line to the third-order one and the solid line to the fourth-order one (from ref. [72]).

formula of the nonrelativistic electron–proton cross section through different orders versus  $\kappa^2$ , for a fixed  $Q^2 = 4.82 \text{ fm}^{-2}$ . The shape of the curves does not change with  $Q^2$ , while their size is strongly dependent on  $Q^2$ . The large variation at  $\kappa^2 > 0$  corresponds to decreasing values of the squared scattering amplitude. Provided the incident electron energy  $E_0$  is larger than 500 MeV, the percentage deviation of the nonrelativistic result through second order does not exceed 5–10% up to  $Q = 2.5 \text{ fm}^{-1}$ , consistently with the claim of ref. [71]. The results through third and fourth order approach the exact result from the opposite side. Thus the approximation through fourth order remains within 5–10% up to  $Q \simeq 3.5 \text{ fm}^{-1}$ .

The off-shell behaviour can also be compared with the extrapolated Rosenbluth formula. In order to avoid ambiguities arising from whether the total electron–proton energy is calculated in the initial state or in the final state, an intermediate prescription can be adopted, where the total energy is averaged over the initial and the final state. This amounts to describing the bound initial proton as a free particle with an effective mass. The off-shell scattering amplitude depends on three independent invariants  $Q^2$ ,  $\kappa^2$  and  $\kappa'^2$ , as in this case  $\kappa^2 \neq \kappa'^2$ . The deviation of  $\kappa'^2$  from  $\kappa^2$  is a measure of the off-shell degree. Figure 8 shows the percentage deviation of the extrapolated Rosenbluth formula from the nonrelativistic cross section at fourth order, for values of  $Q^2$  and  $\kappa'^2$  fixed at  $4.82 \text{ fm}^{-2}$  and  $-1.49 \text{ fm}^{-2}$ , respectively. The deviations of the second- and third-order cross sections are also given. The shape of the curves does not change in a large range of  $Q^2$  and  $\kappa'^2$ . Deviations are within 5% in a large range of kinematic variables corresponding to the typical experimental situation explored with present facilities in (e, e'p) reactions [72].

Going beyond the IA one has also to consider two-body currents produced by meson exchanges. In dealing with electromagnetic processes the gauge invariance of the underlying lagrangian and its consequences, such as the continuity equation, are important issues. In order to ensure current conservation two-body currents must be consistently derived from the basic nucleon–nucleon interaction [74]. This program has, however, practical limitations and has been followed only in some specific cases (see, e.g., ref. [75]) or within simplified models such as the relativistic Fermi gas (for a recent discussion, see ref. [76]). Starting from a relativistic description involving a gauge

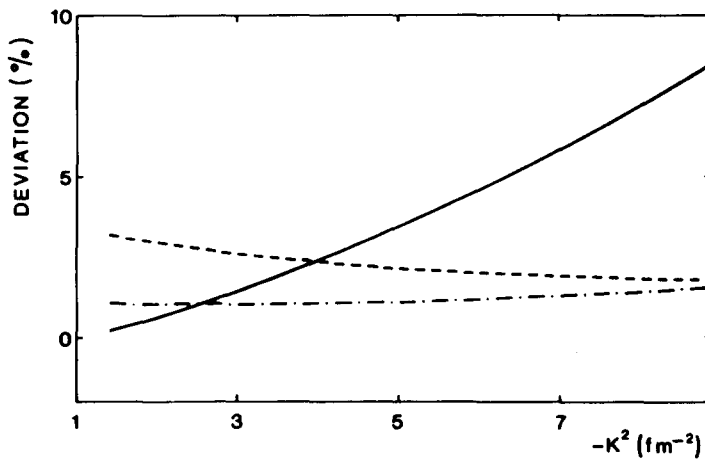


Fig. 8. The percentage deviation of the free electron–proton scattering cross section from the nonrelativistic formula correct through fourth order versus the initial relative four-momentum  $\kappa^2$ , calculated in off-shell kinematics. The solid line refers to the relativistic cross section. The dashed (dot-dashed) line refers to the nonrelativistic second- (third-)order approximation (from ref. [72]).

invariant, covariant lagrangian containing only nucleons and pions, the continuity equation is valid at the level of an operator equation, provided pion exchange currents are present together with pionic correlations in the dynamics originating from the one-pion exchange potential. This situation is not necessarily achieved in a many-body framework with model wave functions, where usually only low order terms in a nonrelativistic expansion are retained. Thus a problem of consistency arises from the dual role played by pions in the nuclear current and dynamics.

In order to obtain a nonrelativistic two-body current a natural scale can be identified with  $Q/2M$ . On the other hand, in electromagnetic interactions a new scale emerges essentially related to the large anomalous magnetic moment of the nucleon [76]. Therefore,  $\mu_N Q/2M$  ( $\mu_N$  being the nucleon magnetic moment) must also be considered and combinations like  $(Q^2/4M^2)G_M^2$  must be treated as being of the same order as  $G_E^2$ , in contrast to making a naive expansion in powers of  $M^{-1}$ . A consistent inclusion of correlations in a relativistic Fermi gas [76] shows that the approximation of truncating at the order  $(q/2M)^2$  turns out to be sufficiently reliable for the inclusive  $(e, e')$  response at momentum transfers up to about  $1 \text{ GeV}/c$ . At the lower momenta, where data for the exclusive  $(e, e'p)$  reaction are available, one then expects that the expansion in powers of  $M^{-1}$  can be safely truncated to second order.

Although in principle one can construct nonrelativistic interaction currents which satisfy current conservation and permit the use of different electromagnetic form factors for the pion and the nucleon [77], such a program has not yet been developed for complex nuclei.

Expressions for the two-body current matrix elements can be derived from the chirally invariant effective lagrangian with pseudovector coupling of ref. [78]. In momentum space representation they are obtained by a nonrelativistic reduction of the lowest order Feynman diagrams with one-pion exchange and/or isobar excitation in the nucleon intermediate state [79] (fig. 9). To order  $1/M^2$ , the pair current  $j^p$  vanishes identically, and the currents due to the pion-in-flight diagram ( $j^\pi$ ) and to the contact diagrams ( $j^c$ ) coincide in this approximation with the result obtained in

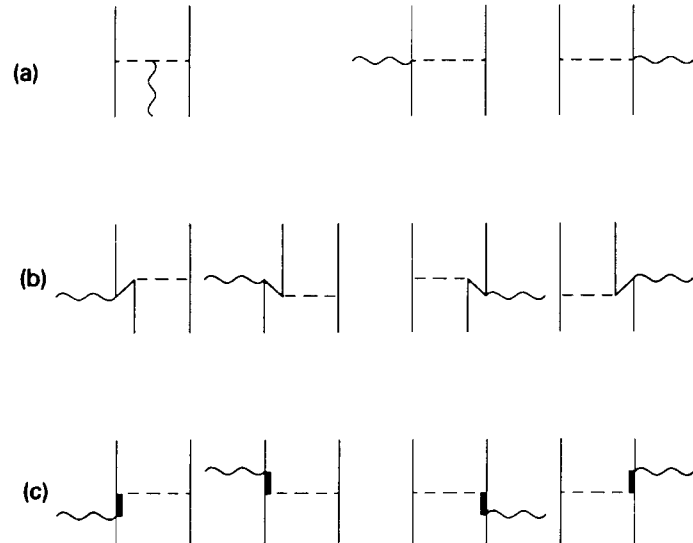


Fig. 9. Contributions to the two-body current from meson exchange and isobar excitation in the intermediate state. (a) The pion-in-flight and the two contact terms; (b) the pair current; (c) isobar contributions.

refs. [80, 81] with pseudoscalar coupling, i.e.,

$$\mathbf{j}^\pi(\mathbf{k}_1, \mathbf{k}_2) = -i \frac{f^2}{\mu^2} G^V(Q^2) [\boldsymbol{\tau}^{(1)} \times \boldsymbol{\tau}^{(2)}]_3 \frac{\boldsymbol{\sigma}^{(1)} \cdot \mathbf{k}_1}{\mu^2 + k_1^2} \frac{\boldsymbol{\sigma}^{(2)} \cdot \mathbf{k}_2}{\mu^2 + k_2^2} (\mathbf{k}_2 - \mathbf{k}_1), \quad (5.32)$$

$$\mathbf{j}^c(\mathbf{k}_1, \mathbf{k}_2) = -i \frac{f^2}{\mu^2} G^V(Q^2) [\boldsymbol{\tau}^{(1)} \times \boldsymbol{\tau}^{(2)}]_3 \left( \boldsymbol{\sigma}^{(1)} \frac{\boldsymbol{\sigma}^{(2)} \cdot \mathbf{k}_2}{\mu^2 + k_2^2} - \boldsymbol{\sigma}^{(1)} \frac{\boldsymbol{\sigma}^{(2)} \cdot \mathbf{k}_1}{\mu^2 + k_1^2} \right), \quad (5.33)$$

$$\mathbf{j}^p(\mathbf{k}_1, \mathbf{k}_2) = 0. \quad (5.34)$$

Here,  $\mu$  is the pion mass,  $\mathbf{k}_1$  and  $\mathbf{k}_2$  are the momenta transferred to the nucleons, and  $f^2/4\pi = 0.08$ . According to ref. [74] and in agreement with ref. [79], at the one-meson exchange level here considered, all terms are multiplied by the same form factor to ensure current conservation. This is the origin of the isovector electromagnetic form factor  $G^V = 2F_1^V$  appearing in eqs. (5.32) and (5.33), while no pion form factor is included here.

The current corresponding to diagrams with intermediate isobar configurations is

$$\begin{aligned} \mathbf{j}^\Delta(\mathbf{k}_1, \mathbf{k}_2) = & -i \frac{\kappa^* h f}{3 M \mu^2} F(Q^2) \mathbf{q} \times \left[ 2 M_1 \tau_3^{(1)} \mathbf{k}_1 \frac{\boldsymbol{\sigma}^{(1)} \cdot \mathbf{k}_1}{\mu^2 + k_1^2} + 2 M_1 \tau_3^{(2)} \mathbf{k}_2 \frac{\boldsymbol{\sigma}^{(2)} \cdot \mathbf{k}_2}{\mu^2 + k_2^2} \right. \\ & \left. + M_2 [\boldsymbol{\tau}^{(1)} \times \boldsymbol{\tau}^{(2)}]_3 \left( (\mathbf{k}_2 \times \boldsymbol{\sigma}^{(1)}) \frac{\boldsymbol{\sigma}^{(2)} \cdot \mathbf{k}_2}{\mu^2 + k_2^2} - \frac{\boldsymbol{\sigma}^{(1)} \cdot \mathbf{k}_1}{\mu^2 + k_1^2} (\mathbf{k}_1 \times \boldsymbol{\sigma}^{(2)}) \right) \right], \end{aligned} \quad (5.35)$$

$$M_1 = \frac{2 M_\Delta + 3 M}{M_\Delta^2 - M^2}, \quad M_2 = \frac{2 M_\Delta + M}{M_\Delta^2 - M^2}, \quad (5.36)$$

where  $M_\Delta = 1232$  MeV is the isobar mass. The constants  $h^2 = 0.290$  and  $\kappa^* = 5.0$  were taken from ref. [78]. The dipole form factor

$$F(Q^2) = [1 + Q^2/(855 \text{ MeV})^2]^{-2} \quad (5.37)$$

takes into account the electromagnetic form factor of the isobar which corresponds to the isovector Sachs form factor  $G_M^V$  used in the static quark model [80, 81]. With the above values of the constants  $h^2$  and  $\kappa^*$ , at  $Q^2 = 0$  the strength of  $j^\Delta$  is larger by  $\sim 50\%$  than the corresponding strength in the static quark model.

## 5.2. Nuclear response in inclusive inelastic scattering

The nuclear response in inclusive electron scattering is dominated by quasi-free processes. In fact the  $(e, e')$  cross section exhibits a universal behaviour for different nuclei and is characterized by two large, broad peaks, associated with direct ejection of fast nucleons from the nucleus (the quasi-elastic peak) and with the quasi-free excitation of  $\Delta$  isobars (the  $\Delta$  peak), appearing at approximately the energy loss for elastic electron–nucleon scattering and for  $\Delta$  production from unbound nucleons.

The  $\Delta$  peak is broader than the quasi-elastic (QE) peak and has the same shape for all the nuclei which have been experimentally considered [82, 83]. In comparison with the free nucleon case, it is broadened by Fermi motion by an additional width beyond the natural  $\Delta$ -decay width (115 MeV), and the location of the apparent  $\Delta$  centroid linearly depends on  $Q^2$ , being shifted to lower energy loss at low  $Q^2$  and to higher invariant mass for  $Q^2 \gtrsim 0.4$  (GeV/c) $^2$  than for the nucleon, where it is independent of  $Q^2$ .

The quasi-elastic peak is also broadened by Fermi motion. Its width is directly proportional to the Fermi momentum  $k_F$ . As the area under the peak is essentially the same, the peak cross section per nucleon is inversely proportional to its width. The peak location,  $\omega_{QE} = |\mathbf{q}|^2/2M + \bar{\epsilon}$ , is shifted from the nucleon scattering value by a quantity determined by the average binding energy  $\bar{\epsilon}$  of the nucleons. Such a simple interpretation in terms of the nuclear Fermi gas model was able to provide a remarkably accurate description of the cross section in the QE region [84].

However, this same model is not able to simultaneously describe QE longitudinal and transverse responses, whose Rosenbluth separation has been experimentally achieved on a variety of nuclei and over a large range of momentum transfers [85–96] (see also ref. [48]). Indeed, although the position and size of the transverse response are reasonably described, the longitudinal response displays a different shape and its size appears considerably quenched with respect to the prediction of the Fermi gas model (fig. 10). This means that the theoretical analysis of the nuclear response for inclusive electron scattering is much more complex than originally inferred from the success of the Fermi gas results. A more sophisticated treatment is required, which provides a severe test both of nuclear structure description and of the reaction mechanism.

Only the diagonal elements of the hadronic tensor contribute to the inclusive response. In principle they can be expressed in terms of the Green function  $G$  related to the total nuclear hamiltonian or, equivalently, of the polarization propagator  $\Pi$  [97], as

$$W^{\mu\mu}(\omega, Q^2) = -(1/\pi) \text{Im} \langle \Psi_i | J^{\mu\dagger} G(\omega + E_0) J^\mu | \Psi_i \rangle = -(1/\pi) \text{Im} \Pi^{\mu\mu}(\omega, Q^2). \quad (5.38)$$

In this form the hadronic tensor contains the full  $A$ -body propagator of the nuclear system, consisting of nucleons interacting with realistic potentials. As such, it is an extremely complicated object, whose evaluation represents a prohibitive task. Only an approximate treatment allows one

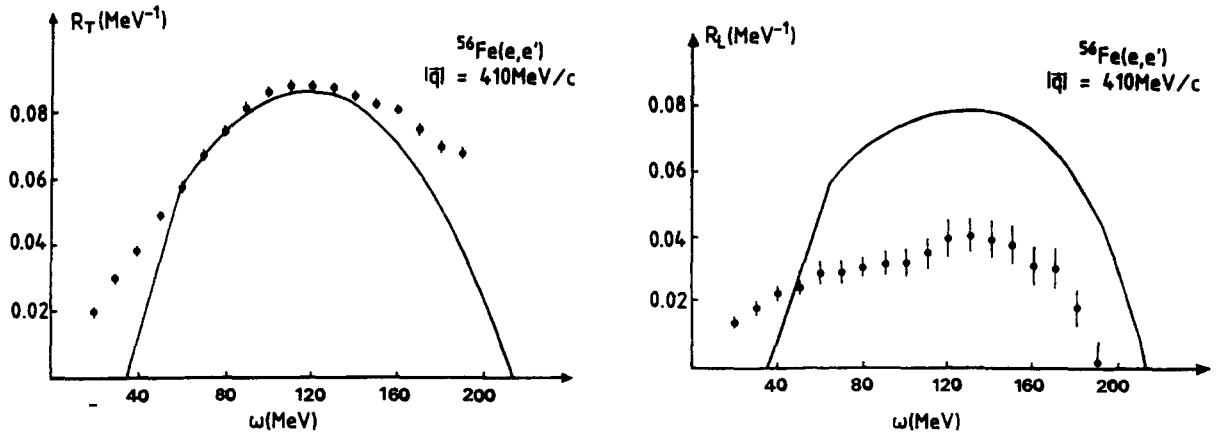


Fig. 10. Longitudinal and transverse response function in inclusive electron scattering off  $^{56}\text{Fe}$ . Solid lines are results of Fermi gas calculations (from ref. [89]).

to reduce the problem to a tractable form. In the simplest case of a noninteracting Fermi gas, the intermediate excited states are particle-hole (p-h) states and the polarization propagator simply reduces to the Lindhard function [97]

$$\begin{aligned} \Pi^{(0)}(\omega, Q^2) = 4 \int \frac{d\mathbf{k}}{(2\pi)^3} \Theta(k_F - k) \Theta(|\mathbf{q} + \mathbf{k}| - k_F) \\ \times \left( \frac{1}{\omega - \omega_{\mathbf{q}+\mathbf{k}} + \omega_k + i\epsilon} - \frac{1}{\omega + \omega_{\mathbf{q}+\mathbf{k}} - \omega_k - i\epsilon} \right), \end{aligned} \quad (5.39)$$

whose imaginary part gives the shape of the QE peak in fig. 10.

The transverse response is dominated by the spin-magnetic current, which is proportional to  $\kappa^V F_2^V(e/2M)\tau_3\sigma \times \mathbf{q}$ . Therefore  $R_T$  is governed by isovector spin-isospin ( $\sigma, \tau$ ) excitations, produced in the random phase approximation (RPA) framework by the p-h force  $V_{ph}^{(\sigma, \tau)}$ , which is derived from  $\rho$ -meson exchange [98, 99]. As a result, the transverse response for nuclear matter is proportional to the imaginary part of the universal response function  $\Pi(\omega, Q^2)$ , which describes the bulk properties of nuclear matter, i.e. [98, 99],

$$R_T(\omega, Q^2) = -\frac{6\pi |\mathbf{q}|^2}{k_F^3 2M} \{Z[G_M^p(Q^2)]^2 + N[G_M^n(Q^2)]^2\} \text{Im } \Pi(\omega, Q^2), \quad (5.40)$$

$$\text{Im } \Pi(\omega, Q^2) = \frac{\text{Im } \Pi^{(0)}(\omega, Q^2)}{[1 - V_{ph}^{(\sigma, \tau)}(\omega, Q^2) \text{Re } \Pi^{(0)}(\omega, Q^2)]^2 + [V_{ph}^{(\sigma, \tau)}(\omega, Q^2) \text{Im } \Pi^{(0)}(\omega, Q^2)]^2}. \quad (5.41)$$

This universal behaviour of the transverse response is indeed confirmed by observation (fig. 11) and a theoretical description based on infinite nuclear matter can reasonably account for the data when also subnuclear degrees of freedom, such as meson exchange currents (MEC) and isobar excitations together with 2p-2h states are included [99] (fig. 12).

A similar RPA theory of spin-isospin nuclear response, subsequently developed for finite nuclei [100], gives also good agreement with the  $R_T$  data of ref. [87].

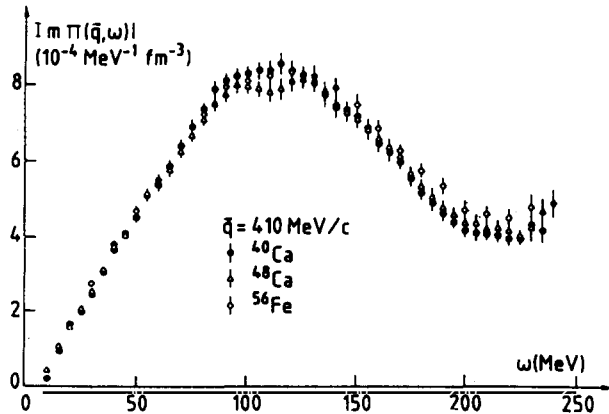


Fig. 11. Inclusive response function  $\text{Im } \Pi$  of eq. (5.40) (from ref. [89]).

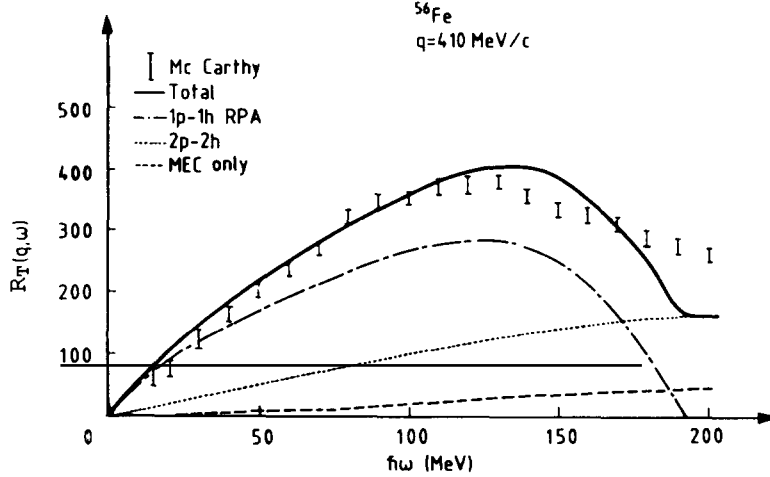


Fig. 12. The separated transverse response in  $^{56}\text{Fe}$  at  $q = 410 \text{ MeV}/c$  as a function of  $\hbar\omega$ . The dot-dashed line is the 1p-1h RPA response; the dotted line is the global 2p-2h response, the dashed line its contribution from the two-body current alone; and the continuous line represents the total 1p-1h, 2p-2h transverse response (from ref. [99]).

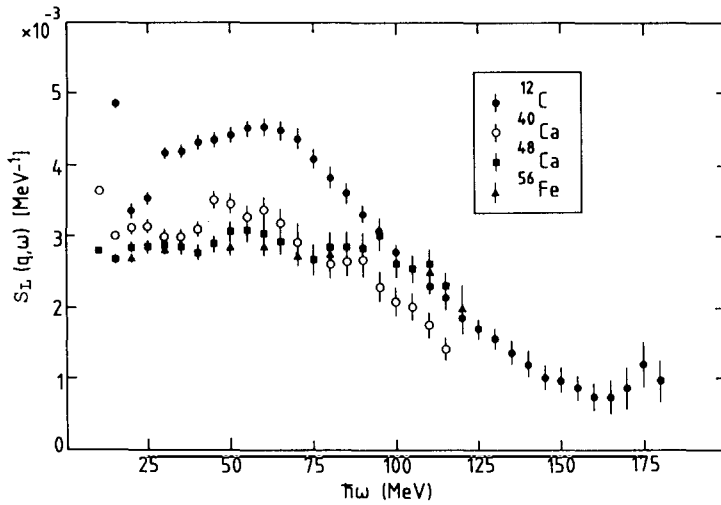


Fig. 13. Longitudinal response (divided by  $Z$ ) in inclusive electron scattering off nuclei at  $|q| = 300 \text{ MeV}/c$  (from ref. [101]).

On the other hand, and especially at low momentum transfer, the longitudinal response exhibits large collective effects [101, 102] (fig. 13). Collectivity acts differently in the isoscalar ( $\tau = 0$ ) and in the isovectors ( $\tau = 1$ ) channels, since it tends to concentrate their strength in different energy domains. It is also significantly associated with the nuclear surface thus producing different responses for different nuclei, which makes a nuclear matter description inappropriate. Although the electrons are actually exploring the whole nuclear volume, the surface character is given by the nature of the isoscalar p-h force, which is somewhat repulsive in the nuclear interior, but becomes strongly attractive at the surface in the  $\tau = 0$  channel. The corresponding response is therefore softened and enhanced, whereas the response due to the  $\tau = 1$  channel is concentrated at higher  $\omega$  [101].

Extensive calculations have been carried out for specific nuclei, in order to take into account ph correlations, in the Tamm–Dancoff or RPA framework [103–105]. These calculations are successful in improving the description of the longitudinal response at low momentum transfers, but at higher momenta ( $q \gtrsim 400$  MeV/c) they only give a small effect, which cannot account for the observed quenching of  $R_L$ . A similar quenching of  $R_L$  is obtained in the calculation of the dynamic structure function of nuclear matter, where realistic interactions and an orthonormalized correlated basis are considered, in an approximation in which only correlated 1p–1h states are retained and 2p–2h excitations are included via the optical potential [106].

Various more or less exotic approaches have been proposed as an explanation of the observed quenching of  $R_L$ . One approach invokes an effective increase in the radius of the nucleon in the nuclear medium (swollen nucleon), resulting from partial deconfinement of the quarks inside the nucleon embedded in the nuclear environment [107–112] (see also ref. [48]). The increased nucleon size modifies the nucleon form factors and reduces  $R_L$ . Other calculations attempt to improve agreement with the data by including relativistic [113] and off-shell [114] effects. Also relativistic  $\sigma$ – $\omega$ – $\rho$  models within the framework of quantum hadrodynamics and the RPA scheme have been used to calculate  $R_L$  and  $R_T$  [115–118]. Although these models reduce the discrepancy between theory and experiment, they generally fail to reproduce both response functions. Thus so far a consistent and satisfactory description of the data for both responses over the full range of the available data has not yet been achieved.

An important mechanism, which leads to a reduction of the QE peak cross section, or equivalently to a redistribution of the strength, and which should be carefully considered before advocating other possible explanations, is represented by nuclear final state interactions (FSI). This effect is of fundamental relevance in exclusive ( $e, e'p$ ) reactions, whose experimental cross sections are fairly well described by a treatment based on the distorted wave impulse approximation (DWIA) (see section 6.4). However, the absorption produced in a given final channel by the imaginary part of the optical potential, which is appropriate for the exclusive process, seemed inconsistent for the inclusive process, where all the allowed final channels contribute and the total flux must be conserved. This resulted at first in calculations where FSI were simply ignored or included by means of a real optical potential.

A proper description of FSI for inclusive electron scattering is provided by the Green function approach [119–121], where, under suitable approximations, the components of the nuclear response are written in terms of the optical model Green function. In ref. [119] this result is derived by arguments based on multiple scattering theory, whereas in refs. [120, 121] the same result is obtained by means of Feshbach projection operator techniques. Then, confining to protons, the matrix element in eq. (5.38) is decomposed into the sum of various contributions,

$$\text{Im} \langle \Psi_i | J^{\mu\dagger} G J^\mu | \Psi_i \rangle \sim Z \sum_n \text{Im} \langle \Psi_i | j_1^{\mu\dagger} G_n j_1^\mu | \Psi_i \rangle , \quad (5.42)$$

where

$$G_n = P_n G P_n, \quad P_n = \int |\mathbf{r}, n\rangle d\mathbf{r} \langle \mathbf{r}, n| , \quad (5.43)$$

is the projection of the full Green function onto the channel subspace spanned by the orthonormalized set of states  $|\mathbf{r}, n\rangle$  corresponding to a proton at the point  $\mathbf{r}$  and to the residual

$(A - 1)$ -nucleus in the state  $|n\rangle$ . A similar expression occurs for neutrons.  $G_n$  is the Green function associated with the Feshbach optical model hamiltonian, which describes elastic scattering of a nucleon by an  $(A - 1)$ -nucleus in the state  $|n\rangle$ . The sum over  $n$  includes discrete eigenstates and resonances embedded in the continuum [121].

The approximation in eq. (5.42) has been derived neglecting nondiagonal terms  $P_n G P_m$  and retaining only the one-body part  $j_1^\mu$  of the current operator. It is basically a single-particle approach, where one assumes that  $j_1^\mu$  connects the initial state  $|\Psi_i\rangle$  only with states in the channel subspace spanned by the vectors  $|\mathbf{r}, n\rangle$ , i.e., with states asymptotically corresponding to single-nucleon knockout. However, not only these states, but all of the allowed final states are correctly included in the inclusive response, as  $G_n$  contains the full propagator  $G$  and these states are taken into account by the optical potential.

A similar philosophy motivated the extension of the RPA to second RPA (SRPA), which includes multiple-nucleon knockout by calculating all particle lines in the continuum via the optical potential [105, 106]. Indeed, for high values of  $q$ , where the effect of long range correlations becomes negligible, the Green function approach and the SRPA should converge [120].

The complexity of a practical calculation of  $G_n$  can be avoided by means of its spectral representation, based on a biorthogonal expansion in terms of the eigenfunctions of the Feshbach hamiltonian [121]. In the single-particle representation one obtains

$$W^{\mu\mu}(\omega, Q^2) = \sum_n \left( \operatorname{Re} T_n^{\mu\mu}(E_f) + \frac{1}{\pi} \mathcal{P} \int_0^{+\infty} dE \frac{1}{E_f - E} \operatorname{Im} T_n^{\mu\mu}(E) \right), \quad (5.44)$$

where  $\mathcal{P}$  denotes the principal value,  $E_f$  is the energy of the final state and

$$T_n^{\mu\mu}(E) = \lambda_n \int d\mathbf{r} \tilde{\chi}_E^{(-)*}(\mathbf{r}) j^\mu(\mathbf{r}) \phi_n(\mathbf{r}) \left( \int d\mathbf{r} \chi_E^{(-)*}(\mathbf{r}) j^\mu(\mathbf{r}) \phi_n(\mathbf{r}) \right)^*. \quad (5.45)$$

In eq. (5.45)  $j^\mu$  is the single-particle current,  $\tilde{\chi}_E^{(-)}$  and  $\chi_E^{(-)}$  are eigenfunctions belonging to the eigenvalue  $E$  of the single-particle optical potential and of its hermitian conjugate, respectively, and  $\lambda_n$  is the spectral strength [122] of the hole state  $\phi_n$ , which is the normalized overlap integral between  $|\Psi_i\rangle$  and  $|n\rangle$ .

The integrals in eq. (5.45) are of the same kind as those obtained in the DWIA treatment of the exclusive ( $e, e'p$ ) reaction [see eq. (6.20), section 6.1]. However, now both eigenfunctions  $\tilde{\chi}_E^{(-)}$  and  $\chi_E^{(-)}$  must be considered. It is conceptually interesting to observe that the components of the inclusive response, although containing eigenfunctions of a complex potential, are not affected by a spurious attenuation of the strength due to flux absorption. In fact, for a particular channel  $n$ , the loss of flux in  $\chi_E^{(-)}$ , which contributes to excitation of the other final states, is compensated by a gain of flux in  $\tilde{\chi}_E^{(-)}$ , due to the flux lost, towards the channel  $n$ , by the other final states asymptotically originating from different channels. In this approach it is just the imaginary part of the optical potential that causes the difference between  $\tilde{\chi}_E^{(-)}$  and  $\chi_E^{(-)}$  and takes into account the redistribution of the strength among different channels. The resulting expansion emphasizes both the common conceptual basis and the different physical content of exclusive and inclusive electron scattering and allows a consistent treatment of both processes.

The Green function approach can be improved by replacing the eigenfunctions of the Feshbach optical potential by [121]

$$\sqrt{1 - dv_L^\dagger(E)/dE} \chi_{L,E}^{(-)}(\mathbf{r}), \quad (5.46)$$

where  $\chi_{L,E}^{(-)}$  is an eigenfunction belonging to the eigenvalue  $E$  of the local equivalent phenomenological optical potential  $v_L^\dagger$ . The term in the square root, the so-called “de Forest factor” [121, 123], removes the whole energy dependence of the local optical potential. It represents a simple prescription that improves the treatment and allows one to take into account two different contributions: the effect of interference between different discrete channels, represented by terms  $P_n G P_m$ , which are neglected in the approximation of eq. (5.42), and the spurious energy dependence due to the locality of  $v_L$ , usually considered by means of the Perey factor [124]. Moreover, eq. (5.46) also motivates the use of a phenomenological optical potential for the inclusive response on the basis of a theoretical result and not only because of the poor practical knowledge of the Feshbach optical potential.

FSI give a large and similar effect on both components of the nuclear response. The height of the QE peak is substantially quenched and the total strength is redistributed among various channels. The further reduction of the peak height resulting when also interference between discrete channels and the nonlocality of the optical potential are considered by means of the de Forest factor, in combination with the same phenomenological ingredients able to describe quasi-free ( $e, e'p$ ) data, gives satisfactory agreement with experimental longitudinal response, for values of momentum transfer between 400 and 550 MeV/c (fig. 14). For higher values relativistic effects should be considered. The systematic underestimate of the transverse response produced by FSI in the present approach is not surprising. Indeed any discussion of the transverse response cannot exclude MEC, which because of their two-body nature excite 2p–2h states, whose contribution should restore the transverse response [99, 102]. Even though a simultaneous and consistent description of both components of the nuclear response has not been achieved so far, the great amount of work carried out on this subject seems to indicate that inelastic electron scattering in the quasi-elastic region can be reasonably explained in terms of conventional nuclear physics.

### 5.3. The Coulomb sum rule

The general features of the nuclear response to electron scattering are better exploited by means of sum rule techniques. A detailed analysis of a variety of sum rules is performed in a recent review [128] and is beyond the present purposes. Here attention is focussed on the so-called Coulomb sum rule, which can be verified with the successful experimental separation of the longitudinal and transverse inclusive data.

Theoretically, the Coulomb sum rule is obtained by integrating the longitudinal response  $R_L$  over the energy loss  $\omega$ :

$$C'_L(|\mathbf{q}|) = \int_0^\infty d\omega R_L(\omega, Q^2) = \overline{\sum_i} [\langle \Psi_i | \hat{\rho}^\dagger(\mathbf{q}) \hat{\rho}(\mathbf{q}) | \Psi_i \rangle - |\langle \Psi_i | \hat{\rho}(\mathbf{q}) | \Psi_i \rangle|^2]. \quad (5.47)$$

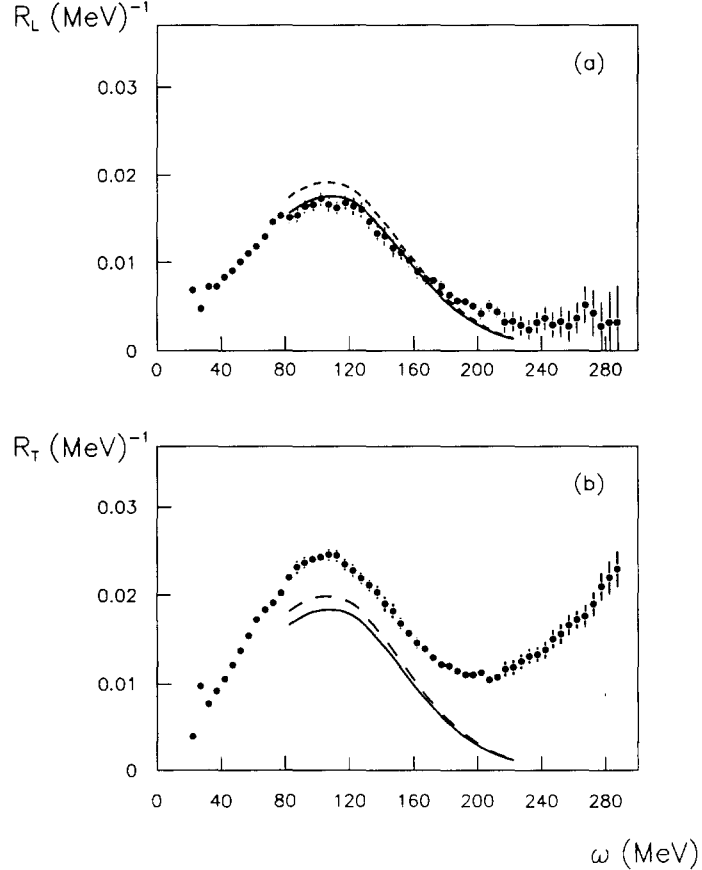


Fig. 14. (a) Longitudinal and (b) transverse response functions for  $^{12}\text{C}$  at  $q = 400 \text{ MeV}/c$  as a function of energy transfer. The data are from ref. [86]. Solid line gives the inclusive response with the de Forest factor, dashed line is without the de Forest factor. Hole states are from ref. [125] and optical potential from ref. [126]. A pure shell model is assumed for the nuclear structure (from ref. [127]).

For point-like charges, the one-body and the two-body densities are

$$\begin{aligned} \rho_1(\mathbf{r}) &= \overline{\sum_i} \langle \Psi_i | \sum_{k=1}^Z \delta(\mathbf{r} - \mathbf{r}_k) | \Psi_i \rangle, \\ \rho_2(\mathbf{r}, \mathbf{r}') &= \frac{1}{Z(Z-1)} \overline{\sum_i} \langle \Psi_i | \sum_{k \neq l}^Z \delta(\mathbf{r} - \mathbf{r}_k) \delta(\mathbf{r}' - \mathbf{r}_l) | \Psi_i \rangle. \end{aligned} \quad (5.48)$$

One can also define a proton-proton correlation function as follows:

$$c_2(\mathbf{r} - \mathbf{r}') = \int d\mathbf{R} \rho_2(\mathbf{r}, \mathbf{r}'), \quad (5.49)$$

where  $\mathbf{R} = \frac{1}{2}(\mathbf{r} + \mathbf{r}')$ . Therefore

$$C'_L(|\mathbf{q}|) = Z + Z(Z-1)\tilde{c}_2(|\mathbf{q}|) - Z^2 |F_{ch}(|\mathbf{q}|)|^2, \quad (5.50)$$

where  $F_{\text{ch}}$  is the target charge form factor for point-like protons and  $\tilde{c}_2(|\mathbf{q}|)$  is the Fourier transform of the proton–proton correlation function. For  $|\mathbf{q}| \rightarrow \infty$  both  $\tilde{c}_2(|\mathbf{q}|)$  and  $F_{\text{ch}}(|\mathbf{q}|)$  vanish, so that

$$(1/Z) C'_L \xrightarrow[|\mathbf{q}| \rightarrow \infty]{} 1 . \quad (5.51)$$

As such, under the basic assumptions of point-like nonrelativistic nucleons, the Coulomb sum rule provides a sensitive tool for appreciating dynamic nucleon–nucleon correlations as a function of  $\mathbf{q}$  and its comparison with data is a challenge for any many-body theory of the nuclear system.

Experimentally, one has to limit the integration range of the longitudinal response up to the maximum explored value  $\omega_{\max}$  of the electron energy loss. Extracting the nucleon form factor, one then defines

$$C_L(|\mathbf{q}|) = \frac{1}{Z} \int_0^{\omega_{\max}} d\omega \frac{R_L(\omega, Q^2)}{G_E^2(Q^2)} , \quad (5.52)$$

which also should go to 1 in the limit of high momenta.

In practice the integral in eq. (5.52) is performed over the quasi-elastic peak at increasing values of  $|\mathbf{q}|$ . The model independent asymptotic limit is reached rather quickly in light nuclei [92–94] and the general behaviour of the Coulomb sum rule is reproduced by calculations [129] (fig. 15). In heavy and medium-heavy nuclei [85–91, 95, 96] (fig. 16) there is still up to 40% missing strength in the experimental  $C_L$  at  $|\mathbf{q}| = 2.5 \text{ fm}^{-1}$ . According to recent data [130] on the separated longitudinal and transverse response functions in  $^{56}\text{Fe}(e, e')$  at momentum transfer near  $1 \text{ GeV}/c$  the Coulomb sum rule continues to be lower than the calculation at this high momentum transfer by about 30%, with an uncertainty of about 20%.

At the highest measured momentum transfer, which is much larger than twice the Fermi momentum, one would expect that correlations were not effective: thus the lack of strength is a puzzle stimulating one to go beyond the approximations used in the derivation of the Coulomb sum rule. On the one hand one could advocate some mechanism, related to short range and tensor correlations, pushing the missing strength to higher energies. On the other hand one could take into account relativistic corrections and nuclear medium effects, modifying the nucleon form factors. Moreover, a reliable comparison between experimental and theoretical Coulomb sum rules cannot neglect the role played by FSI and Coulomb distortion of electron waves. We refer the reader to ref. [128] for an extensive discussion of the available literature. Here we only note that a convincing explanation of the missing strength of the Coulomb sum rule in medium and heavy nuclei still remains an unsolved problem.

#### 5.4. Deep inelastic scattering

It is useful to compare the expressions for the cross section obtained in different cases, i.e., eq. (4.24) for the point-like Dirac particle, eq. (4.36) with the definitions (4.38) for a physical nucleon [or, equivalently, eqs. (4.41)–(4.43)], and eq. (5.11) for inclusive inelastic scattering. In the elastic

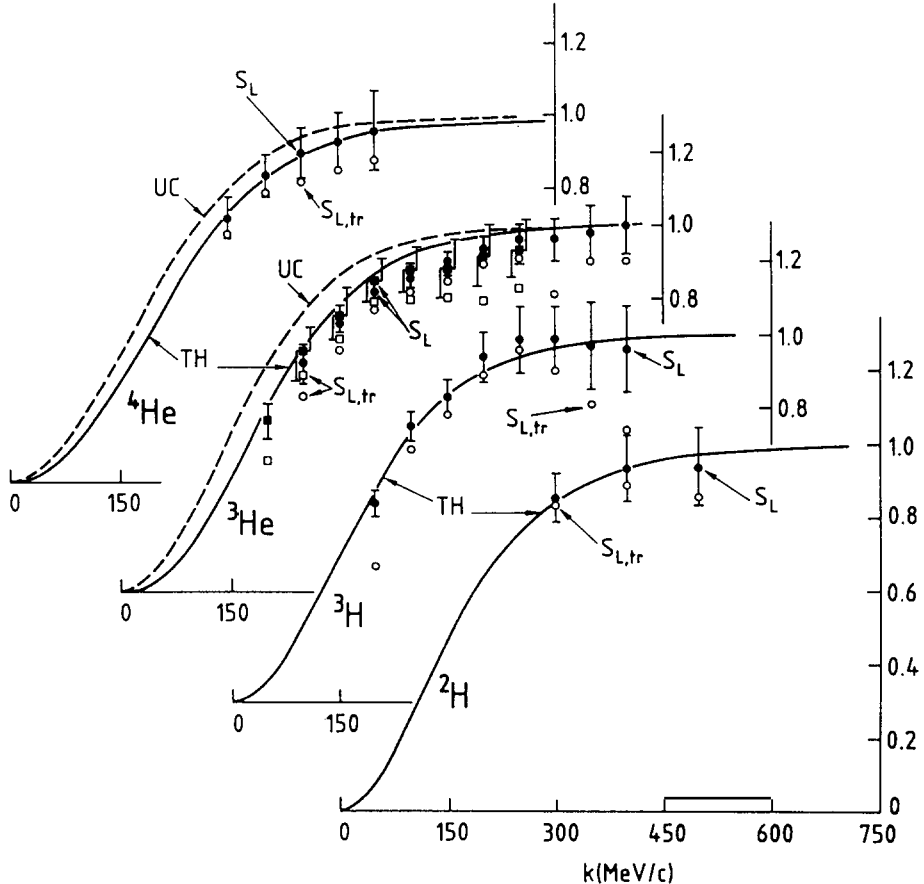


Fig. 15. Coulomb sum rule for few-nucleon systems. The dashed and full lines show results obtained with and without pair correlations. The integrals of the observed response at  $\omega < \omega_{\max}$  are shown by open circles and squares, while the filled circles and squares include the estimated  $\omega > \omega_{\max}$  tail contribution (from ref. [129] by courtesy of R. Schiavilla).

limit for the nucleon, eq. (5.11) thus implies

$$\begin{aligned} W_1 &\rightarrow (Q^2/4 M^2) G_M^2 \delta(\omega - Q^2/2 M), \\ W_2 &\rightarrow (1 + Q^2/4 M^2)^{-1} [G_E^2 + (Q^2/4 M^2) G_M^2] \delta(\omega - Q^2/2 M). \end{aligned} \quad (5.53)$$

In turn, for a point-like Dirac particle one has

$$W_1 \rightarrow (Q^2/4 M^2) \delta(\omega - Q^2/2 M), \quad W_2 \rightarrow \delta(\omega - Q^2/2 M), \quad (5.54)$$

i.e.,

$$\begin{aligned} 2M W_1(\omega, Q^2) &= (Q^2/2 M \omega) \delta(1 - Q^2/2 M \omega) \equiv 2 F_1(x), \\ \omega W_2(\omega, Q^2) &= \delta(1 - Q^2/2 M \omega) \equiv F_2(x), \end{aligned} \quad (5.55)$$

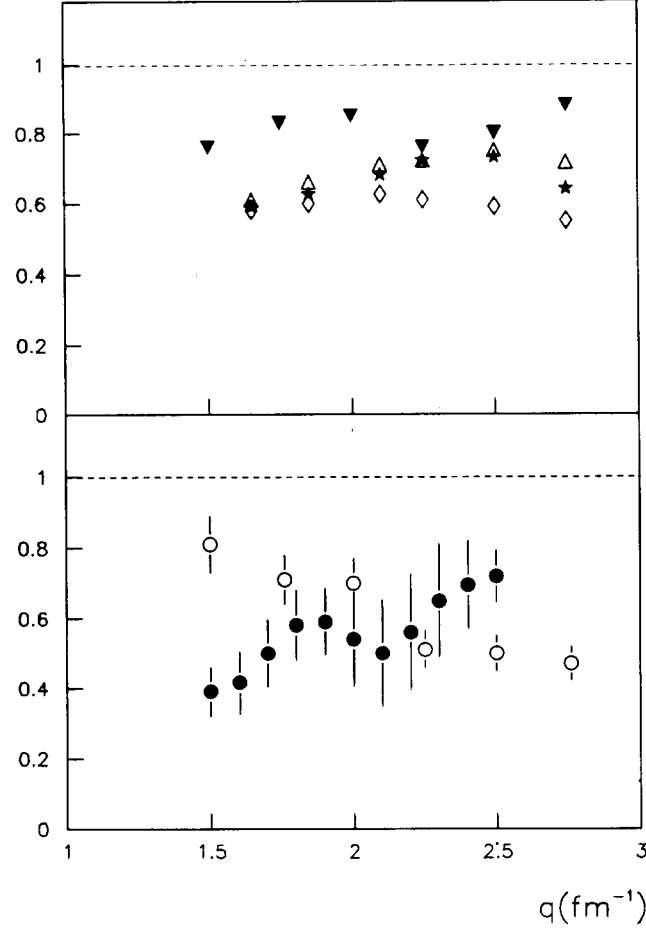


Fig. 16. Coulomb sum rule for complex nuclei:  $^{12}\text{C}$  (filled triangles),  $^{40}\text{Ca}$  (open diamonds),  $^{48}\text{Ca}$  (stars),  $^{56}\text{Fe}$  (open triangles),  $^{208}\text{Pb}$  (open dots),  $^{238}\text{U}$  (filled dots) (adapted from ref. [128]).

where

$$x = Q^2/2M\omega \quad (5.56)$$

is the Bjorken scaling variable [131]. While in electron scattering one can vary  $\omega$  and  $Q^2$  independently, the structure functions  $F_{1,2}$  depend on one variable  $x$  only. As a consequence, for fixed  $x$  the structure functions do not depend on  $Q^2$ , i.e., are independent of any mass scale. In fact this occurs in high energy inelastic scattering on the proton for  $Q^2 \gg M^2$  and an invariant hadron mass  $W \gg M$ ; it is known as the scaling behaviour of deep inelastic scattering [132–134] (fig. 17). It can be interpreted as due to incoherent elastic scattering from point-like constituents in the proton and is the experimental basis for the quark–parton model.

A useful quantity related to eqs. (5.17) is

$$R = 2 \frac{Q^2}{|\mathbf{q}|^2} \frac{R_L}{R_T} = \frac{W_2}{W_1} \frac{Q^2 + \omega^2}{Q^2} - 1 . \quad (5.57)$$

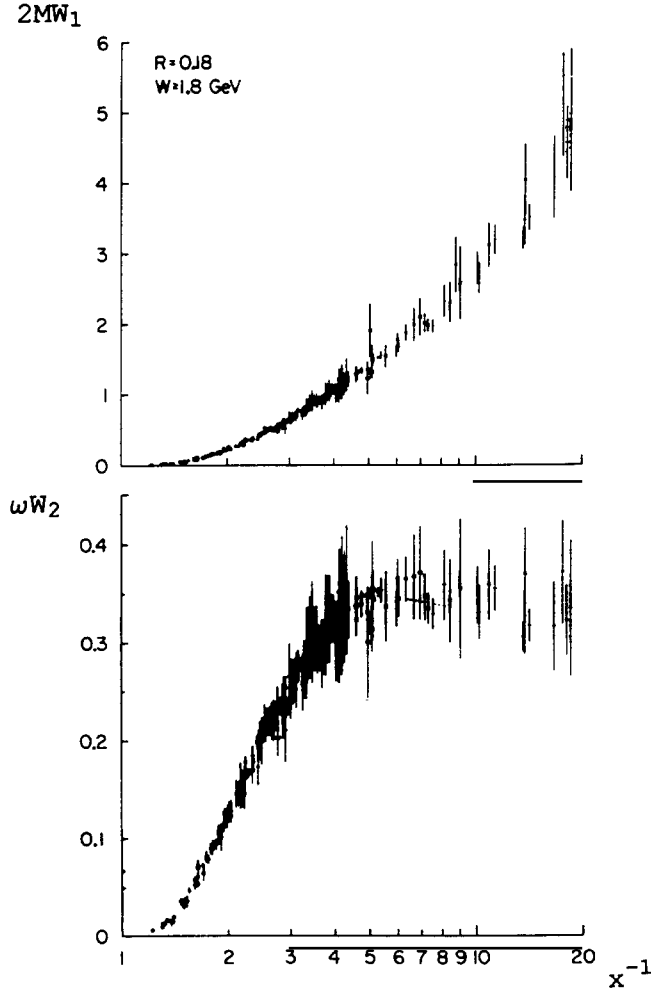


Fig. 17. Scaling behaviour of the proton structure functions in deep inelastic scattering (from ref. [134]).

In terms of this ratio one has

$$\frac{2F_1}{F_2} = \frac{2MW_1(\omega, Q^2)}{\omega W_2(\omega, Q^2)} = \frac{1}{x} \frac{1}{1+R} \left( 1 + \frac{2Mx}{\omega} \right). \quad (5.58)$$

At high energy and momentum transfer the observed ratio  $R$  is consistent with zero [135], thus indicating that the longitudinal response drops to zero and

$$2xF_1(x) = F_2(x), \quad (5.59)$$

which is known as the Callan–Gross relation [136].

Similar scaling behaviour occurs in nuclei and will be discussed in section 6.8.

## 6. The hadron tensor in semi-inclusive inelastic scattering

Semi-inclusive inelastic reactions are produced when one particle of mass  $M$  ejected from the target of mass  $M_T$  during the scattering process is detected in coincidence with the scattered electron. The kinematic variables are shown in fig. 18.

For unpolarized particles the hadron tensor is symmetric and its general structure is given in terms of the independent four-vectors  $q^\mu$ ,  $P^\mu$  and  $p'^\mu$  as follows:

$$\begin{aligned} W^{\mu\nu} &= W^{\nu\mu} \\ &= Ag^{\mu\nu} + Bq^\mu q^\nu + C \frac{1}{M_T^2} P^\mu P^\nu + D \frac{1}{M_T} (P^\mu q^\nu + P^\nu q^\mu) + E \frac{1}{p \cdot P} \frac{1}{2} (P^\mu p'^\nu + P^\nu p'^\mu) \\ &\quad + F \frac{1}{M_T} (p'^\mu q^\nu + p'^\nu q^\mu) + G \frac{1}{M^2} p'^\mu \sigma^{\nu\mu}. \end{aligned} \quad (6.1)$$

The coefficients  $A, \dots, G$  are functions of the four independent scalars  $Q^2$ ,  $q \cdot P$ ,  $q \cdot p'$  and  $p' \cdot P$ . Gauge invariance, eq. (5.7), however, gives three relations among them. Therefore only four independent structure functions result, say

$$W_1 = -A, \quad W_2 = C, \quad W_3 = E, \quad W_4 = G. \quad (6.2)$$

Moreover, electron current conservation, eq. (2.21), suppresses terms linear in  $q^\mu$ , which do not contribute when contracted with the lepton tensor. Therefore one finally obtains [137]

$$W^{\mu\nu} = -W_1 g^{\mu\nu} + W_2 \frac{1}{M_T^2} P^\mu P^\nu + W_3 \frac{1}{p \cdot P} \frac{1}{2} (P^\mu p'^\nu + P^\nu p'^\mu) + W_4 \frac{1}{M^2} p'^\mu p'^\nu. \quad (6.3)$$

Taking into account eq. (2.44) in a spherical basis one has

$$W_{\lambda\lambda'} = (-)^{\lambda+\lambda'} W_{\mu\nu} \varepsilon_\lambda^\mu \varepsilon_{\lambda'}^\nu. \quad (6.4)$$

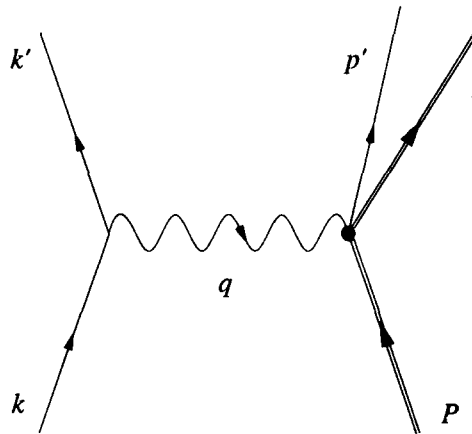


Fig. 18. Semi-inclusive inelastic electron scattering.

In the laboratory frame (fig. 19), where the initial nucleus is assumed at rest [ $P^\mu = (M_T, 0)$ ] and  $p'^\mu = (E', \mathbf{p}')$ , the independent elements of the hadron tensor are [16]

$$\begin{aligned} W_{00} &= -W_1 + \frac{|\mathbf{q}|^2}{Q^2} \left( W_2 + cW_3 + \frac{E'^2}{M^2} c^2 W_4 \right), \quad W_{11} = W_1 + \frac{|\mathbf{p}'|^2}{2M^2} W_4 \sin^2 \gamma, \\ W_{01} &= -\frac{1}{\sqrt{2}} \frac{|\mathbf{q}|}{Q} \frac{|\mathbf{p}'|}{E'} \left( \frac{1}{2} W_3 + \frac{E'^2}{M^2} c W_4 \right) \sin \gamma e^{-i\alpha}, \quad W_{1-1} = -\frac{|\mathbf{p}'|^2}{2M^2} W_4 \sin^2 \gamma e^{2i\alpha}, \end{aligned} \quad (6.5)$$

where

$$c = 1 - (\omega |\mathbf{p}'| / E' |\mathbf{q}|) \cos \gamma, \quad (6.6)$$

$\gamma$  is the angle between  $\mathbf{p}'$  and  $\mathbf{q}$ , and  $\alpha$  is the angle of rotation about  $\mathbf{q}$  to bring the electron scattering plane to coincide with the plane of the final hadron system. In this frame the structure functions  $W_i$  depend on  $\omega$ ,  $|\mathbf{q}|$ ,  $|\mathbf{p}'|$  and  $\gamma$ . The remaining elements of the hadron tensor are obtained from the ones of eq. (6.5) making use of the hermiticity of  $W_{\mu\nu}$  and the reflection symmetry property (2.40) of the photon polarization vectors:

$$W_{\lambda\lambda'} = W_{\lambda'\lambda}^* = (-)^{\lambda+\lambda'} W_{-\lambda'-\lambda}. \quad (6.7)$$

In general out-of-plane kinematics can be conceived, whereas for  $\alpha = 0, \pi$ , one has coplanar kinematics. When  $\gamma = 0(\pi)$ , i.e., when  $\mathbf{p}'$  and  $\mathbf{q}$  are parallel (antiparallel), one deals with the so-called parallel kinematics. In this case  $\alpha$  is not defined. However, this does not introduce ambiguities in the hadron tensor because only  $W_{00}$  and  $W_{11} = W_1$  survive in this case.

If the hadron tensor is evaluated in the CM frame of the final hadron system, one has to transform it to the laboratory frame where the cross section is measured. In particular, this implies a rotation through  $-\alpha$  about  $\mathbf{q}$  to bring the plane of final hadrons to coincide with the electron

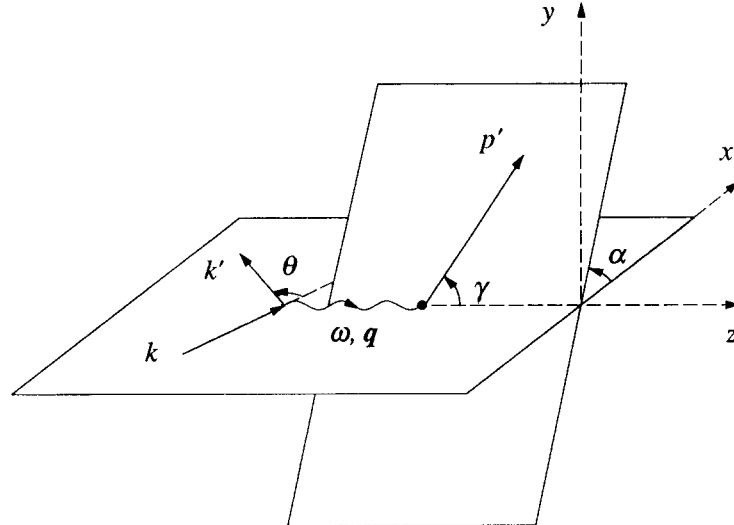


Fig. 19. Kinematics for the semi-inclusive scattering process.

scattering plane in the laboratory frame. This rotation leaves the longitudinal polarization vector unchanged, but changes the phase of the transverse components. Hence on a spherical basis the effect of the transformation is a phase factor between  $W'_{\lambda\lambda'}$  in the CM frame and  $W_{\lambda\lambda'}$  in the laboratory frame [14],

$$W_{\lambda\lambda'} = e^{i\alpha(\lambda - \lambda')} W'_{\lambda\lambda'}. \quad (6.8)$$

This phase introduces the same nontrivial  $\alpha$  dependence of eqs. (6.5) into the contraction (5.3), which can be explicitly extracted defining new structure functions [138]:

$$\begin{aligned} f_{00} &= (|\mathbf{q}|^2/Q^2) W'_{00}, & f_{11} &= W'_{11} + W'_{-1-1}, \\ f_{01} &= (|\mathbf{q}|/Q) 2 \operatorname{Re}(W'_{01} - W'_{0-1}), & f_{1-1} &= 2 \operatorname{Re} W'_{1-1}. \end{aligned} \quad (6.9)$$

Thus, neglecting recoil, the coincidence cross section becomes [139, 137, 140, 15, 138]

$$\frac{d\sigma}{dE' d\Omega dp'} = \sigma_M (\rho_{00} f_{00} + \rho_{11} f_{11} + \rho_{01} f_{01} \cos \alpha + \rho_{1-1} f_{1-1} \cos 2\alpha), \quad (6.10)$$

where the coefficients  $\rho_{\lambda\lambda'}$  only depend on the electron kinematics and are defined in table 2.

Alternatively, one could also define

$$W_L = 2f_{00}, \quad W_T = f_{11}, \quad W_{TL} = f_{01}, \quad W_{TT} = -f_{1-1}, \quad (6.11)$$

so that the coincidence cross section becomes

$$\frac{d\sigma}{dE' d\Omega dp'} = \frac{e^2 \pi}{2|\mathbf{q}|} \Gamma [W_T + \varepsilon_L W_L + \sqrt{\varepsilon_L(1+\varepsilon)} W_{TL} \cos \alpha + \varepsilon W_{TT} \cos 2\alpha]. \quad (6.12)$$

In this form the close connection between electronuclear and photonuclear processes is better seen [7, 3]. In contrast to the case of real photons, where only the pure transverse response  $W_T$  occurs, now there are also the pure longitudinal response function  $W_L$  and the two interference responses  $W_{TL}$  and  $W_{TT}$ . Integrating over the ejectile momentum  $p'$ , i.e. for a situation where only the scattered electron is detected, these two interference responses are averaged to zero and eq. (6.12) goes over to the form (5.18), which holds for the inclusive inelastic electron scattering.

Explicit expressions of the hadron tensor depend on the specific process under investigation. However, one can always determine the general structure of the nuclear current from basic symmetry requirements. As an example, in pion electroproduction where a (pseudoscalar) pion is emitted by electron scattering, the nuclear current must be a Lorentz covariant pseudo-four-vector. In the case of pion electroproduction on the nucleon its electromagnetic current can then be written in terms of the eight independent pseudovectors that one can obtain starting from the kinematic variables of the process [8]. As a consequence of current conservation, which imposes two conditions, the scattering matrix in the one-photon exchange approximation results as a sum of six scalar amplitudes, which reduce to four in the case of pion photoproduction [141]. A similar situation occurs in kaon photo- [142] and electro-production [143]. In any case the coincidence electroproduction cross section always has the form (6.10) or (6.12) (see, e.g., refs. [144, 145]).

In the following, attention is focussed on single-nucleon emission.

### 6.1. The hadron tensor in $(e, e'N)$ reactions

In this section the exclusive  $(e, e'N)$  reaction is considered where one nucleon  $N$  is directly emitted from the target and detected in coincidence with the scattered electron, while the residual nucleus is left in a state with energy  $E$ . The typical reaction is proton knockout, i.e., the  $(e, e'p)$  reaction under quasi-free kinematics.

The basic ingredient of the hadron tensor is the matrix element of the nuclear charge current density operator between the initial target state  $|\Psi_i\rangle$  and the final hadron state  $|\Psi_f\rangle$ , i.e.,

$$J_\mu = \int d\mathbf{r} e^{i\mathbf{q}\cdot\mathbf{r}} \langle \Psi_f | \hat{J}_\mu(\mathbf{r}) | \Psi_i \rangle. \quad (6.13)$$

The amplitude (6.13) in principle requires the solution of the full  $A$ -body problem for the initial and final states. One can calculate  $J_\mu$  in a Hartree–Fock (HF) frame, e.g., using a Skyrme force as an effective nucleon–nucleon interaction, followed by a consistent treatment in the RPA model [146, 149]. However, it is shown below that  $J_\mu$  can be equivalently rewritten in a one-body representation.

A natural choice for  $|\Psi_f\rangle$  is suggested by the experimental conditions of the reaction selecting a final state which behaves asymptotically as a recoiling residual nucleus and a knockout nucleon. For a specific value of the energy  $E$ , the residual nucleus is in an eigenstate  $|Ea\rangle$  of its hamiltonian, characterized by the additional set of quantum numbers  $a$ . Then  $|\Psi_f\rangle$  can be projected out of the entire Hilbert space of the total hamiltonian  $H$  into the specific channel subspace by the following projection operator [150]:

$$P = \sum_v a_v^\dagger |Ea\rangle \frac{1}{1 - n_v} \langle Ea| a_v, \quad (6.14)$$

where  $a_v^\dagger$  ( $a_v$ ) creates (annihilates) a particle with quantum numbers  $v$  on top of the residual nucleus state  $|Ea\rangle$ . Thus

$$|\Psi_f\rangle = \sum_v \chi_{Ea, v}^{(-)} a_v^\dagger |Ea\rangle, \quad (6.15)$$

where

$$\chi_{Ea, v}^{(-)} = \frac{1}{1 - n_v} \langle Ea| a_v | \Psi_f \rangle \quad (6.16)$$

describes the (single-particle) distorted wave function of the ejectile with incoming wave boundary condition. The index  $v$  labels the natural orbitals of  $|Ea\rangle$  corresponding to an occupation number  $n_v \neq 1$ .

The amplitudes  $J_\mu$  can be calculated in the  $P$ -subspace provided one uses the appropriate effective charge current density operator  $\tilde{J}_\mu(\mathbf{r})$ . In fact,

$$|\Psi\rangle = \left( P + \frac{1}{W - QHQ} QHP \right) P |\Psi\rangle, \quad (6.17)$$

where  $Q = 1 - P$  projects onto the complementary part of the Hilbert space and  $P|\Psi\rangle$  satisfies the following eigenvalue equation:

$$\mathcal{H}(W)P|\Psi\rangle = WP|\Psi\rangle. \quad (6.18)$$

The effective hamiltonian  $\mathcal{H}(W)$  is defined as

$$\mathcal{H}(W) = PHP + PHQ \frac{1}{W - QHQ} QHP \quad (6.19)$$

and is nonlocal, nonhermitian and energy dependent. It leads to a one-body hamiltonian  $\tilde{\mathcal{H}}(W)$ ,

$$\tilde{\mathcal{H}}_{vv'}(W) = (Ea|a_v \mathcal{H}(W) a_{v'}^\dagger |Ea\rangle \frac{1}{1 - n_{v'}}), \quad (6.20)$$

which has the form of a Feshbach hamiltonian, but is referred to the state  $|Ea\rangle$  of the residual nucleus.

Using eq. (6.17) for both the initial and the final hadron states in eq. (6.13), the amplitudes  $J_\mu$  in momentum space (and for the time being disregarding spin degrees of freedom) become

$$\begin{aligned} J_\mu &= \int d\mathbf{p} d\mathbf{p}' \delta(\mathbf{p}' - \mathbf{p} - \mathbf{q}) \chi_{Ea}^{(-)*}(\mathbf{p}') \tilde{J}_\mu(\mathbf{p}', \mathbf{p}) \phi_{Ea}(\mathbf{p}) [S_a(E)]^{1/2} \\ &= \int d\mathbf{p} \chi_{Ea}^{(-)*}(\mathbf{p} + \mathbf{q}) \tilde{J}_\mu(\mathbf{p}, \mathbf{q}) \phi_{Ea}(\mathbf{p}) [S_a(E)]^{1/2}, \end{aligned} \quad (6.21)$$

where  $\tilde{J}_\mu(\mathbf{p}', \mathbf{p})$  is defined in terms of  $\hat{J}_\mu(\mathbf{p}', \mathbf{p})$  in the same way as  $\tilde{\mathcal{H}}(W)$  is defined in terms of  $H$  in eq. (6.19). The (single-particle) bound state wave function  $\phi_{Ea}(\mathbf{p})$  describes the final residual state  $|Ea\rangle$  as a hole produced in the target state  $|\Psi_i\rangle$ , i.e.,

$$\phi_{Ea}(\mathbf{p}) [S_a(E)]^{1/2} = \langle Ea|a(\mathbf{p})|\Psi_i\rangle, \quad (6.22)$$

and is a normalized solution of  $\tilde{\mathcal{H}}(E_0)$  belonging to the eigenvalue  $E_0$ ;  $\chi_{Ea}^{(-)}(\mathbf{p})$  is an eigenfunction of  $\tilde{\mathcal{H}}^\dagger(E_0 + \omega)$  belonging to  $E_0 + \omega$ . As such,  $\chi_{Ea}^{(-)}(\mathbf{p})$  and  $\phi_{Ea}(\mathbf{p})$  are not orthogonal. However, the use of an effective transition operator in eq. (6.21) removes the orthogonality defect of the model wave functions, besides taking into account space truncation effects [150].

The hadron tensor is then built as follows:

$$W_{\mu\nu} \sim \sum_a \int d\mathbf{p} d\mathbf{p}' \chi_{Ea}^{(-)*}(\mathbf{p} + \mathbf{q}) \tilde{J}_\mu(\mathbf{p}, \mathbf{q}) \phi_{Ea}(\mathbf{p}) S_a(E) \phi_{Ea}^*(\mathbf{p}') \tilde{J}_\nu^\dagger(\mathbf{p}', \mathbf{q}) \chi_{Ea}^{(-)}(\mathbf{p}' + \mathbf{q}). \quad (6.23)$$

It is useful to introduce the definition of the hole spectral density:

$$S(\mathbf{p}, \mathbf{p}'; E) = \sum_a S_a(\mathbf{p}, \mathbf{p}'; E) = \sum_a \phi_{Ea}(\mathbf{p}) S_a(E) \phi_{Ea}^*(\mathbf{p}'). \quad (6.24)$$

Then

$$W_{\mu\nu} \sim \sum_a \int d\mathbf{p} d\mathbf{p}' \chi_{Ea}^{(-)*}(\mathbf{p} + \mathbf{q}) \tilde{J}_\mu(\mathbf{p}, \mathbf{q}) S_a(\mathbf{p}, \mathbf{p}'; E) \tilde{J}_\nu^\dagger(\mathbf{p}', \mathbf{q}) \chi_{Ea}^{(-)}(\mathbf{p}' + \mathbf{q}). \quad (6.25)$$

## 6.2. The spectral density

From eq. (6.24) one can write the following explicit expression for the hole spectral density:

$$S(\mathbf{p}, \mathbf{p}'; E) = \sum_a \int dE' \langle \Psi_i | a^\dagger(\mathbf{p}') | E' a \rangle \langle E' a | a(\mathbf{p}) | \Psi_i \rangle \delta(E - E'), \quad (6.26)$$

i.e.,

$$S(\mathbf{p}, \mathbf{p}'; E) = \langle \Psi_i | a^\dagger(\mathbf{p}') \delta(E - H) a(\mathbf{p}) | \Psi_i \rangle. \quad (6.27)$$

Therefore, the diagonal element of the hole spectral density,

$$S(\mathbf{p}, E) = \sum_a |\phi_{Ea}(\mathbf{p})|^2 S_a(E), \quad (6.28)$$

can be interpreted as the joint probability of removing a particle with momentum  $\mathbf{p}$  from the target nucleus leaving the residual one in a state with energy  $E$ . As such,  $S(\mathbf{p}, E)$  is a weighted sum of momentum distributions  $|\phi_{Ea}(\mathbf{p})|^2$  related to the residual nucleus, which is pictured as a hole produced in the target.  $S_a(E)$  is the spectroscopic factor measuring the probability that the residual nucleus can indeed be considered as a pure hole generated in the target nucleus by the knockout process. Due to the energy conservation the hole spectral density is only defined at the discrete energy values corresponding to bound states of the residual nucleus and for a continuum spectrum starting at the threshold of the first particle emission of the residual nucleus. Therefore,  $S(\mathbf{p}, E)$  is different from zero only if some  $S_a(E)$  is.

In finite nuclei the spectral density is nondiagonal in the momentum representation. Thus the hadron tensor in eq. (6.23) involves a two-fold integration over momenta. Only in nuclear matter, where translational invariance holds, is the spectral density diagonal.

We list here some general properties of the hole spectral density which follow from its definition (see, e.g., ref. [151]):

$$\int d\mathbf{p} S(\mathbf{p}, \mathbf{p}; E) = \sum_a S_a(E) \equiv S(E), \quad (6.29)$$

$$\int dE S(\mathbf{p}, \mathbf{p}'; E) = \langle \Psi_i | a^\dagger(\mathbf{p}') a(\mathbf{p}) | \Psi_i \rangle \equiv \rho(\mathbf{p}, \mathbf{p}'), \quad (6.30)$$

$$\int dE \int d\mathbf{p} S(\mathbf{p}, \mathbf{p}; E) = A. \quad (6.31)$$

Equation (6.29) defines the total spectroscopic factor  $S(E)$  for an excitation energy  $E$  of the residual nucleus. Equation (6.30) gives the (nondiagonal) one-body density matrix in momentum space,  $\rho(\mathbf{p}, \mathbf{p}')$ , whose diagonal elements  $n(\mathbf{p}) \equiv \rho(\mathbf{p}, \mathbf{p})/A$  define the nucleon momentum distribution. Equation (6.31) shows that the total strength must be equal to the total number  $A$  of nucleons present in the target nucleus.

According to a well-known theorem on density matrices [152],  $|\Psi_i\rangle$  possesses the following natural expansion:

$$|\Psi_i\rangle = A^{-1} \sum_v \sqrt{n_v} a_v^\dagger |K_v\rangle, \quad (6.32)$$

where the normalized vector

$$|K_v\rangle = \frac{1}{\sqrt{n_v}} a_v |\Psi_i\rangle \quad (6.33)$$

is an eigenvector of the  $(A - 1)$ -particle density matrix (corresponding to  $|\Psi_i\rangle$ ) belonging to the same eigenvalue  $n_v$  of the single-particle density matrix.

The discrete set  $|K_v\rangle$  appears to be a suitable basis to describe the states of the residual nucleus in terms of one-hole states with respect to  $|\Psi_i\rangle$ . Actually, the projection operator  $P$  can also be written as

$$P = \sum_v |K_v\rangle \langle K_v| = \sum_v a_v |\Psi_i\rangle \frac{1}{n_v} \langle \Psi_i| a_v^\dagger, \quad (6.34)$$

and acting on  $|K_v\rangle$  it projects out its hole part.

With the aid of the natural expansion (6.32),  $S_a(E)$  can be rewritten as

$$S_a(E) = \sum_v n_v |\langle E a | K_v \rangle|^2. \quad (6.35)$$

It is interesting to consider some particular cases.

(i)  $|\Psi_i\rangle$  is a Slater determinant. Then  $n_v$  are either 1 or 0, and

$$S_a(E) = \langle E a | P | E a \rangle \leq 1, \quad (6.36)$$

the equality sign holding true only if also  $|E a\rangle = P |E a\rangle$ . However, if  $P |E a\rangle = 0$ , the spectroscopic strength vanishes, confirming the fact that it gives a measure of the extent to which the state  $|E a\rangle$  of the residual nucleus can be considered to be a one-hole state.

(ii)  $|E a\rangle = |K_v\rangle$ , no assumptions on  $|\Psi_i\rangle$ . Then

$$S_a(E) = n_v (\leq 1). \quad (6.37)$$

This case originated the misleading nomenclature of occupation number for the spectral strength, though the condition  $|E a\rangle = |K_v\rangle$  is far from being satisfied in practice.

(iii) In the general case, nothing can be said about the value of  $S_a(E)$ , except for the sum rule (6.31), i.e.,

$$\int dE S(E) = A. \quad (6.38)$$

The partial sum rule

$$\int dE S_{vv'}(E) = \int dE \sum_a \langle \Psi_i | a_v^\dagger | Ea \rangle \langle Ea | a_v | \Psi_i \rangle = n_v \delta_{vv'} \quad (6.39)$$

produces the occupation number for the orbit  $v$  only if the natural orbital basis is assumed. Otherwise nondiagonal terms appear on the right-hand side of eq. (6.39) as in eq. (6.30).

From a strict mathematical point of view the hole spectral density is given by the discontinuity across the real energy axis of the hole part of the single-particle Green function [153]. Thus the definition of the spectral density requires knowledge of the whole dynamics related to the single-particle motion in nuclei. Equations have been devised to produce the spectroscopic amplitudes  $\phi_{Ea}$  once the model nuclear hamiltonian has been chosen [122, 154].

A unified approach has been developed [155–157], where hole and particle states are treated on an equal footing. A complex shell model potential is constructed extrapolating the mean field from positive towards negative energies. The extrapolation makes use of the constraint provided by the dispersion relation which connects the real to the imaginary part of the mean field. This complex field then describes not only the scattering of a nucleon by a target nucleus with  $A$  nucleons but also quasiparticle excitations in both the  $(A + 1)$ - and  $(A - 1)$ -nucleon systems.

Direct calculations of the hole spectral density are available in few-nucleon systems based either on variational methods [158–160] or Faddeev equations [161–163]. In nuclear matter results have been obtained in the frame of correlated orthogonal basis theory [164, 165] and in the self-consistent Green function approach [166].

In the case of finite nuclei, only recently self-consistent solutions for the single-particle Green function have started to become available [167, 168]. They are obtained by solving the Dyson equation in an iterative scheme with the self-energy up to second order in the interaction. However, drastic approximations are necessary to reduce the complexity of the technical problems. As a consequence the fragmentation of the spectral strength, while in agreement with the expectation of the role of correlations in nuclei, only qualitatively compares with the data.

These correlations are introduced from the very beginning in the nuclear many-body theory of refs. [164, 165]. It is based on a nonrelativistic hamiltonian with the realistic Urbana  $V_{14} +$  three-nucleon interaction [169], which in principle pretends to describe the properties of all nuclei, starting from the deuteron to nuclear matter. The strong repulsive core of the nucleon–nucleon force is handled in the variational approach to the ground state wave function. All the possible spin-isospin and tensor correlations are included in the orthogonalized correlated basis states. An accurate approximation to the spectral density is obtained for nuclear matter by taking advantage of its translational invariance, which reduces the spectral density in momentum space to diagonal form. Two-body correlations lead to two effects. (i) For  $p > p_F$  ( $p_F$  being the Fermi momentum) about 15% of the single-particle strength is spread over a missing energy region several hundreds of MeV wide; this effect is caused by mixing of the 1h state with high lying 2p–1h states in the  $A - 1$  system. (ii) The corresponding depletion of about 15% of the strength of normally occupied states

( $p < p_F$ ) is spread over a large  $p, E$  region; this is due to the presence of 2p–2h admixtures in the initial ground state. As a consequence, the single-particle occupancies near the Fermi surface are given by  $\sim 0.79$  at  $p = p_F - \varepsilon$  and  $\sim 0.06$  at  $p = p_F + \varepsilon$  [164, 170]. Thus the quasi-particle strength  $Z_F$ , which is the discontinuity of the occupancy at  $p_F$ , is  $Z_F = 0.73$ , in reasonable agreement with the experimental value  $Z_F \sim 0.6$  obtained on heavy nuclei (see section 6.4). Other interesting quantities are the mean removal energy,

$$\langle E \rangle = A^{-1} \int dE \int dp ES(p, E), \quad (6.40)$$

and the mean kinetic energy,

$$\langle T \rangle = A^{-1} \int dE \int dp \frac{p^2}{2m} S(p, E), \quad (6.41)$$

appearing in the energy sum rule [171] for the ground state energy  $E_0$  of the  $A$  system:

$$E_0 = A^{\frac{1}{2}} (\langle T \rangle - \langle E \rangle). \quad (6.42)$$

Equation (6.42) is satisfied if only two-body forces are present. A large value of  $\langle E \rangle$  is produced by correlations ( $\langle E \rangle = 71$  MeV), about 40% of it coming from  $p > p_F$ . Correspondingly,  $\langle T \rangle = 36$  MeV, with about 50% of this value coming from  $p > p_F$ . Thus  $E_0/A$  from eq. (6.42) is  $-17$  MeV, to be compared with the accepted value of  $-16$  MeV for nuclear matter. This is an indication of the role of three-body forces included in the calculation [164, 165].

### 6.3. Nucleon and electron distortion

The nucleon scattering state  $\chi_{Ea}^{(-)}$  is in principle an eigenfunction of the Feshbach (nonlocal) hamiltonian  $\tilde{\mathcal{H}}^\dagger(E_0 + \omega)$ , eq. (6.20). In practice the solution of this problem is simplified by approximating  $\tilde{\mathcal{H}}$  by phenomenological (local) optical model potentials. They simulate the medium-field interaction between the residual nucleus and the emitted nucleon with (energy dependent) parameters determined through a best fit on elastic nucleon–nucleus scattering data including cross section and polarizations.

Usually [126, 172–175] central and spin-orbit components with both a real and an imaginary part are included in the optical potential together with a Coulomb term  $V_C(r)$  describing (for the proton case) the interaction with a uniformly charged sphere of radius  $R_C$ . The charge exchange effect can be taken into account in the final state by also considering an isospin dependent term [176]. The shapes are chosen in most cases as a Woods–Saxon function,

$$f(x) = (1 + e^x)^{-1}, \quad (6.43)$$

with  $x = (r - R)/a$ ,  $R = r_0 A^{1/3}$ , or a derivative of it,  $f'(x) = df(x)/dx$ , for the spin-orbit ( $S$ ) part and surface-peaked ( $D$ ) contributions:

$$\begin{aligned} V_{\text{opt}} = & V_C(r) - V(E)f(x_V) - iW(E)f(x_W) + 4ia_D W_D(E)f'(x_D) \\ & + (2/r)[V_S(E)f'(x_S) + iW_S(E)f'(x_{WS})]\mathbf{l} \cdot \boldsymbol{\sigma}, \\ & - 2[V_T(E)f(x_T) + iW_T(E)f(x_{WT}) - 4ia_{TD} W_{TD}(E)f'(x_{TD})](\boldsymbol{\tau} \cdot \mathbf{T})/A. \end{aligned} \quad (6.44)$$

Optical potentials are also obtained by folding density dependent nucleon-nucleon effective interactions with the nuclear density in the local density approximation [177, 178].

The energy dependence of the strengths is partly due to the fact that the optical potential is, in principle, a nonlocal operator. The effect of the nonlocality can be taken into account in the distorted wave functions by means of the Perey factor [124, 179]

$$f(E) = [1 - dV_{\text{opt}}(E)/dE]^{1/2}. \quad (6.45)$$

An alternative form of the Perey factor is given by [180]

$$f(E) = [1 - \alpha V_{\text{opt}}(E)]^{-1/2}, \quad (6.46)$$

where  $\alpha = \beta^2 M/2\hbar^2$  is the range of nonlocality in a gaussian model [181].

Roughly, the effect of the optical potential  $V_{\text{opt}}$  can be obtained by replacing the initial momentum  $\mathbf{p}$  of the nucleon by an effective momentum [182–184]

$$\mathbf{p}_{\text{eff}} = \mathbf{p} + (E'/p'^2)|\bar{V}_{\text{opt}}|\mathbf{p}, \quad (6.47)$$

where  $\bar{V}_{\text{opt}}$  is some average depth.

The main effect of the real part of the optical potential is to shift the cross section, while the imaginary part gives a reduction by a factor between 0.5 and 0.7 [185]. Moreover, the distortion fills the minima of the PWIA result. The spin-orbit component produces an asymmetry of the response for different directions of the outgoing nucleon momentum with respect to the momentum transfer [186] (see figs. 20 and 21 below).

The two-step charge exchange mechanism, where a direct proton knockout is followed by a  $(p, n)$  transition as a consequence of isospin dependence of the optical model potential, has been shown to give an important contribution in photonuclear  $(\gamma, n)$  reactions [187, 188]. However, a similar treatment of the  $(e, e'n)$  reaction indicates only a small effect [189, 190], in agreement with the result obtained within a self-consistent HF and continuum RPA model [184], where exchange two-step processes are taken into account. The effect is even smaller in the  $(e, e'p)$  reaction [190].

Another correction to PWIA concerns the distortion of electron wave functions in the Coulomb field of the nucleus. This is essential in the analysis of reactions on heavy nuclei. On the contrary, dispersive effects arising from a direct interaction with exchange of more than one photon are less important and are of the order of  $1/Z$  at high energy and large angles [59]. As in the inclusive case, both these effects do not allow one to write the cross section in terms of structure functions.

An exact treatment of Coulomb distortion requires the solution of a Dirac equation for a large number of partial waves. This has been done for inclusive scattering (see, e.g., ref. [61]) and turns out to be a hard task for nucleon emission reactions, due to the combined presence of nucleon distortion [191, 192].

An approximate treatment of Coulomb distortion uses the eikonal approximation [193] or, equivalently, a high energy expansion in inverse powers of the electron energy [194], which has been applied to the inclusive [63] and the exclusive ( $e, e'p$ ) reactions [195, 63]. The numerical results of this method are comparable with those obtained in the relativistic DWIA [192]. The two calculations are in good agreement, thus indicating the absence of significant relativistic effects in the energy region experimentally investigated up to now. Only for heavy nuclei does the approximate treatment overestimate the effect of Coulomb distortion.

The electron distorted wave functions are expanded in powers of  $Z\alpha$ , where  $\alpha$  is the fine structure constant, as

$$\Phi_h^{(\pm)} = e^{\pm i\delta_{1/2}(\bar{k}/k)} e^{ik \cdot r} u_h [1 + Z\alpha g^{(1)}(\bar{k}, r) + (Z\alpha)^2 g^{(2)}(\bar{k}, r) + \dots]. \quad (6.48)$$

The sign ( $\pm$ ) refers to the two scattering solutions with outgoing or incoming spherical waves,  $u_h$  is the Pauli spinor for the electron with a given helicity  $h$  and  $\bar{k}$  is an effective momentum given by

$$\bar{k} = k - V(0)\hat{k}, \quad (6.49)$$

where  $V(0)$  is a mean value of the electrostatic nucleon potential. For a uniform spherical charge distribution with radius  $R$  one has

$$V(0) = -3Z\alpha/2R. \quad (6.50)$$

The expansion of eq. (6.48) is truncated at second order in  $Z$ . The main effect of distortion is twofold: the momentum transfer  $q$  is changed to an effective momentum (see also ref. [196]),

$$\bar{q} = q - \frac{V(0)}{E_i} (q - \omega \hat{k}'_f), \quad (6.51)$$

where the subscripts  $i$  and  $f$  refer to incident and final electrons, respectively. In addition a focusing of electron waves is produced which increases the electron flux close to the target.

The first effect, i.e., the effective momentum approximation (EMA), is simple to consider and can be easily included in the analysis of experimental data. Its contribution is proportional to the momentum transfer and also depends on the direction. Moreover, it is increasing with decreasing incident electron energy. The EMA can reasonably take into account Coulomb distortion for light nuclei.

The main effect of focusing results in an enhancement of the cross section, which can be large for heavy nuclei and is almost independent of the energy. Different effects are obtained for nucleons coming from different nucleon orbits.

In figs. 20 and 21 the 3 s hole state in  ${}^{208}\text{Pb}$  is considered. The reduced cross section given there is the quantity that is usually extracted from experiments. It is obtained by dividing the cross section by the off-shell electron–proton cross section (specifically,  $\sigma_i^{\text{cc}}$  of ref. [64]). In PWIA this

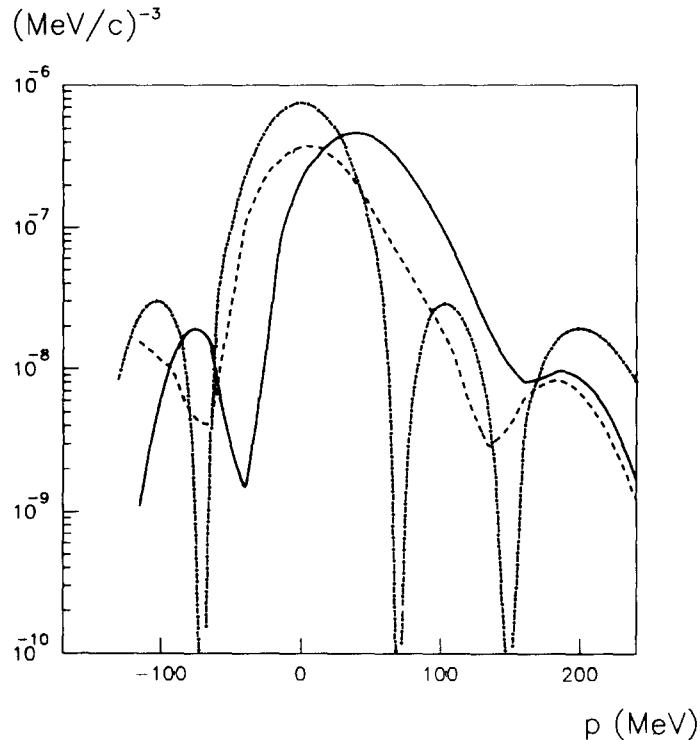


Fig. 20. The reduced cross section for the 3s hole state in  $^{208}\text{Pb}$  under parallel kinematics versus recoil momentum for an incident electron of 410 MeV and an emitted proton of 100 MeV. The bound state was taken from ref. [125] and the optical potential from ref. [175]. The dot-dashed curve was calculated in PWIA. Dashed and solid curves include proton and full distortion, respectively. Positive (negative)  $p$  values refer to situations where  $q < p'$  ( $q > p'$ ).

quantity gives the momentum distribution of protons in the target nucleus (see section 6.4). The curves including the proton distortion confirm the general trend discussed above of FSI. On the contrary, electron distortion shows a strong dependence on the selected kinematics. In parallel kinematics its effect can be understood in terms of a shift, given by EMA, and an enhancement, of about 30% in the present situation, given by focusing. In the kinematics with constant  $(\mathbf{q}, \omega)$ , where the proton is emitted in a direction approximately perpendicular to  $\mathbf{q}$ , the global effect is different; this is due to the different influence of EMA, which changes the momentum transfer and therefore cuts some values of the recoil momentum, thus giving a strong reduction of the cross section, while the effect of focusing is roughly the same as in parallel kinematics.

#### 6.4. Comparison with experiment

In PWIA, where FSI are neglected, the scattering wave function  $\chi_{Ea}^{(-)}(\mathbf{p})$  in eq. (6.23) becomes a delta function centred at the observed momentum of the ejectile. Thus in PWIA the integrations in eq. (6.23) can be performed immediately with the result that in the coincidence  $(e, e'p)$  cross section a factorization is possible between the nuclear structure part, given by the (diagonal) spectral density, and the electron–nucleon interaction, i.e.,

$$d\sigma/dE' d\Omega dp' = K \sigma_{eN} S(p, E), \quad (6.52)$$

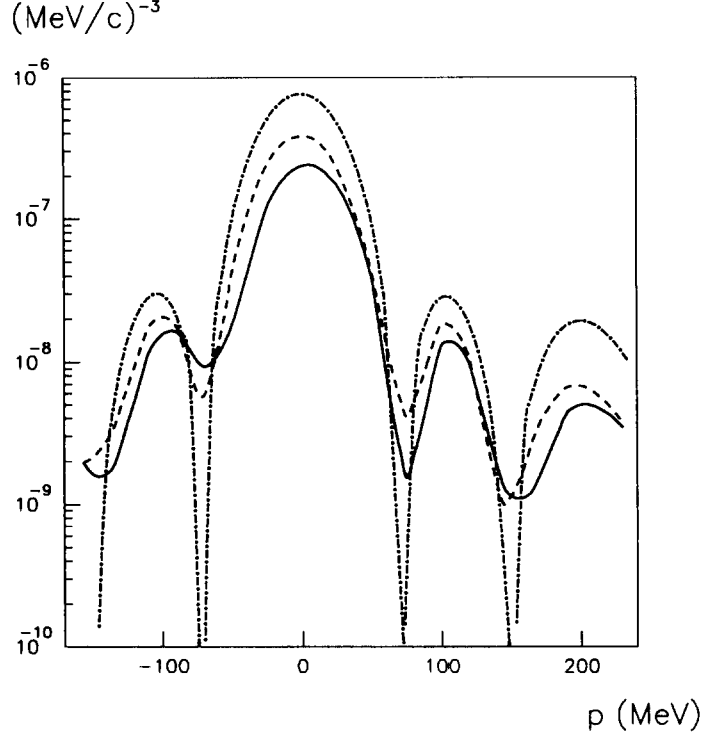


Fig. 21. The same as in fig. 20, but for a kinematics with constant  $(\mathbf{q}, \omega)$ . Positive (negative)  $p$  values refer to situations where the angle between  $\mathbf{p}'$  and  $\mathbf{k}$  is larger (smaller) than the angle between  $\mathbf{q}$  and  $\mathbf{k}$ .

where  $\sigma_{eN}$  is the (half off-shell) electron–nucleon cross section and  $K$  is a suitable kinematic factor. Equation (6.52) shows that this type of reaction is able to give detailed information on the single-particle properties of nuclei. The process is depicted in fig. 22, where the factorization is shown between the electron–nucleon (off-shell) interaction and the virtual nucleon emission by the target represented by the hadron vertex. The invariant function describing the hadron vertex becomes the hole spectral density in the nonrelativistic approximation [197].

However, interpretation of the data is complicated by many effects which have been neglected in eq. (6.52) and whose importance must be ascertained. First, FSI are not negligible. In addition, they destroy the simple factorization (6.52). If one neglects the spin–orbit term of the optical potential and the  $\mathbf{p}$ -dependence of the nucleon current, a factorized form of the cross section can be recovered in terms of a distorted spectral density:

$$S^D(\mathbf{p}, E) = \sum_a |\phi_{Ea}^D(\mathbf{p})|^2 S_a(E), \quad (6.53)$$

where the distorted momentum distribution  $|\phi_{Ea}^D(\mathbf{p})|^2$  is obtained from

$$\phi_{Ea}^D(\mathbf{p}) = \int d\mathbf{p}' \chi_{Ea}^{(-)*}(\mathbf{p}' + \mathbf{q}) \phi_{Ea}(\mathbf{p}'), \quad (6.54)$$

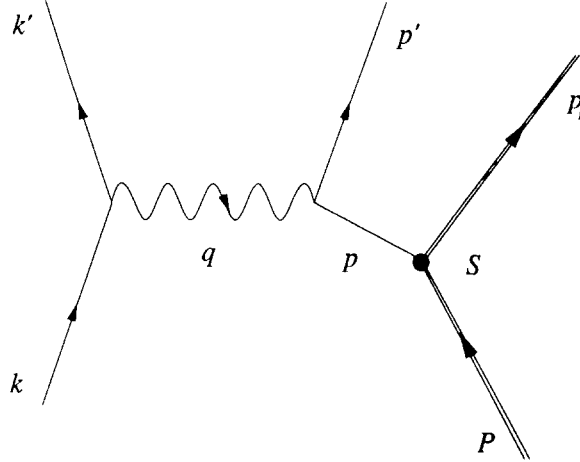


Fig. 22. The exclusive ( $e, e' N$ ) process in PWIA.

and its dependence on  $\mathbf{p}$  is implicitly contained in the fact that  $\chi^{(-)}$  is peaked around  $\mathbf{p}$ . The validity of such a factorized approximation has been discussed in ref. [184]. It depends critically on the kinematic conditions and on the type of optical potential used. In particular, the spin-orbit content of the optical potential automatically destroys the factorization and introduces significant asymmetries in the nuclear response, which is no longer invariant under rotations about  $\mathbf{q}$  [184, 198].

The second point concerns the single-particle wave functions  $\phi_{Ea}$ . In principle  $\phi_{Ea}$  is also given by the solution of the problem for  $\mathcal{H}$ , eq. (6.20). In practice the bound state  $\phi_{Ea}$  is obtained either phenomenologically or from self-consistent Hartree–Fock solutions. The successful comparison with the data obtained in ref. [185] has shown that for discrete final states and up to the explored momenta  $\phi_{Ea}$  is satisfactorily approximated by the natural orbital of the target nucleus. The result has been confirmed in all subsequent experiments [5, 199].

The data analysis is based on the assumption that the knockout process is governed by a one-body transition operator. In principle the effective current  $\tilde{J}_\mu$  in eq. (6.21) also takes care of restoring orthogonality between bound and scattering states. Actually, the orthogonality defect in standard kinematic conditions for ( $e, e' p$ ) reactions is negligible [150]. Therefore one can safely approximate  $\tilde{J}_\mu$  by  $\hat{J}_\mu$ .

The analysis is performed by taking advantage of the energy structure of the cross section presenting well-defined peaks corresponding to individual bound states of the residual nucleus. Assuming that in the energy interval  $\Delta E$  only nucleons emitted from the hole  $\alpha$  contribute, one builds a reduced cross section by dividing the coincidence cross section by  $K\sigma_{eN}$  and integrating over the energy interval  $\Delta E$  as follows:

$$\int_{\Delta E} dE \frac{d\sigma}{dE' d\Omega dp'} \frac{1}{K\sigma_{eN}} = Z_\alpha S_\alpha n_\alpha(\mathbf{p}). \quad (6.55)$$

In eq. (6.55) it has been further assumed that  $n_\alpha(\mathbf{p})$  is independent of energy in the interval  $\Delta E$  and the degeneracy of the final states of the residual nucleus is simply taken into account by the factor

$Z_\alpha$ . For a fully occupied shell  $\alpha$ ,  $Z_\alpha = 2j_\alpha + 1$ . Moreover

$$S_\alpha = \int_{\Delta E} dE S_a(E). \quad (6.56)$$

In PWIA

$$n_\alpha(\mathbf{p}) = |\phi_{Ea}(\mathbf{p})|^2. \quad (6.57)$$

Equation (6.55) defines a theoretical reduced cross section which is to be compared with the experimental momentum distribution,

$$\int_{\Delta E} dE \left( \frac{d\sigma}{dE' d\Omega d\mathbf{p}'} \right)_{\text{exp}} \frac{1}{K\sigma_{eN}} \equiv \rho_{\text{exp}}(\mathbf{p}), \quad (6.58)$$

obtained by dividing the experimental cross section by the same product  $K\sigma_{eN}$ . In this way the information contained in a five-fold cross section is reduced to a two-fold function (depending on energy and momentum). In this reduction the role played by  $\sigma_{eN}$  is crucial. This quantity can be calculated in many different approximations, as we do not know the off-shell form factors of nucleons. In the analysis of experimental data one usually adopts  $\sigma_1^{\text{rc}}$  of ref. [137]. However,  $\sigma_1^{\text{rc}}$  is calculated in a relativistic frame, which could be inconsistent with the nonrelativistic calculation of the cross section. At high energy a nonrelativistic calculation of  $\sigma_{eN}$  [200] has to face the problem of simulating the relativistic behaviour. This is usually done through an expansion in the inverse mass of the nucleon (see section 5.1).

The proportionality factor  $Z_\alpha S_\alpha$  in eq. (6.55) is the spectroscopic factor of the hole involved. If the data are taken over the energy band  $\Delta E$  in a sufficiently large range of momenta, one can obtain a reliable experimental value for  $S_\alpha$  by equating (6.55) and (6.58) integrated over  $\mathbf{p}$ :

$$Z_\alpha S_\alpha = \frac{\int d\mathbf{p} \rho_{\text{exp}}(\mathbf{p})}{\int d\mathbf{p} n_\alpha(\mathbf{p})}. \quad (6.59)$$

However, in practice, due to the limited kinematic range explored by experiment,  $S_\alpha$  is simply determined by a fit to the experimental momentum distribution  $\rho_{\text{exp}}(\mathbf{p})$ .

A representative sample of the comparison between the experimental momentum distributions and the theoretical reduced cross sections is shown in fig. 23 for the closed shell nuclei  $^{16}\text{O}$ ,  $^{40}\text{Ca}$  and  $^{90}\text{Zr}$ . Transitions involving proton knockout from the valence shells are given. The curves represent the nonrelativistic DWIA calculations where also Coulomb distortion of the electron waves is taken into account [195]. The spectroscopic factors for each transition are obtained by fitting the theoretical curves to the experimental ones. Figure 23 clearly shows that the shape of the experimental momentum distributions is well described for different transitions to discrete states.

Traditionally, spectroscopic factors or, more generally, the distribution of single-particle strength,  $S_a(E)$ , have been measured in stripping and pickup reactions. Reasonable agreement between the data is found for the shape of the energy dependence of the distribution, whereas the

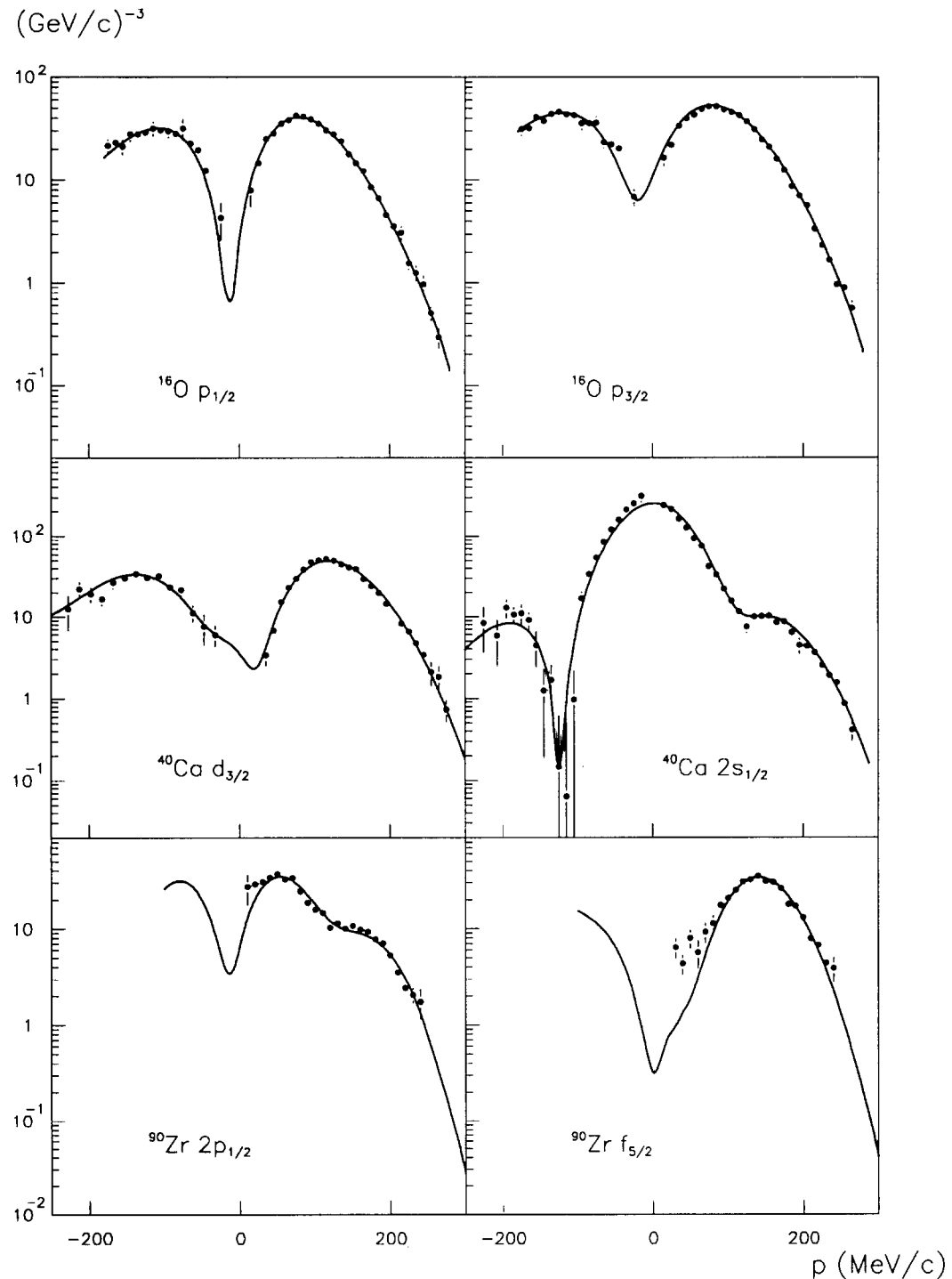


Fig. 23. Experimental momentum distributions for different transitions in the  $(e, e' p)$  reactions on  $^{16}\text{O}$  [201],  $^{40}\text{Ca}$  [202] and  $^{90}\text{Zr}$  [203, 204]. The curves represent DWIA calculations including electron distortion as described in the text (adapted from ref. [205]).

norm of the spectroscopic factors varies from one experiment to another. In general the determination of absolute spectroscopic factors from transfer reactions, such as, e.g., the pick-up reaction ( $d, {}^3He$ ), appears very difficult because the reaction mechanism, involving a strongly interacting hadron probe, is not completely under control and is in any case only sensitive to the surface part of the wave function of the transferred nucleon. On the contrary, the data for electromagnetic knockout determine the overlap functions quite precisely by means of the procedure explained above.

For valence orbits the strength measured in recent high resolution ( $e, e'p$ ) experiments is integrated over a small energy interval (typically  $\Delta E \sim 5\text{--}10 \text{ MeV}$ ) in order to also include possible fragmentation due to recoupling for nonclosed shell nuclei and long range RPA-type correlations. One finds that the absolute spectroscopic strengths amount to about 55–70% of what one would expect on the basis of the independent particle model for atomic nuclei [199, 206–208].

In the case of medium-weight nuclei, such values are in good agreement with those derived from pick-up experiments, provided that in both cases one adopts the same radial shape for the single-particle wave function. The uncertainty on the measured spectroscopic factor is about 10% and originates from FSI, which are responsible for an absorption factor, which is typically  $\sim 0.6$ , with a range of uncertainty around 10% depending on the particular optical model potential used. A further uncertainty is introduced by the effect of the two-body currents, which typically reduce the different cross section by  $\sim 10\%$  at  $Q \sim 400 \text{ MeV}/c$  [209].

The situation is controversial in the case of  ${}^{208}\text{Pb}(e, e'p)$ . Here DWIA calculations do not yield good fits to the measured cross sections [210, 207]. This has been ascribed to an inaccuracy in the treatment of Coulomb distorted electron waves [68]. However, a Combined Evaluation of Relative spectroscopic factors and Electron Scattering [211] (CERES) applies to this case rather well. Combining the relative spectroscopic factors extracted for  ${}^{208}\text{Pb}$  [210, 212, 213] with the charge density difference between isotope pairs such as  ${}^{205}\text{Tl}$  and  ${}^{206}\text{Pb}$  [214], information on the occupation of the 3 s shell can be extracted due to the particular radial shape of the  $3s_{1/2}$  wave function. Although some of the assumptions of the method are questionable [157], the merit of the CERES method is to determine the occupation of the  $3s_{1/2}$  in  ${}^{208}\text{Pb}$  in terms of ratios of spectroscopic factors of the three involved nuclei, with results which are reconciled with those obtained in recent many-body calculations [215].

The spectroscopic factors are independent of  $Q$ , i.e., constant. However, the recent analysis of four strong transitions in the reaction  ${}^{90}\text{Zr}(e, e'p) {}^{89}\text{Y}$  in the range  $0.92 \text{ fm}^{-1} < Q^2 < 4.20 \text{ fm}^{-1}$  clearly indicates a decrease of the deduced spectroscopic factors with  $Q^2$  of about 15%. This was accomplished by simultaneous fitting of proton elastic scattering data with several energy dependent parametrizations of the optical potentials and no significant sensitivity to the choice of the parametrization, as long as it described the proton scattering data well [205, 216]. A consistent description of the data is obtained [205, 217] if one includes the effects of two-body currents produced by meson exchanges and intermediate isobar configurations according to eqs. (5.32)–(5.35).

### 6.5. Structure functions

The coincidence ( $e, e'N$ ) cross section is written in eq. (6.10) in terms of four structure functions  $f_{\lambda\lambda'}$ , eq. (6.9). Their explicit expressions are easily obtained in PWIA. In this case the factorization between the nuclear structure part and the electron–nucleon interaction gives

$$f_{\lambda\lambda'} = S(\mathbf{p}, E) g_{\lambda\lambda'}, \quad (6.60)$$

where the  $g_{\lambda\lambda'}$  contain the separated contributions to the elementary electron–nucleon scattering cross section. For the nonrelativistic nucleon charge current operator [eqs. (5.30) and (5.31)] truncated to first order in  $M^{-1}$  one has

$$\begin{aligned} g_{00} &= F_1^2, \quad g_{11} = F_1^2 (|\mathbf{p}'|^2/M^2) \sin^2 \gamma + \frac{1}{2M^2} (F_1 + \kappa F_2)^2 |\mathbf{q}|^2, \\ g_{01} &= -2\sqrt{2} F_1^2 (|\mathbf{p}'|/M) \sin \gamma, \quad g_{1-1} = -F_1^2 (|\mathbf{p}'|^2/M^2) \sin^2 \gamma. \end{aligned} \quad (6.61)$$

Combining  $g_{\lambda\lambda'}$  with  $\rho_{\lambda\lambda'}$  from table 2 gives the (half off-shell) electron–nucleon cross section  $\sigma_{eN}$ , which fulfills gauge invariance and is consistent with the nonrelativistic calculation of the cross section.

A careful treatment of FSI requires considering the full (nondiagonal) spectral function (6.24) entering the hadron tensor (6.23). The factorized approximation (6.52), even with a distorted spectral density such as (6.53), is acceptable only to within  $\sim 10\%$  and is not able to account for violation of rotational symmetry about  $\mathbf{q}$  of the experimental momentum distribution [184, 185]. Much larger effects are expected on the different structure functions [138].

In general, structure functions are expected to be particularly sensitive to different ingredients entering the cross section. Therefore their separation is very helpful in investigating all these ingredients and in particular the behaviour of the nuclear response with respect to the different components of the interaction.

As an example the four structure functions  $f_{00}, f_{11}, f_{01}, f_{1-1}$  for the  $p_{1/2}$  hole in  $^{16}\text{O}$  are given in fig. 24.

In principle the structure functions can be experimentally separated in the cross section under suitable kinematic conditions. However, as in the corresponding situation for inclusive  $(e, e')$  scattering, in eq. (6.10) one-photon exchange is assumed and Coulomb distortion of electron waves is neglected. In the one-photon exchange approximation the quasi-free  $(e, e'\mathbf{p})$  cross section can always be written [195] in terms of four structure functions decomposing the response of the nucleus according to the different components of the electromagnetic interaction. However, due to Coulomb distortion these structure functions depend on electron kinematic variables as well. If one assumes the validity of eq. (6.10) or eq. (6.12) an incorrect separation is obtained. In particular, in parallel kinematics where only the longitudinal and transverse structure functions  $f_{00}$  and  $f_{11}$  survive as in the  $(e, e')$  reaction, the cross sections are still aligned in a Rosenbluth plot, but the separation gives wrong structure functions [195]. Only after the experimental cross sections have been purified from Coulomb distortion effects, can expression (6.10) be retrieved and separation procedures based on that expression be applied. In light nuclei it is in general sufficient to correct for the contribution of EMA. In medium and heavy nuclei, on the contrary, a complete and reliable treatment of Coulomb distortion is needed.

In general the complete separation is possible only with out-of-plane experiments, which are on the borderline of present capabilities. In the case of pion electroproduction only pioneering measurements have been performed with the purpose of separating the different structure functions [219, 220]. As for  $(e, e'\mathbf{p})$  reactions, the only case is for the deuteron target at relatively low energy [221].

In coplanar kinematics [138], which is at present the only one accessible in high resolution experiments with two spectrometers, a partial determination can be achieved. The structure function  $f_{01}$  can be completely determined by comparing the two symmetric kinematics with

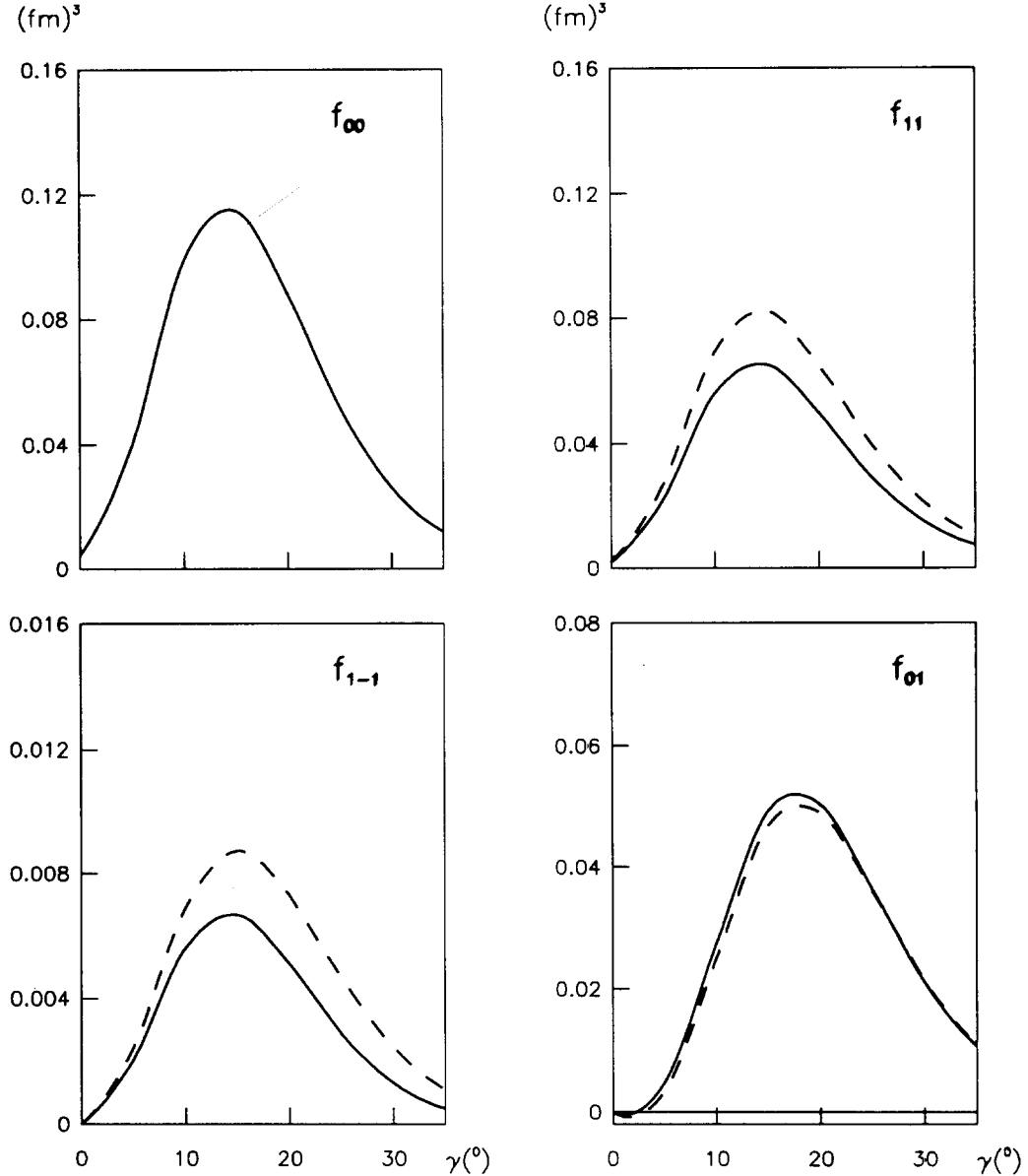


Fig. 24. Structure functions  $f_{00}$ ,  $f_{11}$ ,  $f_{01}$ ,  $f_{1-1}$  for the  $p_{1/2}$  hole in  $^{16}\text{O}$  versus the angle  $\gamma$  of the emitted proton, as calculated at  $Q = 400$  MeV/c both in DWIA (dashed lines) and including two-body currents (solid lines) [218].

$\cos \alpha = +1$  and  $\cos \alpha = -1$  [222, 204]. As  $f_{01}$  is an interference term between longitudinal and transverse contributions, its determination is quite interesting. The first separation was carried out for the  $^{16}\text{O}(\text{e}, \text{e}'\text{p})^{15}\text{N}$  reaction at Saclay for transitions to the ground state and to the first excited state of the residual nucleus [222]. The data are shown in fig. 25 together with theoretical results obtained in the nonrelativistic DWIA [138] of section 6.1. Fair agreement is obtained, but different spectroscopic factors  $S_\alpha$  are required to fit the cross sections and  $f_{01}$ . They are 0.48 and 0.73 for the  $p_{1/2}$  hole and 0.56 and 0.64 for the  $p_{3/2}$  hole. A similar result, but with larger  $S_\alpha$ , is given by a relativistic DWIA calculation [67, 222].

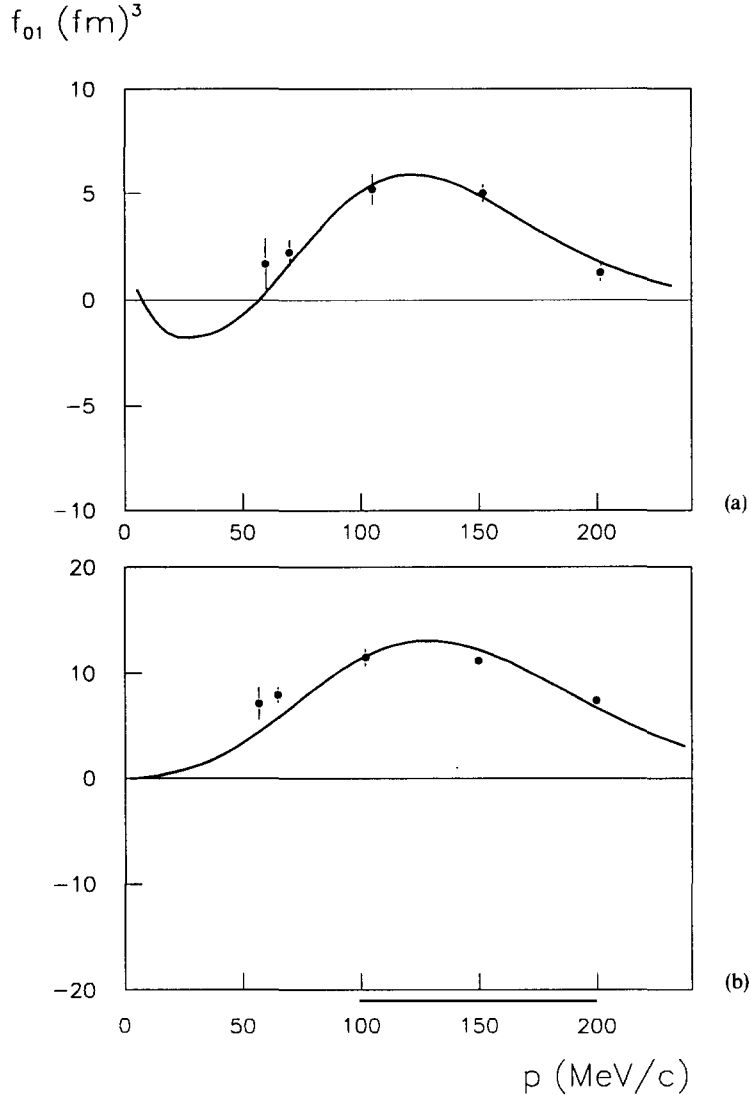


Fig. 25. The longitudinal-transverse interference structure function  $f_{01}$  versus recoil momentum in  $^{16}\text{O}(\text{e}, \text{e}'\text{p})^{15}\text{N}$  at  $|\mathbf{q}| = 570 \text{ MeV}/c$  with a proton of 160 MeV emitted from the (a)  $p_{1/2}$  and (b)  $p_{3/2}$  orbit. Data from ref. [222], optical potential from ref. [175].

The two-body currents, as calculated in ref. [218], help to decrease the discrepancy between the values of  $S_\alpha$  obtained from the cross sections and  $f_{01}$ . In the considered kinematics they decrease the cross section by about 10%, thus increasing  $S_\alpha$  by the same amount, while leaving  $f_{01}$  practically unchanged. Further data from NIKHEF are expected [204, 223], which hopefully will shed light on this problem. Incidentally, the role of two-body currents is emphasized in  $(\text{e}, \text{e}'\text{n})$  reactions [224].

When  $f_{01}$  has been separated,  $f_{11}$  can be determined by varying electron kinematics, i.e.,  $\varepsilon$ , while keeping  $\omega, q, p'$  and  $\gamma$  fixed [138]. One is thus left with the quantity  $(Q^2/|\mathbf{q}|^2)f_{00} - \frac{1}{2}f_{1-1}$ . Various theoretical approaches always give  $f_{00} \gg f_{1-1}$ . Then neglecting  $f_{1-1}$ ,  $f_{00}$  is obtained [138]. A recent measurement in the quasi-elastic region has been performed for the deuteron target [225].

A remarkable simplification occurs in the constrained kinematics, where  $\mathbf{p}'$  is parallel or antiparallel to  $\mathbf{q}$  (parallel kinematics). In this case only the pure longitudinal  $f_{00}$  and the pure transverse  $f_{11}$  survive and can be separated through a Rosenbluth plot. Results of such experiments are usually presented in terms of the ratio

$$R_G = [(4M^2/Q^2)W_T/W_L]^{1/2}, \quad (6.62)$$

which in PWIA becomes the ratio between the magnetic and the electric proton form factor, i.e.,  $R_G = G_M^p/G_E^p = \mu_p$ . This observable is well suited to investigate possible nucleon modification in the nucleus.

Some  $R_G$  measurements have been carried out in different laboratories over the last few years for complex nuclei [226–233, 208]. The interpretation of these data has sometimes been controversial. At missing energies below the two-particle emission threshold data do not indicate deviations larger than 10% with respect to standard nonrelativistic DWIA calculations for  $Q^2$  up to 0.25 (GeV/c)<sup>2</sup>. However, a deviation of  $\sim 30\%$  has been obtained [226, 229] at higher values of  $Q^2$  for <sup>40</sup>Ca. Future experiments, involving a full determination of the separated response functions for individual transitions and in a wide range of  $Q^2$  are needed for a deeper understanding of this issue.

### 6.6. Inelastic scattering above threshold for two-particle emission

Above threshold for two-nucleon emission the process is expected to be of mainly transverse character. First evidence for this was obtained in an (e, e'p) experiment carried out at MIT over a large range of missing energy [230]. An enhanced transverse response is also observed [234] in <sup>6</sup>Li(e, e'p); the energy dependence of the transverse to longitudinal ratio, which starts to deviate from unity at the two-body emission threshold, makes plausible the occurrence of a two-body reaction component.

Between the QE and  $\Delta$  production peaks in the inclusive (e, e') response, i.e., in the so-called dip region, the observed yield for nuclei with  $A \geq 4$  is much larger than predicted by simple models based on QE nucleon knockout, quasi-free pion production and meson exchange currents [235]. This suggests the presence of a new reaction mechanism, which can be better explored with exclusive experiments. At present only a measurement [236] is available for the reaction <sup>12</sup>C(e, e'p) under parallel kinematics. It indicates that 65% of the proton knockout cross section for  $Q^2$  near 0.1 (GeV/c)<sup>2</sup> and an invariant mass of 1066 MeV is due to other than one-nucleon processes. A uniform continuum strength is observed, extending from beyond the p shell to the highest measured missing energies. For missing energies above 50 MeV, the transverse response shows significant strength and the longitudinal response is essentially zero. In addition, there is a dramatic rise above the two-body knockout threshold of 28 MeV suggesting the presence of a transverse two-body reaction component in the region of the s shell.

A theory for two-nucleon knockout has been developed recently [237] and applied to both ( $\gamma$ , pn) and (e, e'2N) reactions [238, 239]. In principle such reactions are able to give information on the two-body density matrix and nucleon–nucleon correlations. However, uncertainties are introduced by FSI. Experimentally, coincidence experiments with two-nucleon emission are at a preliminary stage [240, 241] and unable to disentangle the different reaction mechanisms. With the advent of continuous wave electron accelerators this field will certainly receive more attention.

On the other hand, the uniform strength at large missing energy in the dip region cannot be accounted for within the framework of two-body processes [242]. This conclusion was reached through an analysis of FSI in the  $(e, e'p)$  reaction under parallel kinematics, where forward proton scattering is important and can be related to the study of the inclusive  $(p, p')$  reaction. In the inclusive  $(p, p')$  reaction the single scattering process, where the incident proton interacts inelastically with the target nucleon only once before coming out, is dominant at small proton scattering angles and can be treated in DWIA by using the effective nucleon–nucleon interaction. It is found that the calculated cross section for the two-body-type of FSI is very small compared with the data and with a different qualitative behaviour of the separated longitudinal and transverse responses. Thus one has to look for multinucleon knockout in the dip region [242].

Electroexcitation of the  $\Delta$  has been studied in the inclusive  $(e, e')$  reaction for a large variety of nuclei [82, 83]. For these data the cross section per nucleon is independent of  $A$ . Nuclear medium effects are clearly evident in the broadening of the  $\Delta$  peak and the shift of the  $\Delta$  centroid with respect to the case of production from free nucleons. However, the cross section is  $\sim 15\%$  larger than predicted by the  $\Delta$ -hole model [243]. As this model successfully describes pion–nucleus scattering, pion photoproduction and elastic photon scattering, the disagreement raises the question of whether the  $\Delta$  is adequately described in the high momentum transfer region or whether the many-body processes not involving the  $\Delta$  are important. In fact, in the missing energy spectrum [232] two distinct structures are observed, which correspond to multinucleon knockout and quasi-free pion production processes, in qualitative agreement with the  $(\gamma, p)$  spectra [244–247].

No data are yet available for exclusive reactions  $(e, e'p\pi)$  in the  $\Delta$  region where the dominant exit channel is  $\Delta$  de-excitation through pion emission. The coincidence cross section for pion detection exhibits the familiar form with four structure functions already discussed for nucleon knockout. However, now the different contributions of the current are governed by the dominantly transverse character of the  $\Delta$  resonance. The longitudinal–transverse interference is thus very interesting to study the small electric quadrupole component of the  $\Delta$  resonance [248].

### 6.7. $y$ -scaling

The concept of  $y$ -scaling has been introduced by West [249] in deep inelastic electron scattering by nuclei. For a system of nonrelativistic and noninteracting particles, he showed that the inclusive cross section at large momentum transfer can be written as a product of the elementary electron–nucleon cross section, times a nuclear structure function depending only upon the “scaling variable”

$$y_0 = (M/|\mathbf{q}|)(\omega - |\mathbf{q}|^2/2M), \quad (6.63)$$

which represents the longitudinal momentum  $p_{||}$  of a nucleon embedded in a free Fermi gas. Some successful tests [250–253] have encouraged the idea that high momentum components in the nuclear wave function could be extracted by a suitable analysis of the data (see also ref. [254]). The basic assumptions for scaling are the validity of the one-photon exchange mechanism in the nonrelativistic approximation with nucleon degrees of freedom only and the possibility that the reaction proceeds via single nucleons undergoing a transition from one free state ( $|\mathbf{p}_i|^2/2M$ ) to another ( $|\mathbf{p}_i + \mathbf{q}|^2/2M$ ) disregarding the convective current and any interaction of the emitted

nucleon with the other nucleons of the residual system. Under such conditions, the response  $R_L$ , e.g., of the inclusive ( $e, e'$ ) reaction in momentum representation becomes

$$\begin{aligned} R_L(\omega, Q^2) &= \sum_i \langle \Psi_i | \delta(\omega - [(p_i + q)^2 - |p_i|^2]/2M) | \Psi_i \rangle \\ &= A \int d\mathbf{p} n(\mathbf{p}) \delta(\omega - (\mathbf{p} + \mathbf{q})^2/2M + |\mathbf{p}|^2/2M), \end{aligned} \quad (6.64)$$

where  $n(\mathbf{p})$  is the nucleon momentum distribution. Introducing now the longitudinal ( $p_{||}$ ) and perpendicular ( $p_{\perp}$ ) components of  $\mathbf{p}$  along  $\mathbf{q}$ , one gets [249]

$$R_L(\omega, Q^2) = \left| \frac{d\omega}{dp_{||}} \right|^{-1} 2\pi A \int_{|y_0|}^{\infty} p dp n(p), \quad (6.65)$$

where  $d\omega/dp_{||} = d\omega/dy_0 = |\mathbf{q}|/M$  is a phase space factor arising from the dependence of the energy delta function upon  $p_{||}$ . On the quasi-elastic peak,  $y_0 = 0$ , while  $y_0 < 0$  for  $\omega$  lower than the quasi-elastic peak energy where only nucleon degrees of freedom are reasonably active.

From eq. (6.65) one obtains that the quantity

$$f(y_0) = A^{-1} \frac{d\omega}{dy_0} R_L(\omega, Q^2) = 2\pi \int_{|y_0|}^{\infty} p dp n(p) \quad (6.66)$$

is a function of one variable  $y_0$  only, i.e., is a “scaling function” representing the nucleon longitudinal momentum distribution.

In fact the inclusive quasi-elastic cross section in PWIA at high momentum transfer can be written by integrating eq. (6.52) over energy and momenta of the knocked out nucleons, i.e. [255],

$$\frac{d\sigma}{dE' d\Omega'} = \left( \frac{Z}{A} \sigma_{ep} + \frac{N}{A} \sigma_{en} \right) \left| \frac{d\omega}{dp_{||}} \right|^{-1} 2\pi \int_{E_{\min}}^{E_{\max}} dE \int_{p_{\min}}^{p_{\max}} p dp S(p, E), \quad (6.67)$$

where  $E_{\max} = E_{\max}(q, \omega)$ ,  $p_{\max} = p_{\max}(q, \omega, E)$  and  $p_{\min} = p_{\min}(q, \omega, E)$  are fixed by energy conservation;  $E_{\min}$  is fixed by the experimental conditions. Since the spectral function is a rapidly decreasing function of  $p$  and  $E$ , the upper limits of the integrals can be safely extended to  $\infty$ . Thus the scaling properties of the function

$$F(q, \omega) = 2\pi A \int_{E_{\min}}^{E_{\max}} dE \int_{p_{\min}}^{p_{\max}} p dp S(p, E) \quad (6.68)$$

are mainly governed by the  $q$  dependence of  $p_{\min}$ . The latter is determined through the equation giving the energy conservation for quasi-elastic scattering of an electron off a nucleon having

minimal values of the momentum and of the removal energy. In the case of relativistic kinematics this reads

$$\omega + M_T = \sqrt{M^2 + (q - p_{\min})^2} + \sqrt{(M_r + E_r^*)^2 + p_{\min}^2}, \quad (6.69)$$

where  $M_r$  and  $E_r^*$  are the mass and the excitation energy of the residual nucleus. Therefore  $p_{\min}$  depends on  $q$ ,  $\omega$  and  $E_r^*$ , so that in general it cannot be taken as a scaling variable. A scaling variable  $y$  valid for any nucleus can be defined by putting  $E_r^* = 0$ . It represents the momentum of a nucleon bound with minimal removal energy  $E = E_{\min}$ . For the deuteron,  $y = p_{\min}$  for any value of  $q$ , and

$$F(q, \omega) \equiv F(q, y) \xrightarrow[q \rightarrow \infty]{} F(y) = 2\pi \int_{|y|}^{\infty} p \, dp \, n(p), \quad (6.70)$$

where the scaling function  $F(q, y)$  reduces to the longitudinal momentum distribution as a result of performing the integral of the spectral function over the energy.

The importance of  $y$ -scaling analysis in terms of the scaling function  $F(q, y)$  stems from the observation that, if only nucleonic degrees of freedom are considered and the basic reaction mechanism is supposed to be the PWIA, then, at sufficiently high values of  $q$ , the scaling function  $F(q, y)$  becomes a quantity which depends only upon  $y$  (i.e., which scales in  $y$ ) and which represents an integral of the nucleon spectral function. Therefore the analysis of  $y$ -scaling in the region where scaling is observed allows one to obtain information on nucleon dynamics, e.g., nucleon momentum distribution, whereas the analysis in the region where scaling is not observed yields information on those effects which break down the impulse approximation and the independent particle model for the nuclear system. In particular, since different kinds of contribution to the quasi-elastic cross section are singled out for different values of  $y$  ( $y \sim 0$ , scattering from quasi-free nucleons;  $y > k_F$ , surface effects;  $y \gg k_F$  scattering from correlated nucleons, etc.), plotting the  $q$  dependence of  $F(q, y)$  for various values of  $y$  yields unique information on many-particle effects in different regimes of nucleon dynamics. If in addition separated longitudinal and transverse contributions to  $F(q, y)$  are also investigated [256], valuable information is obtained about the most relevant features of the nucleon–nucleon effective interaction inside the nuclear medium [257].

Quite generally, one can separate the momentum distribution into two pieces as follows [258]:

$$\begin{aligned} n(p) &= A^{-1} \int_{E_{\min}}^{\infty} dE S(p, E) \equiv n_{\text{gs}}(p) + n_{\text{ex}}(p) \\ &= A^{-1} \int_{E_{\min}}^{\infty} dE S_{\text{gs}}(p, E) + A^{-1} \int_{E_{\min}}^{\infty} dE S_{\text{ex}}(p, E), \end{aligned} \quad (6.71)$$

where  $S_{\text{gs}}(p, E)$  yields the probability distribution that the final  $(A - 1)$  system is left in its ground state (corresponding to  $E_r^* = 0$  and  $E = E_{\min} = |E_A| - |E_{A-1}|$ ), whereas  $S_{\text{ex}}(p, E)$  yields the probability distribution that the final  $(A - 1)$  system is left in the excited state with excitation energy  $E_r^* = E - E_{\min}$ .

Correspondingly, the scaling function  $F(q, y)$  is split into two contributions: the one from  $n_{\text{gs}}(p)$  trivially scales in  $y$ , whereas the second one, because of the explicit dependence of  $p_{\min}$  upon the momentum transfer, does not. Such a “scaling violation” is entirely due to the nucleon binding. Thus in the case of the deuteron  $n(p)$  turns out to be the ground state momentum distribution  $n_{\text{gs}}(p)$ . Comparison with data allows one in this case to directly extract  $n_{\text{gs}}(p)$  [258, 259]. Otherwise, for  $E_r^* \neq 0$ , deviations from the scaling behaviour in  $y$  are expected due to the effect of binding and  $y$  is no longer the longitudinal momentum. In particular, integrating the spectral function over the energy one includes both  $n_{\text{gs}}(p)$  and a contribution  $n_{\text{ex}}(p)$  which contains the effects of nuclear correlations.

In fig. 26 a comparison is presented [260] between experimental and theoretical scaling functions. Binding corrections are important at high negative values of  $y$  [259]. However, the largest effect responsible for scaling violation at large negative values of  $y$  is produced by FSI. In fact, independently of the form of the momentum distribution, for fixed  $y$ ,  $F(q, y)$  increases with  $q$  because of the increase of  $p_{\max}$  with  $q$ . If not so, a breaking of the PWIA assumption must occur [257, 258]. Including FSI complicates the description considerably and the problem arises of why and under what conditions  $y$ -scaling occurs and which scaling variable one has to choose [261].

### 6.8. Lepton–nucleus deep inelastic scattering

The discovery by the European Muon Collaboration (EMC) that the nucleon structure functions  $F_2$  in iron and deuterium are significantly different came as a surprise [262]. In nuclei one would expect that the corresponding structure function  $F_2^A$  is a weighted sum of proton and neutron structure functions, i.e.,

$$F_2^A(x) = (1/A)[Z F_2^p(x) + N F_2^n(x)]. \quad (6.72)$$

However, this is not the case. The ratio  $R(x) = F_2^A(x)/F_2^D(x)$  of the nucleon structure function of iron to that of deuterium was found larger than unity at small values of the Bjorken scaling variable,  $x = Q^2/2M\omega$ , and decreasing to values lower than unity in the region of large  $x$ . The effect was named the EMC effect and was confirmed in the region above  $x = 0.3$  in electron scattering experiments at SLAC [263]. The BCDMS collaboration at CERN [264] also confirmed the effect at  $x > 0.3$ , whereas for  $x < 0.3$  the BCDMS ratio was smaller than the original EMC effect. A compilation of measured ratios for different nuclei in successive experiments [265] is exhibited in fig. 27. The present situation (see ref. [266] for a recent review) gives the following picture: structure functions are sensitive to the nuclear medium and the effects depend on the kinematic region. At very small  $x$ , only accessible for small  $Q^2$ , the ratios are considerably smaller than unity as suggested by the shadowing phenomenon [267], which is dominated by the large (hadronic) size of the  $q\bar{q}$  pairs [268]. This is a direct consequence of the colour transparency property of the total cross section, which is sensitive to the transverse size of the  $q\bar{q}$  pair. In the region  $x = 0.1–0.3$ , where the contribution from sea quarks may be important, the ratio exceeds unity by a few percent. In the medium range,  $x = 0.3–0.8$ , the structure function is significantly smaller for a nucleus than for a free nucleon. This depletion is approximately proportional to  $\log A$ , with little or no  $Q^2$  dependence [263]. For  $x$  approaching 1, the ratio is predicted to rise due to the effects on the bound nucleons of the Fermi motion [269, 270].

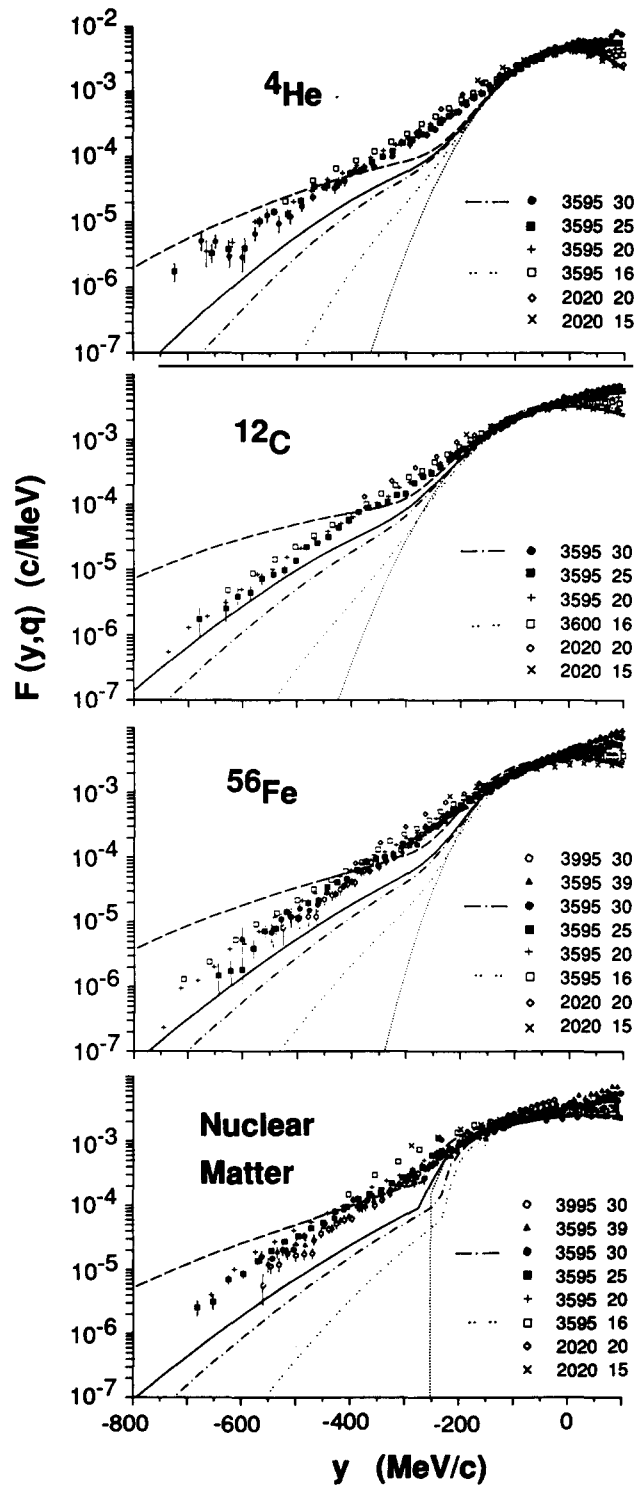


Fig. 26. Comparison between experimental and theoretical scaling functions. Dotted line for the one-body contribution (for finite nuclei divided by 0.8), double-dotted and dash-dotted lines including many-body contributions (eq. 6.68), solid line for the asymptotic scaling function [eq. (6.68) for  $q \rightarrow \infty$ ] and dashed line for the longitudinal momentum distribution (eq. 6.70) (from ref. [260]).

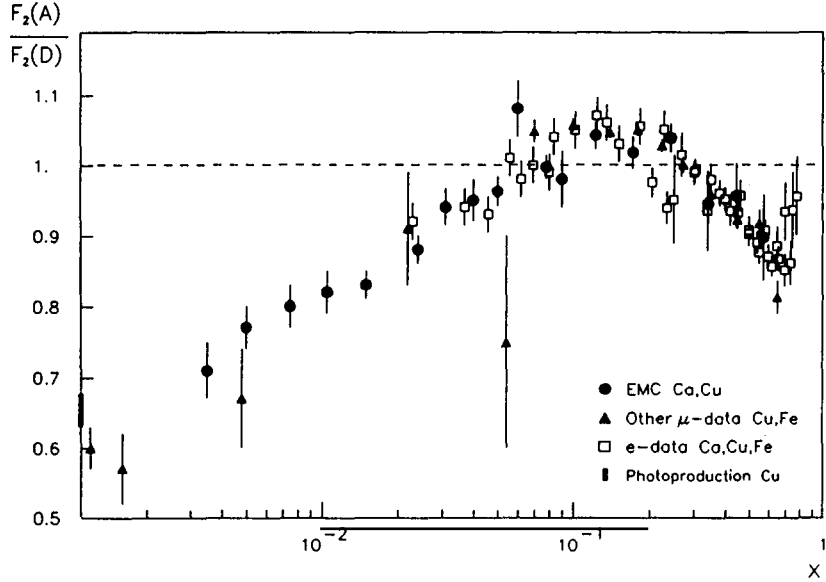


Fig. 27. Compilation of the data on the nuclear to nucleon structure function ratio for the  $\langle A \rangle = 55$  nuclei (from ref. [265]).

The role played by nucleonic degrees of freedom in deep inelastic scattering of leptons has been widely discussed (see, e.g., ref. [11]). In particular, the nucleon removal energy and nucleon–nucleon correlations have important effects [271–276]. Assuming that the deep inelastic process can be described in the IA with the undetected emission of a nucleon, the hadron tensor is obtained by the following convolution formula [274, 275]:

$$W_{\mu\nu}^A = \sum_s \int d^{(4)}p \left( \frac{Z}{A} \mathcal{S}_A^p(P, p, s) W_{\mu\nu}^p(p, q, s) + \frac{N}{A} \mathcal{S}_A^n(P, p, s) W_{\mu\nu}^n(p, q, s) \right), \quad (6.73)$$

where  $\mathcal{S}_A^{p(n)}$  is the invariant function describing the nuclear vertex with an outgoing virtual proton (p) or neutron (n) and  $W_{\mu\nu}^{p(n)}$  is the hadron tensor for the off-shell proton (neutron) with spin  $s$ :

$$W_{\mu\nu}^{p(n)} = \left( -W_1^{p(n)}(x, Q^2) \tilde{g}_{\mu\nu} + W_2^{p(n)}(x, Q^2) \frac{1}{M^2} \tilde{p}_\mu \tilde{p}_\nu \right) \bar{u}(p, s) \mathcal{K} u(p, s), \quad (6.74)$$

with

$$\bar{u}(p, s) \mathcal{K} u(p, s) = [\bar{u}(p, s) \not{q} u(p, s) + \bar{u}(p, s) \not{p} u(p, s) + M] M / (p \cdot q). \quad (6.75)$$

Expression (6.74) is the off-shell generalization of eq. (5.8) where the nucleon off-shellness has been disregarded in the nucleon structure functions  $W_{1,2}$ .

By taking appropriate linear combinations of the components of the nucleon and nuclear hadronic tensors in the Bjorken limit one finally obtains the following convolution formula for the

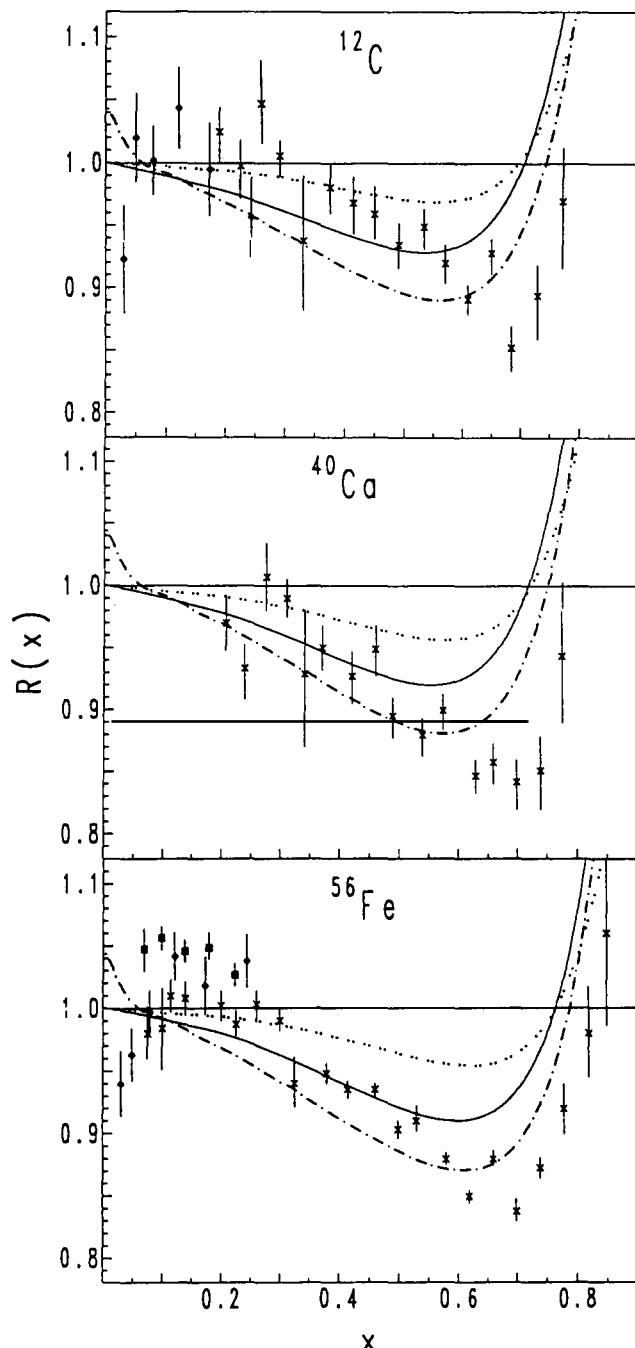


Fig. 28. The ratio  $R(x) = F_2^A(x)/F_2^D(x)$  and the EMC effect in nuclei. Dotted lines: HF results; full lines: correlated many-body approach; dot-dashed lines: correlated many-body approach including  $Q^2$ -rescaling of quark confinement radius (from ref. [275]).

nuclear structure function:

$$F_2^A(x, Q^2) = \int_{x \leq z} dz \left( \frac{Z}{A} f_A^p(z) F_2^p(x/z, Q^2) + \frac{N}{A} f_A^n(z) F_2^n(x/z, Q^2) \right), \quad (6.76)$$

where

$$f_A^{p(n)}(z) = \int d^{(4)}p \mathcal{S}_A^{p(n)}(p) z \delta\left(z - \frac{M_A}{M} \frac{\mathbf{p} \cdot \mathbf{q}}{P_A \cdot q}\right) \quad (6.77)$$

is the light cone momentum distribution satisfying the normalization

$$\int_0^\infty dz f_A^{p(n)}(z) = 1. \quad (6.78)$$

The factor  $z$  in eq. (6.77) is also known as the flux factor [197].

The invariant function  $\mathcal{S}_A^{p(n)}$  has the following expansion in the nonrelativistic limit [197]:

$$\sum_s \mathcal{S}_A(P, p, s) = S(|\mathbf{p}|, E) [1 + O(p^2/M^2) + \dots]. \quad (6.79)$$

Thus, neglecting relativistic corrections of order higher than  $p^2/M^2$ , one can relate the nuclear structure function  $F_2^A(x)$  to the hole spectral density and, ultimately, to quantities such as the nucleon momentum distribution, mean removal energy and mean kinetic energy, which are available from many-body theory. Nucleon–nucleon correlations, by strongly increasing the nucleon mean removal and kinetic energies, strongly enhance the EMC effect; as a result, the experimental behaviour is qualitatively reproduced in the region  $0.2 \leq x \leq 0.7$  (fig. 28). However, the results obtained with realistic spectral functions are systematically larger than the data at  $x \sim 0.6–0.7$ . A realistic many-body treatment of nuclear structure effects on the cross sections for deep inelastic scattering is able to reproduce the trend of the EMC effect in the region  $0.2 \leq x \leq 0.5$ , i.e., the slope of  $R(x)$ , but for  $0.5 \leq x \leq 0.9$  and for all nuclei considered (i.e., for nuclei in the range  $4 \leq A \leq 197$ ) a systematic discrepancy between experimental data and theoretical calculations appears to persist [275, 276, 170], with the predicted deviation of  $R(x)$  from unity much smaller than the experimental one, which might represent a clear signature of nonconventional effects. For  $x \geq 0.7$  binding corrections coming from a covariant derivation of the convolution formula [277] are numerically significant and help towards an agreement with the data.

## 7. Spin observables

Polarization experiments represent a rich source of information on the structure functions and in general on the target response [278]. Indeed, only for reactions with polarized particles is it possible to include in the cross section the six hadron responses appearing in eq. (5.3). In general

these reactions depend on a larger number of observables, which are hidden in the unpolarized case, where a sum and/or average over spin states is performed. Some of the polarization observables are expected to be sensitive to small components of the transition amplitude, which cannot be extracted without ambiguity from the unpolarized cross section. Therefore, their determination would impose severe constraints on theoretical models and appears of great interest. Moreover, only measurements of polarization observables allow a complete determination of transition amplitudes [279, 190, 14].

Unfortunately, experiments with polarized targets have to face the difficulty to maintain polarization in external cryogenic targets or to construct polarized jet targets with sufficiently high density, while the measurement of recoil polarization is performed with polarimeters which have a low efficiency. Therefore only few results are available [280, 281] and in the present situation a complete determination of the transition amplitudes represents a too ambitious program [282, 283]. However, a large number of polarization measurements will be carried out in the future when new facilities and improved experimental techniques are available.

In this section the formalism for coincidence reactions with nucleon emission is extended to include polarized electrons and spin degrees of freedom in the construction of the hadron tensor.

### 7.1. Electron polarization

With polarized electrons the lepton tensor  $L_{\mu\nu}$  in eq. (3.12) contains both a symmetric and an antisymmetric part in the Lorentz indices. However, the antisymmetric part,  $L_{\mu\nu}^h$ , enters the cross section only when the hadron tensor  $W_{\mu\nu}$  also contains an antisymmetric part. Current conservation makes it impossible to add a nonvanishing antisymmetric term to  $W_{\mu\nu}$  in the case of inclusive inelastic scattering unless the target is polarized [17]. Therefore in elastic and inelastic scattering the parity violating part does not contribute, and polarized and unpolarized electrons give identical cross sections. Single-arm electron scattering from unpolarized targets can be used to investigate the effect of the parity violating part of the nuclear current [284–287]. In these cases the main contribution to the helicity asymmetry comes from interference between the electromagnetic and the weak interactions, which is proportional to first order to the Fermi constant  $G$ . The effective lagrangian for this process contains both a vector ( $V$ ) and an axial-vector ( $A$ ) component of the hadron current, i.e.,

$$\mathcal{L}_{\text{eff}} = - (G/\sqrt{2}) [\bar{u}_f \gamma^\mu \gamma^5 u_i (\tilde{\alpha} V_\mu^3 + \tilde{\gamma} V_\mu^0) + \bar{u}_f \gamma^\mu u_i (\tilde{\beta} A_\mu^3 + \tilde{\delta} A_\mu^0)], \quad (7.1)$$

where the independent parameters  $\tilde{\alpha}, \tilde{\beta}, \tilde{\gamma}, \tilde{\delta}$  correspond to the isovector–vector, isovector–axial-vector, isoscalar–vector and isoscalar–axial-vector components, respectively.

In terms of quark functions  $u$  and  $d$  and neglecting any strange contribution, the different components of the hadron current are

$$\begin{aligned} V^{3\mu} &= \frac{1}{2}(\bar{u}\gamma^\mu u - \bar{d}\gamma^\mu d), & A^{3\mu} &= \frac{1}{2}(\bar{u}\gamma^\mu \gamma^5 u + \bar{d}\gamma^\mu \gamma^5 d), \\ V^{0\mu} &= \frac{1}{2}(\bar{u}\gamma^\mu u + \bar{d}\gamma^\mu d), & A^{0\mu} &= \frac{1}{2}(\bar{u}\gamma^\mu \gamma^5 u - \bar{d}\gamma^\mu \gamma^5 d). \end{aligned} \quad (7.2)$$

In electron scattering the scale of the effect is set by the quantity

$$A_0 = GQ^2/2\pi\alpha\sqrt{2}. \quad (7.3)$$

The helicity asymmetry is produced in quasi-elastic inclusive scattering by a parity violation contribution [287, 288]

$$A_0[v_L R_L^{\text{PV}}(\omega, Q^2) + v_T R_T^{\text{PV}}(\omega, Q^2) + v'_T R'_T^{\text{PV}}(\omega, Q^2)]. \quad (7.4)$$

The results of inelastic electron scattering [289, 290], combined with the atomic physics experiments of parity violation in heavy atoms, can give a complete determination of the parameters  $\tilde{\alpha}$ ,  $\tilde{\beta}$ ,  $\tilde{\gamma}$ ,  $\tilde{\delta}$ . In addition, the experiments of parity violation in elastic scattering on nuclei with  $S = T = 0$  give a direct determination of the coefficient  $\tilde{\gamma}$  [291].

With unpolarized targets an antisymmetric contribution to the hadron tensor arises when an emitted particle is detected in coincidence with the scattered electron. In terms of the kinematic variables defined in fig. 19 and assuming current conservation in the lepton tensor, it can be written as

$$W_A^{\mu\nu} = W_S \frac{1}{p' \cdot P} \frac{1}{2} (P^\mu p'^\nu - P^\nu p'^\mu). \quad (7.5)$$

Its contribution will show up in a new structure function, which in the laboratory frame on a spherical basis [see eqs. (6.4)] is

$$W_{01}^A = \frac{1}{2\sqrt{2}} \frac{|\mathbf{q}|}{Q} \frac{|\mathbf{p}'|}{E'} W_S \sin \gamma e^{-i\alpha}. \quad (7.6)$$

Correspondingly, with the definition [see eqs. (6.9)]

$$f'_{01} = (|\mathbf{q}|/Q) 2\text{Im}(W_{01} - W'_{0-1}), \quad (7.7)$$

the coincidence cross section (6.10) becomes [292, 16]

$$\frac{d\sigma}{dE' d\Omega dp'} = \sigma_M (\rho_{00} f_{00} + \rho_{11} f_{11} + \rho_{01} f_{01} \cos \alpha + \rho_{1-1} f_{1-1} \cos 2\alpha + h\rho'_{01} f'_{01} \sin \alpha), \quad (7.8)$$

where the coefficients  $\rho_{\lambda\lambda'}$  and  $\rho'_{01}$  depend on the electron kinematics and are defined in table 2 apart from a factor  $\beta$ . Alternatively

$$\begin{aligned} \frac{d\sigma}{dE' d\Omega dp'} &= \frac{\pi e^2}{2|\mathbf{q}|} \Gamma [W_T + \varepsilon_L W_L + \sqrt{\varepsilon_L(1+\varepsilon)} W_{TL} \cos \alpha + \varepsilon W_{TT} \cos 2\alpha \\ &\quad + h\sqrt{\varepsilon_L(1-\varepsilon)} W'_{TL} \sin \alpha], \end{aligned} \quad (7.9)$$

$$W'_{TL} = f'_{01}. \quad (7.10)$$

The fifth structure function  $f'_{01}$  ( $W'_{TL}$ ) arising in this case can only be observed when the emitted particle is detected out of the electron plane ( $\alpha \neq 0$ ) and can be separated by flipping the electron

helicity  $h$ . By definition [eqs. (7.7) and (7.10)] it is constructed from the same components of the hadron tensor as  $f_{01}$  ( $W_{TL}$ ), but for a different combination which is nonvanishing only if  $W_{\mu\nu}$  is antisymmetric. If  $W_{\mu\nu}$  is real and symmetric, as in PWIA or in general when FSI are absent, then the fifth structure function is identically zero [16]. Therefore it turns out to be entirely due and particularly sensitive to FSI, while other effects, e.g., two-body currents, give only a minor contribution (fig. 29).

The fifth structure function also vanishes in the particular case of a reaction proceeding through a channel in which a single phase dominates for all the projections of the current, i.e.,  $J^\mu \sim |J^\mu|e^{i\delta}$ . Then  $W'_{01}$  is real and  $f'_{01}$  vanishes [292]. In first approximation this could be the case of electron scattering in the  $\Delta$ -region, where the isobar excitation is driven to a large degree by the 33-amplitude with the single phase  $\delta_{33}$ . To the extent that  $f'_{01}$  does not vanish one is able to access information concerning interference of the 33-amplitude for other channels which are usually too weak to be investigated directly. In particular this could shed some light on the debated question of how large the electric quadrupole transition is with respect to the magnetic dipole one, whose size is expected to be of a few percent at moderate momentum transfer, but is predicted to be unity in the perturbative QCD limit simply because of helicity conservation [294].

## 7.2. Hadron tensor with polarized particles

For the most general reaction induced by polarized electrons, where also nuclear polarization is considered, the number of four-vectors for constructing the hadron tensor can increase and the problem arises of how many response functions occur in the cross section. The hadron tensor  $W_{\mu\nu}$  is built in terms of bilinear products of the electromagnetic current matrix elements. In turn, the currents are four-vectors which satisfy a continuity equation; this implies that only three components

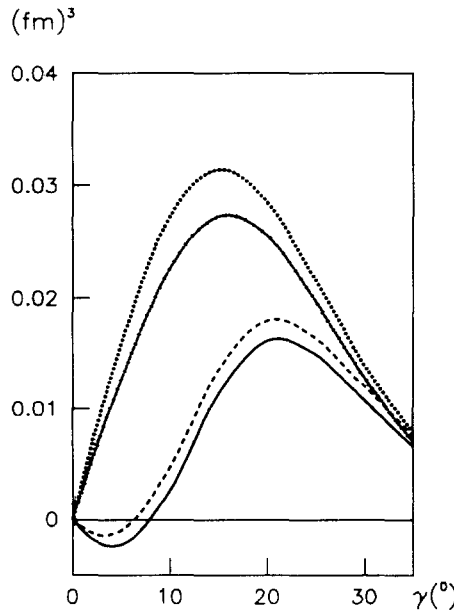


Fig. 29. The fifth structure function  $f'_{01}$  for the  $p_{1/2}$  hole in  ${}^{16}\text{O}$  at  $Q = 400$  MeV/c versus the emitted proton angle  $\gamma$  for different types of FSI. Optical potential from ref. [172] for the solid and the dashed lines, from ref. [126] for the dot-dashed and the dotted lines. The dot-dashed and the solid lines also include the contribution from two-body currents [218].

of the current are independent. Thus in general  $3 \times 3 = 9$  elements of the hadron tensor  $W_{\mu\nu}$  enter the cross section. A similar analysis [287] of the hadron tensor for a weakly interacting probe leads to a general structure with  $4 \times 4 = 16$  terms in the cross section, since in that case we have axial-vector as well as vector currents and the former are not conserved.

Therefore, the most general form for the coincidence cross section for electron scattering is obtained by contracting the lepton tensor with the hadron tensor as in eq. (5.3). Explicitly writing the dependence on the angle  $\alpha$  between the electron and the hadron planes, one thus has to combine the six independent elements of the lepton tensor with the nine independent elements of the hadron tensor as follows [293, 295]:

$$\begin{aligned} \frac{d\sigma}{dE' d\Omega dp'} = & \sigma_M \{ \rho_{00} f_{00} + \rho_{11} f_{11} + \rho_{01} (f_{01} \cos \alpha + \bar{f}_{01} \sin \alpha) \\ & + \rho_{1-1} (f_{1-1} \cos 2\alpha + \bar{f}_{1-1} \sin 2\alpha) \\ & + h [\rho'_{01} (f'_{01} \sin \alpha + \bar{f}'_{01} \cos \alpha) + \rho'_{11} f'_{11}] \}. \end{aligned} \quad (7.11)$$

Alternatively, with the hadron responses defined in table 4,

$$\begin{aligned} \frac{d\sigma}{dE' d\Omega dp'} = & \frac{\pi e^2}{2|\mathbf{q}|} \Gamma \{ W_T + \varepsilon_L W_L + \sqrt{\varepsilon_L(1+\varepsilon)} (W_{TL} \cos \alpha + \bar{W}_{TL} \sin \alpha) \\ & + \varepsilon (W_{TT} \cos 2\alpha + \bar{W}_{TT} \sin 2\alpha) \\ & + h [\sqrt{\varepsilon_L(1-\varepsilon)} (W'_{TL} \sin \alpha + \bar{W}'_{TL} \cos \alpha) + \sqrt{1-\varepsilon^2} W'_{TT}] \}. \end{aligned} \quad (7.12)$$

The structure functions appearing in eqs. (7.11) and (7.12) are defined similarly to the structure functions in eqs. (6.9) and (6.11). They are given in table 5 in terms of the matrix elements of the hadron current calculated in the CM frame on a spherical basis. They agree with the responses  $R$  of ref. [14] and with the structure functions of ref. [293], where they were defined in the laboratory frame with a different definition of the photon polarization vectors. Only, the sign of the structure functions  $f_{1-1}$  and  $\bar{f}_{1-1}$  is reversed with respect to the one of ref. [293].

Table 4  
The hadron responses

---

|   |
|---|
| $W_L = 2f_{00}$   |
| $W_T = f_{11}$  |
| $W_{TL} = f_{01} \quad \bar{W}_{TL} = \bar{f}_{01}$     |
| $W_{TT} = -f_{1-1} \quad \bar{W}_{TT} = -\bar{f}_{1-1}$ |
| $W'_{TL} = f'_{01} \quad \bar{W}'_{TL} = \bar{f}'_{01}$ |
| $W'_{TT} = f'_{11}$                                     |

---

Table 5  
Structure functions and hadron currents in the CM frame

|   |
|---|
| $f_{00} = ( \mathbf{q} ^2/Q^2) \sum_i \int_f  J_0 ^2$                                       |
| $f_{11} = \bar{\sum}_i \int_f ( J_1 ^2 +  J_{-1} ^2)$                                       |
| $f_{01} = ( \mathbf{q} /Q) \bar{\sum}_i \int_f 2\text{Re}(J_0 J_1^* - J_0 J_{-1}^*)$        |
| $\bar{f}_{01} = ( \mathbf{q} /Q) \bar{\sum}_i \int_f 2\text{Im}(J_0 J_1^* + J_0 J_{-1}^*)$  |
| $f_{1-1} = - \bar{\sum}_i \int_f 2\text{Re}(J_1 J_{-1}^*)$                                  |
| $\bar{f}_{1-1} = \bar{\sum}_i \int_f 2\text{Im}(J_1 J_{-1}^*)$                              |
| $f'_{01} = ( \mathbf{q} /Q) \bar{\sum}_i \int_f 2\text{Im}(J_0 J_1^* - J_0 J_{-1}^*)$       |
| $\bar{f}'_{01} = ( \mathbf{q} /Q) \bar{\sum}_i \int_f 2\text{Re}(J_0 J_1^* + J_0 J_{-1}^*)$ |
| $f'_{11} = \bar{\sum}_i \int_f ( J_1 ^2 -  J_{-1} ^2)$                                      |

In the general case, where the polarization of all the nuclear particles is considered, the hadron tensor  $W^{\mu\nu}$  is given by [296, 282, 297]

$$W^{\mu\nu} = \bar{\sum}_{\text{if } \alpha\alpha'} \sum_{\beta\beta'} \sum_{\gamma\gamma'} \langle \alpha\beta | J^\mu | \gamma \rangle \langle \alpha'\beta' | J^\nu | \gamma' \rangle^* \rho_{\alpha\alpha'}^P \rho_{\beta\beta'}^R \rho_{\gamma\gamma'}^T \delta(E_i - E_f), \quad (7.13)$$

where  $\rho^P$ ,  $\rho^R$  and  $\rho^T$  are polarization density matrices of the outgoing nucleon, of the residual nucleus and of the target, respectively. The indices  $\alpha$ ,  $\beta$  and  $\gamma$  label the magnetic quantum numbers of the intrinsic spin of the particles. In the CM frame of each particle the helicity basis can be used and the matrix elements of the electromagnetic current in eq. (7.13) become the helicity amplitudes.

Polarization density matrices can be written in terms of irreducible statistical tensors  $t_{kq}$  as [298]

$$\rho_{\gamma\gamma'} = (2s + 1)^{-1/2} \sum_{kq} (-)^{s-\gamma} (ss\gamma' - \gamma | kq) t_{kq}, \quad (7.14)$$

where  $s$  is the intrinsic spin of the particle. From eq. (7.14) we have

$$t_{00} = \text{Tr } \rho \quad (7.15)$$

and the normalization

$$t_{00} = 1 \quad (7.16)$$

is assumed.

For an unpolarized particle

$$\rho_{\gamma\gamma'} = (2s + 1)^{-1}\delta_{\gamma\gamma'} \quad (7.17)$$

and therefore

$$t_{kq} = 0, \quad \text{for } k \neq 0. \quad (7.18)$$

In the case of a particle with  $s = \frac{1}{2}$ , the polarization density matrix can be written as

$$\rho = \frac{1}{2}(1 + \mathbf{P} \cdot \boldsymbol{\sigma}), \quad (7.19)$$

where  $\mathbf{P}$  is the vector polarization and the cartesian components of  $\boldsymbol{\sigma}$  are given by the Pauli matrices.

### 7.3. Target polarization

When only the target is polarized, the cross section can be written in terms of the statistical tensors  $t_{kq}$  defined in eq. (7.14) as [298]

$$(d\sigma/d\Omega)_{\text{pol}} = \sigma_0 \sum_{kq} t_{kq} T_{kq}^*, \quad (7.20)$$

where  $\sigma_0$  is the unpolarized cross section and the tensors  $T_{kq}$  give the target analyzing power. If the target has spin  $s = \frac{1}{2}$ , a simple form is obtained, i.e.,

$$(d\sigma/d\Omega)_{\text{pol}} = \sigma_0(1 + \mathbf{P}^T \cdot \mathbf{A}^T), \quad (7.21)$$

where  $\mathbf{P}^T$  is the vector target polarization and  $\mathbf{A}^T$  the analyzing power, which can be determined through an asymmetry measurement.

With polarized electrons and  $s = \frac{1}{2}$  targets, the cross section becomes

$$(d\sigma/d\Omega)_{\text{pol}} = \sigma_0[1 + \mathbf{P}^T \cdot \mathbf{A}^T + h(\mathbf{A} + \mathbf{P}^T \cdot \mathbf{A}'^T)], \quad (7.22)$$

where  $\mathbf{A}$  is the electron analyzing power and  $\mathbf{A}'^T$  is the efficiency correlation coefficient.

In the  $s = \frac{1}{2}$  case the structure functions are given by

$$f_{\lambda\lambda'} = f_{\lambda\lambda'}^u + \mathbf{P}^T \cdot \mathbf{f}_{\lambda\lambda'}^T, \quad (7.23)$$

where  $f_{\lambda\lambda'}^u$  are the unpolarized structure functions and  $f_{\lambda\lambda'}^T$  give the contribution coming from polarization. In this case the components of  $A^T$  and  $A'^T$  in the reference frame of fig. 19 are

$$A_y^T = (K/\sigma_0)[2\varepsilon_L f_{00}^{Ty} + f_{11}^{Ty} + \sqrt{\varepsilon_L(1+\varepsilon)} f_{01}^{Ty} \cos \alpha + \varepsilon f_{1-1}^{Ty} \cos 2\alpha], \quad (7.24)$$

$$A_{x,z}^T = (K/\sigma_0)[\sqrt{\varepsilon_L(1+\varepsilon)} \bar{f}_{01}^{Tx,z} \sin \alpha + \varepsilon \bar{f}_{1-1}^{Tx,z} \sin 2\alpha], \quad (7.25)$$

$$A_y'^T = (K/\sigma_0) \sqrt{\varepsilon_L(1-\varepsilon)} f_{01}^{Ty} \sin \alpha, \quad (7.26)$$

$$A_{x,z}'^T = (K/\sigma_0)[\sqrt{1-\varepsilon^2} f_{11}^{Tx,z} + \sqrt{\varepsilon_L(1-\varepsilon)} \bar{f}_{01}^{Tx,z} \cos \alpha]. \quad (7.27)$$

From eq. (7.23) it is clear that the structure functions with target polarization are different from the corresponding unpolarized ones, which can be obtained by averaging the former ones over the direction of the target polarization.

In the general case structure functions depend on a large number of independent scalars, according to the kinematic variables involved in the particular process studied. However, one has at most four independent four-momenta in the Lorentz frame [10]. Therefore the hadron tensor can be built in terms of suitable combinations of those vectors with factors depending on the independent scalars, whose number increases with the number of kinematic variables required to define the hadron system. As a result the general form of the cross section for exclusive- $n$  electron scattering always has the form (7.11) or (7.12), and the general structure of the elements of the hadron tensor entering the cross section is always the same as that given in table 5.

In electromagnetic knockout reactions on polarized targets [293] there are four basic hadron variables, i.e. the target four-momentum  $P^\mu$  and spin  $s^\mu$ , the ejectile four-momentum  $p'^\mu$  and the momentum transfer  $q^\mu$ . In the laboratory frame, with the z-axis along  $\mathbf{q}$  and the hadron plane defining the (xz)-plane ( $\alpha = 0$ ), they are expressed as

$$\begin{aligned} P^\mu &= (M_T, 0), \\ p'^\mu &= (E', \mathbf{p}') = (E', p' \sin \gamma, 0, p' \cos \gamma), \\ q^\mu &= (\omega, \mathbf{q}) = (\omega, 0, 0, |\mathbf{q}|), \\ s^\mu &= (0, \mathbf{s}) = (0, \sin \theta^* \cos \phi^*, \sin \theta^* \sin \phi^*, \cos \theta^*), \end{aligned} \quad (7.28)$$

where the polarization direction of the target is specified by the zenithal angle  $\theta^*$  and the azimuthal angle  $\phi^*$ . In some particular cases the four vectors in eq. (7.28) are not linearly independent. This occurs when any two of the vectors  $\mathbf{q}$ ,  $\mathbf{P}'$  and  $\mathbf{s}$  are parallel or when they are all in the same plane. In order to avoid problems arising in such situations, it is convenient to deal with linearly independent four-vectors  $p'^\mu$ ,  $q^\mu$ ,  $s^\mu$  and  $\xi^\mu$ , where

$$\xi^\mu = \varepsilon^{\alpha\beta\gamma\mu} q_\alpha p'_\beta s_\gamma = (\mathbf{q} \cdot \mathbf{p}' \times \mathbf{s}, \omega \mathbf{p}' \times \mathbf{s} + E' \mathbf{s} \times \mathbf{q}). \quad (7.29)$$

Among them  $p'^\mu$ ,  $q^\mu$  and  $\xi^\mu$  are vectors, while  $s^\mu$  is a pseudovector. These vectors span the four-dimensional space-time. Only in the very particular case of  $\mathbf{q}$ ,  $\mathbf{p}'$  and  $\mathbf{s}$  being all parallel to each

other (superparallel kinematics) are they not independent. In this case only two linearly independent vectors can be considered, e.g.,  $s^\mu$  and  $q^\mu$ . This situation will be treated in a different way (see below).

In the general case current conservation is ensured by replacing  $p'^\mu$  and  $s^\mu$  by the gauge invariant vectors

$$\tilde{p}'^\mu = p'^\mu - \frac{\mathbf{q} \cdot \mathbf{p}'}{q_\lambda^2} q^\mu, \quad \tilde{s}^\mu = s^\mu - \frac{\mathbf{q} \cdot \mathbf{s}}{q_\lambda^2} q^\mu. \quad (7.30)$$

One can then define orthogonal vectors  $Z_i^\mu$  by performing a Gram–Schmidt orthogonalization on the above four vectors [293, 295]. The hadron tensor  $W^{\mu\nu}$  can be developed on the basis of the vectors  $Z_i^\mu$  as

$$W^{\mu\nu} = \sum_{ij} F_{ij} Z_i^\mu Z_j^\nu. \quad (7.31)$$

Current conservation gives

$$\sum_{ij} F_{ij} (\mathbf{q} \cdot \mathbf{Z}_i) Z_j^\nu = \sum_{ij} F_{ij} Z_i^\mu (\mathbf{q} \cdot \mathbf{Z}_j) = 0. \quad (7.32)$$

Orthogonality between  $\mathbf{q}$  and  $\mathbf{Z}_i$  gives  $\mathbf{q} \cdot \mathbf{Z}_i = q_\lambda^2 \delta_{iq}$ , so that

$$q_\lambda^2 \sum_j F_{qj} Z_j^\nu = q_\lambda^2 \sum_i F_{iq} Z_i^\mu = 0. \quad (7.33)$$

Therefore, due to the linear independence of the  $Z_i^\mu$ , one has

$$F_{qj} = F_{iq} = 0. \quad (7.34)$$

As a result of these properties, the hadron tensor  $W^{\mu\nu}$  can be expressed in terms of nine pieces, six of them symmetric and three antisymmetric in its Lorentz indices. One finally has

$$W^{\mu\nu} = W_S^{\mu\nu} + W_A^{\mu\nu}, \quad (7.35)$$

$$W_S^{\mu\nu} = A_1 \tilde{g}^{\mu\nu} + A_2 [\tilde{p}'^\mu \tilde{p}'^\nu]_S + A_3 [\tilde{s}^\mu \tilde{s}^\nu]_S + A_4 [\tilde{p}'^\mu \tilde{s}^\nu]_S + A_5 [\xi^\mu \tilde{p}'^\nu]_S + A_6 [\xi^\mu \tilde{s}^\nu]_S \quad (7.36)$$

$$W_A^{\mu\nu} = A_7 [\tilde{p}'^\mu \tilde{s}^\nu]_A + A_8 [\xi^\mu \tilde{p}'^\nu]_A + A_9 [\xi^\mu \tilde{s}^\nu]_A, \quad (7.37)$$

$$[a^\mu b^\nu]_{S,A} = a^\mu b^\nu \pm a^\nu b^\mu. \quad (7.38)$$

The form factors appearing in eqs. (7.36) and (7.37) are functions of the scalars  $q_\lambda^2$ ,  $\mathbf{q} \cdot \mathbf{p}'$ ,  $\mathbf{q} \cdot \mathbf{P}$ ,  $\mathbf{p}' \cdot \mathbf{P}$  and  $\xi \cdot \mathbf{P}$  and of the pseudoscalars  $\mathbf{q} \cdot \mathbf{s}$  and  $\mathbf{p}' \cdot \mathbf{s}$ . The form factors  $A_4$ ,  $A_6$ ,  $A_7$  and  $A_9$  must be pseudoscalars; they have the form

$$A_i = A'_i \mathbf{q} \cdot \mathbf{s} + A''_i \mathbf{p}' \cdot \mathbf{s}, \quad i = 4, 6, 7, 9, \quad (7.39)$$

where  $A'_i$  and  $A''_i$  are scalar functions.

In the case of target polarization along  $y$ ,  $s^\mu = (0, 0, 1, 0)$  and  $q \cdot s = p' \cdot s = 0$ . Therefore, necessarily the pseudoscalar form factors vanish and the total number of form factors reduces to five. On the other hand, because in this case  $\xi^y = 0$ , one also has

$$W_S^{\mu y} = W_S^{y\mu} = W_A^{\mu y} = W_A^{y\mu} = 0, \quad \mu \neq y. \quad (7.40)$$

As a consequence, in this case in eq. (7.11)  $f'_{11}$ ,  $\bar{f}_{01}$ ,  $\bar{f}_{1-1}$  and  $\bar{f}'_{01}$  vanish. Correspondingly in eq. (7.12),  $W'_{TT} = \bar{W}_{TL} = \bar{W}_{TT} = \bar{W}'_{TL} = 0$ .

In the superparallel kinematics there are only two linearly independent vectors, i.e.,  $q^\mu$  and  $s^\mu = (0, 0, 0, 1)$ . In this case eqs. (7.36) and (7.37) are replaced by the following ones:

$$W_S^{\mu\nu} = A_1 \tilde{g}^{\mu\nu} + A_3 [\tilde{s}^\mu \tilde{s}^\nu]_S, \quad (7.41)$$

$$W_A^{\mu\nu} = B_1 \epsilon^{\alpha\beta\mu\nu} q_\alpha s_\beta. \quad (7.42)$$

As a consequence, one has

$$\begin{aligned} W_S^{\mu\nu} &= 0, \quad \mu \neq \nu, \\ W_S^{xx} &= W_S^{yy} = -A_1, \\ W_A^{\mu z} &= W_A^{\mu 0} = W_A^{z\mu} = W_A^{0\mu} = 0, \\ W_A^{xy} &= -W_A^{yx} = B_1 \omega. \end{aligned} \quad (7.43)$$

Therefore only  $f_{00}$ ,  $f_{11}$  and  $f'_{11}$  survive in this case. Thus in the superparallel kinematics separation of the different responses appears simpler. In fact, a Rosenbluth separation with unpolarized electrons determines  $f_{00}$  and  $f_{11}$ ; then  $f'_{11}$  is simply determined by flipping the electron helicity.

In some cases a further simplification [293] arises from helicity conservation, because the spin projection  $M$  of the target,  $M'$  of the residual nucleus,  $s'$  of the ejectile and the index of the spherical component  $\lambda$  of the nuclear current are related:  $M + \lambda = M' + s'$ . Therefore in conditions such that  $M' = 0$ ,  $M = m = j$ , and  $j \geq \frac{3}{2}$ ,  $f_{00}$  vanishes and  $f_{11} = -f'_{11}$ . In addition, in PWIA also  $f_{11} = 0$  because the effective transverse current reduces in this case to the spin-magnetic current, which is averaged to zero when the orientation of the target spin is along  $q$ . One then expects in the real case a small, but unique response  $f_{11}$  determined by the transverse current. A longitudinal response  $f_{00} \neq 0$  would be a signal of other reaction mechanisms usually present in the cross section as small contributions and up to now overlooked.

In the case of a polarized target nucleon an alternative form of the antisymmetric part of the hadron tensor can be given as

$$W_{\mu\nu}^A = i\epsilon_{\mu\nu\alpha\beta} q^\alpha \left[ s^\beta \left( MG_1(\omega, Q^2) + \frac{p \cdot q}{M} G_2(\omega, Q^2) \right) - s \cdot q \frac{1}{M} p^\beta G_2(\omega, Q^2) \right], \quad (7.44)$$

where  $G_{1,2}(\omega, Q^2)$  are two new structure functions of the nucleon, which can be measured only with both polarized electrons and polarized target nucleons [299, 4].

#### 7.4. Nucleon recoil polarization

Here the specific situation is considered where a longitudinally polarized electron ejects a polarized nucleon from an unpolarized target. As a consequence of the spin- $\frac{1}{2}$  nature of the nucleons, the hadron tensor has at most a linear dependence upon the direction of the spin of the outgoing nucleon. The components of the hadron tensor can therefore be written as the sum of two parts, one independent of and one dependent on the nucleon vector polarization  $\mathbf{P}$  [190]:

$$W^{\mu\nu} = \frac{1}{2} \sum_{\alpha\alpha'} W_{\alpha\alpha'}^{\mu\nu} (1 + \mathbf{P} \cdot \boldsymbol{\sigma})_{\alpha\alpha'}. \quad (7.45)$$

Accordingly, the structure functions in eq. (7.11) are written in a way similar to eq. (7.23), i.e.,

$$f_{\lambda\lambda'} = h_{\lambda\lambda'}^u + \boldsymbol{\sigma}' \cdot \mathbf{h}_{\lambda\lambda'}, \quad (7.46)$$

where  $\boldsymbol{\sigma}'$  is a unit vector in the spin direction of the recoil nucleon.

The first term in the sum gives five spin independent structure functions, which can be written in terms of  $W_{\alpha\alpha'}^{\mu\nu}$  as

$$\begin{aligned} h_{00}^u &= W_{++}^{00}, & h_{11}^u &= W_{++}^{xx} + W_{++}^{yy}, & h_{01}^u &= -2\sqrt{2} \operatorname{Re} W_{++}^{0x}, \\ h_{1-1}^u &= W_{+-}^{xx} - W_{+-}^{yy}, & h_{01}'^u &= -2\sqrt{2} \operatorname{Im} W_{++}^{0x}, \end{aligned} \quad (7.47)$$

where the subscripts  $\pm$  correspond to  $\alpha, \alpha' = \pm \frac{1}{2}$ . These five structure functions depend on the kinematic variables  $\omega, q, p'$  and the angle  $\gamma$  between  $\mathbf{p}'$  and  $\mathbf{q}$ . When the cross section is summed over the magnetic quantum number of the ejectile, the above quantities go over to the five structure functions  $f_{00}, f_{11}, f_{01}, f_{1-1}$  and  $f_{01}'$  of the unpolarized case.

The second term in eq. (7.46) can be projected onto a basis of unit vectors, e.g.  $\hat{\mathbf{L}}$  (parallel to  $\mathbf{p}'$ ),  $\hat{\mathbf{N}}$  (in the direction of  $\mathbf{q} \times \mathbf{p}'$ ) and  $\hat{\mathbf{S}} = \hat{\mathbf{N}} \times \hat{\mathbf{L}}$ , which define the CM helicity frame of the particle. Thirteen new structure functions result, which are functions of the kinematical variables  $\omega, q, p'$  and  $\gamma$  as well as of the polarization direction of the ejectile. They can be measured only when the polarization of the ejectile is detected and they are averaged to zero when sum over the final spin is performed in the cross section. They are given by

$$\begin{aligned} h_{00}^N &= -\operatorname{Im} W_{+-}^{00}, & h_{11}^N &= -\operatorname{Im}(W_{+-}^{xx} + W_{+-}^{yy}), & h_{1-1}^N &= -\operatorname{Im}(W_{+-}^{xx} - W_{+-}^{yy}), \\ h_{01}^N &= 2\sqrt{2} \operatorname{Im} W_{+-}^{x0}, & h_{01}'^N &= 2\sqrt{2} \operatorname{Re} W_{+-}^{x0}, \\ h_{1-1}^S &= -2\operatorname{Re} W_{+-}^{xy}, & h_{01}^S &= 2\sqrt{2} \operatorname{Re} W_{+-}^{y0}, \\ h_{11}^S &= -2\operatorname{Im} W_{+-}^{yx}, & h_{01}'^S &= 2\sqrt{2} \operatorname{Im} W_{+-}^{y0}, \\ h_{1-1}^L &= -2\operatorname{Re} W_{+-}^{xy}, & h_{01}^L &= 2\sqrt{2} \operatorname{Re} W_{+-}^{y0}, \\ h_{11}^L &= -2\operatorname{Im} W_{+-}^{yx}, & h_{01}'^L &= 2\sqrt{2} \operatorname{Im} W_{+-}^{y0}. \end{aligned} \quad (7.48)$$

The sign of the ( $\lambda\lambda' = 1 - 1$ ) structure functions in eqs. (7.47) and (7.48) is reversed with respect to the one in ref. [190].

If the nucleon polarization is made explicit, the coincidence cross section can be written as [190]

$$\frac{d\sigma}{dE' d\Omega dp'} = \sigma_0 \frac{1}{2} [1 + \mathbf{P} \cdot \boldsymbol{\sigma}' + h(A + \mathbf{P}' \cdot \boldsymbol{\sigma}')], \quad (7.49)$$

where  $\sigma_0$  is the unpolarized differential cross section,  $\mathbf{P}$  is the outgoing nucleon polarization,  $A$  the electron analyzing power and  $\mathbf{P}'$  the polarization transfer coefficient. The unpolarized cross section can be written in terms of four structure functions [see eqs. (6.10) and (6.12)]

$$\sigma_0 = K[2\varepsilon_L h_{00}^u + h_{11}^u + \sqrt{\varepsilon_L(1+\varepsilon)} h_{01}^u \cos \alpha + \varepsilon h_{1-1}^u \cos 2\alpha], \quad (7.50)$$

$$K = (\pi e^2 / |\mathbf{q}|) \Gamma. \quad (7.51)$$

The electron analyzing power is

$$A = (K/\sigma_0) \sqrt{\varepsilon_L(1-\varepsilon)} h_{01}^u \sin \alpha. \quad (7.52)$$

The components of  $\mathbf{P}$  and  $\mathbf{P}'$  are

$$P^N = (K/\sigma_0) [2\varepsilon_L h_{00}^N + h_{11}^N + \sqrt{\varepsilon_L(1+\varepsilon)} h_{01}^N \cos \alpha + \varepsilon h_{1-1}^N \cos 2\alpha], \quad (7.53)$$

$$P^{L,S} = (K/\sigma_0) [\sqrt{\varepsilon_L(1+\varepsilon)} h_{01}^{L,S} \sin \alpha + \varepsilon h_{1-1}^{L,S} \sin 2\alpha], \quad (7.54)$$

$$P'^N = (K/\sigma_0) \sqrt{\varepsilon_L(1-\varepsilon)} h_{01}^{N'} \sin \alpha, \quad (7.55)$$

$$P'^{L,S} = (K/\sigma_0) [\sqrt{1-\varepsilon^2} h_{11}^{L,S} + \sqrt{\varepsilon_L(1-\varepsilon)} h_{01}^{L,S} \cos \alpha]. \quad (7.56)$$

The structure functions which are multiplied by  $\sin \alpha$  or  $\sin 2\alpha$  do not contribute to the cross section in coplanar kinematics. As a consequence, in coplanar kinematics

$$A = 0, \quad \mathbf{P} \cdot \boldsymbol{\sigma}' = \mathbf{P} \cdot \hat{\mathbf{N}}, \quad \mathbf{P}' \cdot \hat{\mathbf{N}} = 0, \quad (7.57)$$

and therefore only the components  $P^N$ ,  $P'^S$  and  $P'^L$  survive.

Furthermore, without FSI,  $A$  and  $\mathbf{P}$  vanish identically. This occurs for  $A$  because the corresponding bilinear products of the matrix elements of the nuclear current are real in this case, and for  $\mathbf{P}$  because of rotational invariance about  $\mathbf{q}$ .

In parallel kinematics, where  $\mathbf{p}'$  is parallel to  $\mathbf{q}$ , a great simplification occurs because many structure functions do not contribute. As  $\alpha$  is not defined in parallel kinematics, the simplest way to obtain the appropriate limit of the cross section is to consider it as the limit  $\alpha \rightarrow 0$  ( $\pi$ ) approached with the spin orientation in an arbitrary direction relative to the coordinate system. Assuming that

the cross section is a well-behaved function in this limit, it must become independent of  $\alpha$ . Since the structure functions do not depend on  $\alpha$ , one must have

$$\sigma_0 = K(2\epsilon_L h_{00}^u + h_{11}^u). \quad (7.58)$$

Similar considerations applied to the polarization observables [190, 300] give

$$P^N = (K/\sigma_0) \sqrt{\epsilon_L(1 + \epsilon)} h_{01}^N, \quad (7.59)$$

$$P^L = (K/\sigma_0) \sqrt{1 - \epsilon^2} h_{11}^L, \quad (7.60)$$

$$P^S = (K/\sigma_0) \sqrt{\epsilon_L(1 - \epsilon)} h_{01}^S. \quad (7.61)$$

In addition,  $h_{11}^L = h_{11}^u$  for a nucleon emitted from a  $j = \frac{1}{2}$  shell [190]. Therefore, parallel kinematics in principle represents a good opportunity for separating spin dependent structure functions.

Table 6 contains a summary of the properties of the structure functions [300]. The behaviour of the hadron tensors under time reversal and parity transformation has the property

$$W^{\mu\nu}(s_R, (-)) = W^{\nu\mu}(-s_R, (+)), \quad (7.62)$$

where  $s_R$  is the unit vector in the direction of the ejectile rest frame spin, and the dependence on the final state boundary condition for incoming ( $-$ ) and outgoing ( $+$ ) scattered waves is exhibited. For nucleon knockout, the ( $-$ ) condition is appropriate. When the boundary conditions can be ignored, as in PWIA, eq. (7.62) states that the symmetric part of  $W^{\mu\nu}$  is independent of  $s_R$  and that the antisymmetric part is proportional to  $s_R$ . This is because the dependence of  $W^{\mu\nu}$  on  $s_R$  is at most linear [see eq. (7.46)]. In table 6 the structure functions which survive condition (7.62) when the boundary conditions are ignored are labelled “even” while those which do not are labelled “odd”. Without FSI odd structure functions, and therefore  $A$  and  $P$ , vanish. The last column in table 6 concerns reflection symmetry through the electron scattering plane of the term in the cross section containing the specified structure function. The most easily isolated structure functions are those which can be measured in the electron scattering plane and which are odd under reflection through this plane.

As a consequence of their general properties one expects different sensitivity of the structure functions to different physical effects. In particular, those vanishing in PWIA are suitable for investigating FSI effects, while those which are already different from zero in PWIA will be sensitive to the model dynamics. Such an investigation on complex nuclei has just started for the quasi-free nucleon knockout. Relativistic effects have been studied in ref. [300]. Meson exchange currents and isobar excitation in the intermediate state have been considered in refs. [301, 302, 209, 218].

The nucleon recoil polarization appears to be the first and simplest quantity which can be measured. With an unpolarized electron beam and in coplanar kinematics, only the component  $P^N$  survives. As it vanishes in PWIA, its measurement would give direct information on FSI. A similar situation occurs for the fifth structure function  $f'_{01}$  of section 7.1, whose measurement is, however, more complicated, as its requires both a polarized electron beam and out-of-plane kinematics. A numerical example of  $P^N$  for  $p_{1/2}$  and  $p_{3/2}$  hole in  $^{16}\text{O}$  is shown in fig. 30. It turns out to be only

Table 6  
Properties of the structure functions

| Structure functions | Electron polarization required | Survives in plane | Survives in parallel kinematics | Under time reversal and parity | Reflection symmetry |
|---------------------|--------------------------------|-------------------|---------------------------------|--------------------------------|---------------------|
| $h_{00}^u$          | no                             | yes               | yes                             | even                           | even                |
| $h_{00}^N$          | no                             | yes               | no                              | odd                            | even                |
| $h_{11}^u$          | no                             | yes               | yes                             | even                           | even                |
| $h_{11}^N$          | no                             | yes               | no                              | odd                            | even                |
| $h_{1-1}^u$         | no                             | yes               | no                              | even                           | even                |
| $h_{1-1}^N$         | no                             | yes               | no                              | odd                            | even                |
| $h_{1-1}^L$         | no                             | no                | no                              | odd                            | odd                 |
| $h_{1-1}^S$         | no                             | no                | no                              | odd                            | odd                 |
| $h_{01}^u$          | no                             | yes               | no                              | even                           | odd                 |
| $h_{01}^N$          | no                             | yes               | yes                             | odd                            | odd                 |
| $h_{01}^L$          | no                             | no                | no                              | odd                            | even                |
| $h_{01}^S$          | no                             | no                | yes                             | odd                            | even                |
| $h_{01}^{\prime u}$ | yes                            | no                | no                              | odd                            | even                |
| $h_{01}^{\prime N}$ | yes                            | no                | yes                             | even                           | even                |
| $h_{01}^{\prime L}$ | yes                            | yes               | no                              | even                           | odd                 |
| $h_{01}^{\prime S}$ | yes                            | yes               | yes                             | even                           | odd                 |
| $h_{11}^{\prime L}$ | yes                            | yes               | yes                             | even                           | even                |
| $h_{11}^{\prime S}$ | yes                            | yes               | no                              | even                           | even                |

little affected by MEC and isobar excitation, whereas the strong dependence on FSI is confirmed. The opposite sign between the two hole states stems from the general behaviour of  $\mathbf{P}$  when dealing with the spin-orbit  $j$ -doublet [190] and is determined by an effective polarization of the bound proton, which is produced by the combined effect of spin-orbit coupling and optical potential.

A nontrivial relationship exists between the polarizations which are defined above and those experimentally accessible, due to the use of a spectrometer to measure the kinematical variables of the emitted proton [303, 304]. The presence of the magnetic field in the spectrometer, however, makes it possible to determine the longitudinal recoil polarization without a triple scattering experiment.

The polarization  $P_{sp}$  in the reference frame of a focal plane polarimeter is related to the polarization of the knocked out proton by the relationship [305, 306]

$$\mathbf{P}_{sp} = M_s M_p \mathbf{P}, \quad (7.63)$$

where  $M_s$  is the unitary matrix representing the spin transport through the spectrometer and  $M_p$  is the transformation matrix from the proton system to the spectrometer system.

To first order the spin transport in the spectrometer results in the precession of an angle  $\chi$  around the direction of the magnetic field given by [307]

$$\chi = (E'/M)(\frac{1}{2}g_p - 1)\psi, \quad (7.64)$$

where  $E'$ ,  $M$  and  $g_p$  are the energy, mass and  $g$ -factor of the proton, respectively, and  $\psi$  is the bending angle of the trajectory through the spectrometer.

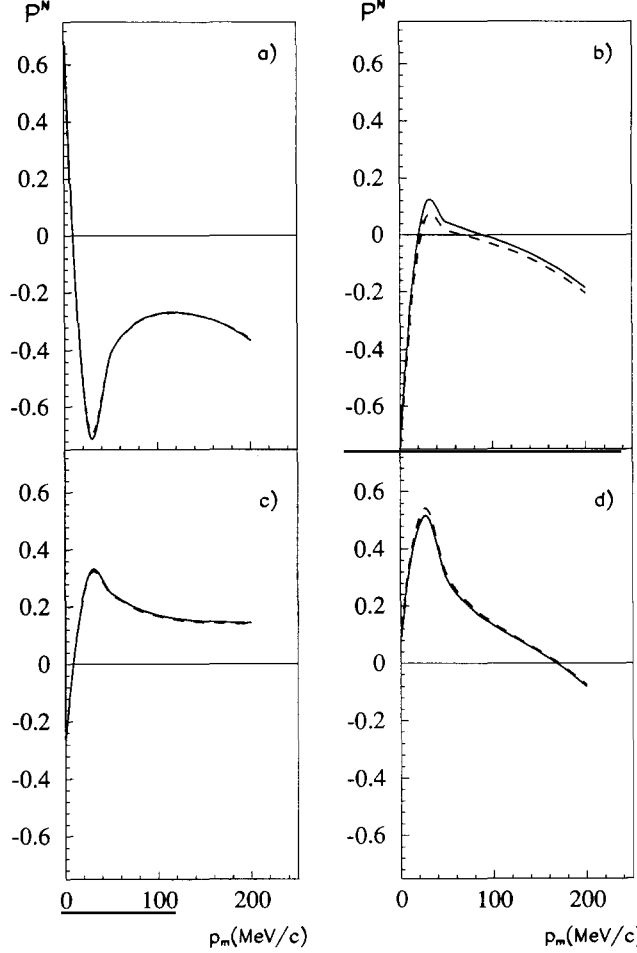


Fig. 30. The polarization normal to the scattering plane of an emitted proton of 150 MeV at constant  $(\omega, \mathbf{q})$  in coplanar kinematics; (a) and (b) for a  $p_{1/2}$  hole in  $^{16}\text{O}$  with optical potential from ref. [126] and from ref. [172], respectively, (c) and (d) for a  $p_{3/2}$  hole in  $^{16}\text{O}$  with optical potential from ref. [126] and from ref. [172], respectively. Dashed line for DWIA and solid line including two-body currents (from ref. [302]).

The effect of  $M_p$  is a rotation around the direction ( $L$ ) of the proton momentum by an angle  $\varepsilon$  given by

$$\cos \varepsilon = \cos \alpha / \cos \phi_{sp}, \quad \text{with} \quad \sin \phi_{sp} = \sin \alpha \sin \gamma, \quad (7.65)$$

where  $\phi_{sp}$  is the angle of the spectrometer with respect to the horizontal plane, which is the scattering plane of the electron.

The polarization components before (SNL) and after (sn'') the spectrometer are related by the equations

$$\begin{aligned} P_{sp}^s &= P^s \cos \varepsilon - P^N \sin \varepsilon, \\ P_{sp}^n &= P^s \cos \chi \sin \varepsilon - P^N \cos \chi \cos \varepsilon - P^L \sin \chi, \\ P'_{sp} &= P^s \sin \chi \sin \varepsilon + P^N \sin \chi \cos \varepsilon + P^L \cos \chi. \end{aligned} \quad (7.66)$$

As  $P'$  cannot be directly measured, the quantities  $P^S$ ,  $P^N$  and  $P^L$  can be extracted by measuring  $P^S$  and  $P^N$  at two different values of  $\chi$ . This can be done by varying the magnetic field of the spectrometer.

If the electrons are polarized, the components of  $P$  and  $P'$  can be disentangled by flipping the electron helicity.

In coplanar kinematics, where  $P^S = P^L = P'^N = 0$ , we have simply

$$P_{sp}^n = P^N \cos \chi, \quad P_{sp}'^n = -P'^L \sin \chi, \quad P_{sp}'^s = P'^S. \quad (7.67)$$

In this case the polarizations can be obtained through a measurement of the right-left asymmetry with respect to the spin orientation [303].

### 7.5. Complete determination of the scattering amplitudes

The most elementary constituents of the cross section are represented by the scattering amplitudes, whose complete determination, although extremely complicated from an experimental point of view, would allow one to extract all of the interesting information available from the considered process and could impose severe constraints on any theoretical calculation. Polarization experiments are essential to any attempt to completely determine the scattering amplitudes. In this section we will discuss the possibility of such an achievement for the  $(e, e'p)$  reaction, without using a specific model.

A scattering process involving  $n$  particles with spin  $s_i$  is completely described by  $N = \prod_{i=1}^n (2s_i + 1)$  scattering amplitudes, which are functions of the dynamical variables [298]. All of the observables can be written as a sum of bilinear products of these scattering amplitudes. Thus, for a given set of dynamical variables there are  $N^2$  observables that can in principle be measured, including coincidence measurements of the polarizations of all the incoming and outgoing particles, which is generally beyond the reach of experimental capabilities. These  $N^2$  possible measurements give  $N^2$  real parameters, from which the  $2N$  real parameters of the amplitudes can be determined. In a parity conserving process the number of independent amplitudes is reduced to  $N/2$ , which give  $N - 1$  real parameters, excluding an overall phase which cannot be determined.

The one-photon exchange mechanism allows one to represent the  $A(e, e'p)B$  reaction as the interaction of a virtual photon with a target  $A$  (with spin  $s_A$ ), leading to a residual nucleus  $B$  (with spin  $s_B$ ) and an outgoing proton, which gives

$$N = 3 \times 2 \times (2s_A + 1)(2s_B + 1) \quad (7.68)$$

scattering amplitudes.  $N/2$  of them are independent and  $N - 1$  real parameters have to be determined. Now we want to investigate which sets of measurements are necessary and sufficient to fully determine the scattering amplitudes. Only a part of the available observables must be measured to achieve this goal.

As the number of real parameters depends on the intrinsic spin of the particles involved in the reaction, the simplest situation occurs for  $s_A = 0$  and  $s_B = \frac{1}{2}$ , or, inversely,  $s_A = \frac{1}{2}$  and  $s_B = 0$ , and gives 6 independent amplitudes and 11 real parameters. All other cases are much more complicated and give a larger number of real parameters. As an example, for deuteron electrodisintegration, where  $s_A = 1$ ,  $s_B = \frac{1}{2}$ , 35 real parameters have to be determined, as discussed in ref. [14].

The situation where  $s_A = 0$  and  $s_B = \frac{1}{2}$  was considered in ref. [190] as an illustrative case. Processes of this type are represented by reactions which have been already experimentally investigated in the unpolarized situation, such as  ${}^4\text{He}(\text{e}, \text{e}'\text{p}){}^3\text{H}$  and  ${}^{16}\text{O}(\text{e}, \text{e}'\text{p}){}^{15}\text{N}$ , leaving the residual nucleus in its ground state, or also  ${}^{12}\text{C}(\text{e}, \text{e}'\text{p}){}^{11}\text{B}^*(2.12 \text{ MeV})$ , where the residual nucleus is left in the excited  $\frac{1}{2}$  state at 2.12 MeV. A similar analysis for the situation corresponding to  $s_A = \frac{1}{2}$  and  $s_B = 0$  was presented in ref. [282]. Processes of this type are represented, e.g., by  $\text{p}(\text{e}, \text{e}'\text{p})\pi^0$  and  ${}^3\text{He}(\text{e}, \text{e}'\text{p})\text{np}$ , where the kinetic energy of the np system is less than few MeV and can be approximated by the  ${}^1\text{S}_0$  final state. In particular, while the latter reaction is sensitive to the neutron electric form factor, a model independent determination seems to be feasible of the quadrupole amplitudes of the N– $\Delta$  transition by looking at the longitudinal–transverse response functions in the  $(\text{e}, \text{e}'\text{p})\pi^0$  reaction [308].

In the CM of each particle, the helicity basis can be used and the scattering amplitudes become the helicity amplitudes [296]  $\langle \alpha\beta|J_\lambda|\gamma \rangle$  of eq. (7.13), where  $\alpha, \beta, \gamma$  and  $\lambda$  denote the helicity of the nucleon, of the residual nucleus, of the target and of the virtual photon, respectively. In the situation, e.g., where  $s_A = 0$  and  $s_B = \frac{1}{2}$ , parity conservation gives

$$\langle -\alpha -\beta|J_{-\lambda}|0 \rangle = (-)^{\lambda+\alpha+\beta} \langle \alpha\beta|J_\lambda|\gamma \rangle \quad (7.69)$$

and the six independent helicity amplitudes are defined as [190]

$$\begin{aligned} H_1 &= \langle -\frac{1}{2} -\frac{1}{2}|J_1|0 \rangle, & H_2 &= \langle -\frac{1}{2}\frac{1}{2}|J_1|0 \rangle, & H_3 &= \langle \frac{1}{2} -\frac{1}{2}|J_1|0 \rangle, \\ H_4 &= \langle \frac{1}{2}\frac{1}{2}|J_1|0 \rangle, & H_5 &= \langle \frac{1}{2}\frac{1}{2}|J_0|0 \rangle, & H_6 &= \langle \frac{1}{2} -\frac{1}{2}|J_0|0 \rangle. \end{aligned} \quad (7.70)$$

The cross section and all other observables can be written in terms of bilinear products of helicity amplitudes. However, they can be derived in a particularly simple way in terms of transversity amplitudes [309]. As an example, when  $s_A = 0$  and  $s_B = \frac{1}{2}$ , they are defined in terms of the  $H_i$  as [190]

$$\begin{aligned} b_{1,2} &= \frac{1}{2}[-H_1 + H_4 \pm i(H_2 + H_3)], & b_{3,4} &= \frac{1}{2}[-H_1 - H_4 \pm i(H_2 - H_3)], \\ b_{5,6} &= (1/\sqrt{2})[H_5 \pm iH_6], \end{aligned} \quad (7.71)$$

where the upper (lower) sign refers to index  $i$  ( $j$ ) of  $b_{i,j}$ . When expressed in terms of the  $b_i$ , the structure functions become the real and imaginary parts of bilinear products of  $b_i$ 's [190, 282]. This form makes it comparatively easy to understand how, through separation of structure functions, the scattering amplitudes can be determined.

Determination strategies cannot be discussed in practice without considering the explicit expression of observables in terms of transversity amplitudes, which are very cumbersome. Moreover, each specific situation has to be individually considered. Some examples are discussed in refs. [190, 282]. Here we only want to give some general indications.

If we must determine  $N - 1$  real parameters, at least  $N - 1$  measurements are needed. However, some further measurements are required in general to resolve discrete ambiguities arising in the determination of the relative phases of the amplitudes [309]. Alternatively, these ambiguities can be solved by taking recourse to the analyticity of the scattering amplitudes, once the parameters have been determined for values of the dynamical variables close to the considered ones [190].

Some observables give only the moduli of the transversity amplitudes, e.g., measurements of the unpolarized structure functions  $h^u$ , and the structure functions  $h^N$ , corresponding to an outgoing nucleon or, equivalently, a recoiling nucleus with a polarization normal to the  $p, q$  plane. Other observables give the real and imaginary parts of bilinear products of the form  $b_i^* b_j$  and allow one to determine the relative phases  $\phi_{ij} = (\phi_i - \phi_j)$ . To completely remove the ambiguity, both the “paired” amplitudes containing the real and the imaginary part must be measured. However, this same measurement will also give, together with, e.g.,  $\phi_{ij}$ , the product  $|b_i||b_j|$  and only one other measurement is needed to determine the two moduli. The program requiring the fewest number of measurements is therefore one in which paired amplitudes, together with only a few moduli, are measured [282]. Unfortunately, measurements of paired amplitudes will generally be more difficult, as they usually involve complicated polarization observables. Therefore the best experimental program may be to measure moduli, if they are easy, and paired amplitudes as needed to eliminate ambiguities.

A complete determination cannot be obtained without out-of-plane experiments and without resorting to polarization measurements. The separation of all structure functions is unnecessary, as some of them depend on others and their measurements does not give any new information [190, 309]. Anyhow, if  $s_B \neq 0$  both measurements of outgoing nucleon and recoil nucleus polarization are needed; otherwise experiments with a polarized target are necessary. However, no measurements for the reaction where more hadrons than one are polarized at the same time are required [190]. Indeed, it is a general result that complete determination always requires double, but never triple polarization experiments [298]. We recall that in the one-photon exchange approximation the structure functions result as components of the virtual photon polarization, and therefore a measurement of a polarized hadron corresponds to a double polarization experiment.

If the incident electron is longitudinally polarized, a new class of structure functions originates. Although in general their measurement is not needed for a complete determination [190], this does not absolutely mean that such experiments are useless. In fact, as structure functions depend on dynamical variables, only the individual analysis of each specific kinematic situation and of available experimental apparatus can decide the best method for separating the amplitudes experimentally. Moreover, a set of measurements which is in general complete, may not be complete in a particular kinematic situation, where additional measurements may become necessary [298, 190]. The example of parallel kinematics for the case  $s_A = 0$  and  $s_B = \frac{1}{2}$  is considered in ref. [190], where only four measurements are needed, one of which requires a polarized electron beam, while no measurements of recoil nucleus polarization are necessary.

## 8. Final discussion

Nuclear phenomena related to inclusive and semi-inclusive electron scattering at intermediate energy have been reviewed; the potentialities of the electromagnetic probe have been discussed in terms of measurable form factors and structure functions representing the response of the hadron system under investigation. In the comparison with the available data the picture of an atomic nucleus built by strongly interacting nucleons and mesons comes out as a successful starting point. The composite nature of nucleons is only reflected in their electromagnetic form factors.

However, some problems are still open. With present day experimentation a large domain of the  $(\omega, q)$ -plane is accessible to study the hadron response under a variety of kinematic conditions. In inclusive scattering only the quasi-elastic region has been investigated in a detailed manner with separation of longitudinal and transverse responses. Only recently have some data been taken

around the  $\Delta$  peak. Here the separation of the different responses is very important for understanding the dynamics of  $\Delta$  formation and propagation inside nuclear matter. Semi-inclusive scattering experiments with detection of the produced pion are the necessary complementary tool both in the dip and in the  $\Delta$  region.

Nucleon knockout has been extensively studied in the quasi-elastic region and reasonably understood for valence nucleons at the cross section level. Separation of the different structure functions is only available in a few cases and under particular kinematic conditions. The existing data already suggest that merely confining oneself to nucleon degrees of freedom could not be sufficient for a consistent description. Deep lying holes are also interesting because they probe short time phenomena and correlations in nuclei. At high energy transfer, however, many-particle emission becomes dominant and requires a careful analysis of the exclusive process, which is probably beyond present capabilities.

Spin observables represent a rich source of spectroscopic information. The experimental difficulties to maintain a polarized beam and/or a polarized target have limited the analysis to very few cases. The field is, however, extremely important and is receiving much attention. In particular, with the construction of polarimeters the recoil polarization of produced particles becomes measurable. This will help towards a complete determination of the transition amplitudes with stringent constraints on the theoretical models.

From the theoretical side, the many-body theory of nuclear matter based on the Schrödinger equation is quite successful in reproducing the response at low energy and momentum transfer. The key ingredient is the spectral density, which can be derived for infinite nuclear matter from first principles and for finite nuclei under suitable approximations. However, the hadron current and final state interactions have to be included in the calculation consistently. While this is in principle possible, heavy approximations are necessary in practice. This introduces some uncertainty in the theoretical results, which, e.g., can be estimated to be of the order of 10% in the spectroscopic factors extracted from nucleon knockout experiments. With separation of the different structure functions a better accuracy is desired.

Increasing the energy and momentum transfer, mesonic and subnucleon degrees of freedom also have to be considered. Together with a better knowledge of the nucleon form factors a fully relativistic treatment is required. A relativistic description of the deuteron has been achieved, but in spite of a big effort the situation of complex nuclei is still far from being satisfactory. With the advent of CEBAF and other multi-GeV electron facilities this is an open problem.

Two-step mechanisms and multi-particle emission have to be included in the formalism. In particular, two-particle emission is in principle interesting for investigating correlations in nuclei. But a consistent theory is only now developing and still unclear indications are available about which are the best kinematic conditions to grasp the relevant information.

In any case, electron scattering remains the best tool for precision nuclear physics and justifies all the efforts done both experimentally and theoretically for improvements and progress.

## Acknowledgements

This review is partially based on work performed by the authors at the Dipartimento di Fisica Teorica e Nucleare of the University of Pavia and within the activities of the Istituto Nazionale di Fisica Nucleare in Pavia, whose computing facilities have been extensively used. The authors are also grateful to F. Cannata, F. Capuzzi, S. Frullani and M. Radici, who collaborated at various stages of the research. Many useful discussions are acknowledged with the scientists of the different

laboratories where intermediate energy nuclear physics is studied, in particular those of CEN Saclay, NIKHEF-K and CEBAF. Special thanks are due to H.P. Blok, S. Fantoni, F. Gross, E. Jans, L. Lapikás, A. Magnon, J. Morgenstern, J. Mougey, G. Orlandini and P.K.A. de Witt Huberts. In the preparation of the manuscript useful suggestions were offered by W.M. Alberico, C. Ciofi degli Atti and G. van der Steenhoven, to whom the authors are deeply indebted.

## References

- [1] J.D. Bjorken and S.D. Drell, *Relativistic Quantum Mechanics* (McGraw-Hill, New York, 1964).
- [2] H. Überall, *Electron Scattering from Complex Nuclei* (Academic Press, London, 1971).
- [3] E. Amaldi, S. Fubini and G. Furlan, *Pion Electroproduction*, Springer Tracts of Modern Physics, vol. 83 (Springer, Berlin, 1979).
- [4] F.E. Close, *An Introduction to Quarks and Partons* (Academic Press, London, 1979).
- [5] S. Frullani and J. Mougey, in: *Advances in Nuclear Physics*, vol. 14, eds. J.W. Negele and E. Vogt (Plenum, New York, 1984) p.1.
- [6] T. de Forest Jr. and J.D. Walecka, *Adv. Phys.* 15 (1966) 1.
- [7] N. Dombey, *Rev. Mod. Phys.* 41 (1969) 236; in: *Hadronic Interactions of Electrons and Photons*, eds. J. Cumming and H. Osborn (Academic Press, London, 1971) p. 17.
- [8] A. Donnachie, in: *High Energy Physics*, vol 5, ed. E.H.S. Burhop (Academic Press, New York, 1972) p. 1.
- [9] C. Ciofi degli Atti, *Prog. Part. Nucl. Phys.* 3 (1980) 163.
- [10] T.W. Donnelly, *Prog. Part. Nucl. Phys.* 13 (1985) 183.
- [11] L.L. Frankfurt and M.I. Strikman, *Phys. Rep.* 160 (1988) 235.
- [12] D. Drechsel and M.M. Giannini, *Rep. Progr. Phys.* 52 (1989) 1083.
- [13] C. Möller, *Z. Phys.* 70 (1931) 786.
- [14] V. Dmitrasinovic and F. Gross, *Phys. Rev. C* 40 (1989) 2479.
- [15] W. Fabian and H. Arenhövel, *Nucl. Phys. A* 314 (1979) 253.
- [16] S. Boffi, C. Giusti and F.D. Pacati, *Nucl. Phys. A* 435 (1985) 697.
- [17] T.W. Donnelly and A.S. Raskin, *Ann. Phys. (NY)* 169 (1986) 247; 191 (1989) 78.
- [18] J. Dechargé and D. Gogny, *Phys. Rev. C* 21 (1980) 1568.
- [19] H. Euteneuer, J. Friedrich and N. Voegler, *Nucl. Phys. A* 298 (1978) 452.
- [20] J.M. Cavedon, B. Frois, D. Goutte, M. Huet, Ph. Leconte, X.H. Phan, S.K. Platchkov, C.N. Papanicolas, S.E. Williamson, W. Boeglin, I. Sick and J. Heisenbeg, *Phys. Rev. Lett.* 58 (1987) 195.
- [21] I. Sick, *Nucl. Phys. A* 218 (1974) 509.
- [22] A.M. Bincer, *Phys. Rev.* 118 (1960) 855.
- [23] S.D. Drell and H.R. Pagels, *Phys. Rev.* 140 (1965) B 397.
- [24] E.M. Nyman, *Nucl. Phys. A* 154 (1970) 97; A 160 (1971) 517.
- [25] H.W.L. Naus and J.H. Koch, *Phys. Rev. C* 36 (1987) 2459.
- [26] P.C. Tiemeijer and J.A. Tjon, *Phys. Rev. C* 42 (1990) 599.
- [27] J.C. Ward, *Phys. Rev.* 77 (1950) 293; 78 (1950) 182; *Proc. Phys. Soc.* 64 (1951) 54.
- [28] Y. Takahashi, *Nuovo Cimento* 6 (1957) 371.
- [29] H.W.L. Naus and J.H. Koch, *Phys. Rev. C* 39 (1989) 1907.
- [30] H.W.L. Naus, J.H. Koch and J.L. Friar, *Phys. Rev. C* 41 (1990) 2852.
- [31] W. Pauli, *Rev. Mod. Phys.* 13 (1941) 203.
- [32] D.R. Yennie, M.M. Levy and D.G. Ravenhall, *Rev. Mod. Phys.* 29 (1957) 144; R.G. Sachs, *Phys. Rev.* 126 (1962) 2256.
- [33] L.N. Hand, D.G. Miller and R. Wilson, *Rev. Mod. Phys.* 35 (1963) 335.
- [34] H. Ahfrenhövel, *Suppl. Prog. Theor. Phys.* 91 (1987) 1.
- [35] M.N. Rosenbluth, *Phys. Rev.* 79 (1960) 615.
- [36] S.J. Brodski and G. Farrar, *Phys. Rev. D* 11 (1975) 1309.
- [37] G.P. Lepage and S.J. Brodski, *Phys. Rev. D* 22 (1980) 2157; S.J. Brodski and G.P. Lepage, *Phys. Scr.* 23 (1981) 945.
- [38] G. Höhler, E. Pietarinen, I. Sabba-Stefanescu, F. Borkowski, G.G. Simon, V.H. Walther and R.D. Wendling, *Nucl. Phys. B* 114 (1976) 505.
- [39] G.G. Simon, Ch. Schmitt, F. Borkowski and V.H. Walther, *Nucl. Phys. A* 333 (1980) 381.
- [40] E.B. Hughes, T.A. Griffy, R. Hofstadter and M.R. Yearian, *Phys. Rev.* 139B (1965) 458.
- [41] S. Galster, H. Klein, J. Mortiz, K.H. Schmidt, D. Wegener and J. Bleckwenn, *Nucl. Phys. B* 32 (1971) 221.
- [42] R.G. Arnold, P.E. Bosted, C.C. Chang, J. Gomez, A.T. Katramatou, C.J. Martoff, G.G. Petratos, A.A. Rahbar, S.E. Rock, A.F. Sill, Z.M. Szalata, D.J. Sherden, J.M. Lambert and R.M. Lombard-Nelsen, *Phys. Rev. Lett.* 57 (1986) 174.

- [43] N. Isgur and G. Karl, Phys. Rev. D 18 (1978) 4187; D 19 (1979) 2653.
- [44] A.W. Thomas, in: Advances in Nuclear Physics, vol. 13, eds. J.W. Negele and E. Vogt (Plenum, New York, 1984) p. 1.
- [45] U.-G. Meissner, N. Kaiser and W. Weise, Nucl. Phys. A 466 (1987) 685.
- [46] F. Iachello, A.D. Jackson and A. Lande, Phys. Lett. B 43 (1973) 191.
- [47] M. Gari and W. Krümpelmann, Z. Phys. A 322 (1985) 689.
- [48] P.J. Mulders, Phys. Rep. 185 (1990) 83.
- [49] R.G. Arnold, C.E. Carlson and F. Gross, Phys. Rev. C 21 (1980) 1426.
- [50] R.G. Arnold, D. Benton, P. Bosted, L. Clogher, G. DeChambrier, A.T. Katramatou, J. Lambert, A. Lung, G.G. Petratos, A. Rahbar, S.E. Rock, Z.M. Szalata, R.A. Gearhart, B. Debebe, M. Frodyma, R.S. Hicks, A. Hotta, G.A. Peterson, J. Alster, J. Lichtenstadt, F. Dietrich and K. van Bibber, Phys. Rev. Lett. 58 (1987) 1723.
- [51] S. Auffret, J.M. Cavedon, J.C. Clemens, B. Frois, D. Goutte, Ph. Leconte, J. Martino, Y. Mizuno, X.-H. Phan, S. Platckov and I. Sick, Phys. Rev. Lett. 54 (1985) 649.
- [52] R. Cramers, M. Renkhoff, J. Drees, U. Ecker, D. Jagoda, K. Koseck, G.-R. Pingel, B. Remenschritter, A. Ritterskamo, B. Boden, V. Burkert, G. Knop, M. Leenen, R. Sauerwein and D. Schablitzy, Z. Phys. C 29 (1985) 513.
- [53] R.G. Arnold, B.T. Chertok, E.B. Dally, A. Grigorian, C.L. Jordan, W.P. Schütz, R. Zdarko, F. Martin and B.A. Mecking, Phys. Rev. Lett. 35 (1975) 776.
- [54] E. Lomon, P. Blunden and P. Sitarski, Phys. Rev. C 36 (1987) 2479.
- [55] M. Gari and H. Hyuga, Nucl. Phys. A 264 (1976) 409.
- [56] D.O. Riska and E. Nyman, Phys. Rev. Lett. 57 (1986) 3007.
- [57] S. Platckov, A. Amroun, S. Auffret, J.M. Cavedon, P. Dreux, J. Duclos, B. Frois, D. Goutte, H. Hachemi, J. Martino, X.H. Phan and I. Sick, Nucl. Phys. A 510 (1990) 740.
- [58] J.L. Friar and M. Rosen, Ann. Phys. (NY) 87 (1974) 289;  
J.L. Friar, in: Proc. Intern. School on Electron and Pion Interaction with Nuclei at Intermediate Energies, eds. W. Bertozzi, S. Costa and C. Schaerf (Harwood, New York, 1980) p. 143.
- [59] A. Bottino, G. Ciocchetti and A. Molinari, Nucl. Phys. 89 (1966) 192.
- [60] E.A.J.M. Offermann, L.S. Cardman, C.W. de Jager, H. Miska, C. de Vries and H. de Vries, Phys. Rev. C 44 (1991) 1096.
- [61] G. Cò and J. Heisenberg, Phys. Lett. B 197 (1987) 489.
- [62] M. Traini, Phys. Lett. B 213 (1988) 1.
- [63] M. Traini, S. Turck-Chièze and A. Zghiche, Phys. Rev. C 38 (1988) 2799.
- [64] T. de Forest Jr., Nucl. Phys. A 392 (1983) 232.
- [65] J.S. Wallace, Annu. Rev. Nucl. Part. Sci. 37 (1987) 267.
- [66] S. Hama, B.C. Clark, E.D. Cooper, H.S. Sherif and R.L. Mercer, Phys. Rev. C 41 (1990) 2737.
- [67] A. Picklesimer, J.W. Van Orden and S.J. Wallace, Phys. Rev. C 32 (1985) 1312.
- [68] Yahne Jin, D.S. Onley and L.E. Wright, Phys. Rev. C 45 (1992) 1333.
- [69] B.D. Serot and J.D. Walecka, in: Advances in Nuclear Physics, vol. 16, eds. J.W. Negele and E. Vogt (Plenum, New York, 1986) p. 1.
- [70] L.L. Foldy and S.A. Wouthuysen, Phys. Rev. 78 (1950) 29.
- [71] K.W. McVoy and L. Van Hove, Phys. Rev. 125 (1962) 1034.
- [72] C. Giusti and F.D. Pacati, Nucl. Phys. A 336 (1980) 427.
- [73] L.L. Foldy, Phys. Rev. 87 (1952) 688;  
C.G. Darwin, Proc. R. Soc. (London) A 118 (1928) 654.
- [74] J.L. Friar and S. Fallieros, Phys. Rev. C 13 (1976) 2571.
- [75] F. Gross and D.O. Riska, Phys. Rev. C 36 (1987) 1928;  
D.O. Riska, Phys. Rep. 181 (1989) 207.
- [76] W.M. Alberico, T.W. Donnelly and A. Molinari, Nucl. Phys. A 512 (1991) 541.
- [77] F. Gross and H. Henning, Nucl. Phys. A 537 (1992) 344.
- [78] R.D. Peccei, Phys. Rev. 176 (1968) 1812; 181 (1969) 1902.
- [79] J.W. Van Orden and T.W. Donnelly, Ann. Phys. (NY) 131 (1981) 451.
- [80] J. Hockert, D.O. Riska, M. Gari and A. Huffman, Nucl. Phys. A 217 (1973) 14.
- [81] D.O. Riska, in: Mesons in Nuclei, vol. II, eds. M. Rho and D. Wilkinson (North-Holland, Amsterdam, 1979) p. 755.
- [82] J.S. O'Connell, W.R. Dodge, J.W. Lightbody Jr., X.K. Maruyama, J.-O. Adler, K. Hansen, B. Schröder, A.M. Bernstein, K.I. Blomqvist, B.H. Cottman, J.J. Comuzzi, R.A. Miskimen, B.P. Quinn, J.H. Koch and N. Ohtsuka, Phys. Rev. C 35 (1987) 1063.
- [83] R.M. Sealock, K.L. Giovanetti, S.T. Thornton, Z.E. Meziani, O.A. Rondon-Aramayo, S. Auffret, J.-P. Chen, D.G. Christian, D.B. Day, J.S. McCarthy, R.C. Minehart, L.C. Dennis, K.W. Kemper, B.A. Mecking and J. Morgenstern, Phys. Rev. Lett. 62 (1989) 1350.
- [84] E.J. Moniz, I. Sick, R.R. Whitney, J.R. Ficenec, R.D. Kephart and W.P. Trower, Phys. Rev. Lett. 26 (1971) 445.
- [85] R. Altemus, A. Caffolla, D. Day, J.S. McCarthy, R.R. Whitney and J.E. Wise, Phys. Rev. Lett. 44 (1980) 965.
- [86] P. Barreau, M. Bernheim, J. Duclos, J.M. Finn, Z. Meziani, J. Morgenstern, J. Mougey, D. Royer, B. Saghai, D. Tarnowski, S. Turck-Chièze, M. Brussel, G.P. Capitani, E. De Sanctis, S. Frullani, F. Garibaldi, D.B. Isabelle, E. Jans, I. Sick and P.D. Zimmermann, Nucl. Phys. A 402 (1983) 515.

- [87] Z.E. Meziani, P. Barreau, M. Bernheim, J. Morgenstern, S. Turck-Chieze, R. Altemus, J.S. McCarthy, L.J. Orphanos, R.R. Whitney, G.P. Capitani, E. De Sanctis, S. Frullani and F. Garibaldi, Phys. Rev. Lett 52 (1984) 2130; 54 (1985) 1233.
- [88] C. Marchand, P. Barreau, M. Bernheim, P. Pradu, G. Fournier, Z.E. Meziani, J. Miller, J. Morgenstern, J. Picard, B. Saghai, S. Turck-Chieze, P. Vernin and M.K. Brussel, Phys. Lett. B 153 (1985) 29.
- [89] Z.E. Meziani, Ph.D. Thesis, Univ. of Paris-Sud at Orsay (1984).
- [90] M. Deady, C.F. Williamson, P.D. Zimmerman, R. Altemus and R.R. Whitney, Phys. Rev. C 33 (1986) 1897.
- [91] G.C. Blatchley, J.J. LeRose, O.E. Pruet, P.D. Zimmerman, C.F. Williamson and M. Deady, Phys. Rev. C 34 (1986) 1243.
- [92] K. Dow, S. Dytman, D. Beck, A. Bernstein, I. Blomqvist, H. Caplan, D. Day, M. Deady, P. Demos, W. Dodge, G. Dodson, M. Farkhondeh, J. Flanz, K. Giovanetti, R. Goloskie, E. Hallin, E. Knill, S. Kowalski, J. Lightbody, R. Lindgren, X. Maruyama, J. McCarthy, B. Quinn, G. Retzlaff, W. Sapp, C. Sargent, D. Skopik, I. The, D. Tieger, W. Turchinetz, T. Ueng, N. Videla, K. von Reden, R. Whitney and C. Williamson, Phys. Rev. Lett. 61 (1988) 1706.
- [93] S.A. Dytman, A.M. Bernstein, K.I. Blomqvist, T.J. Pavel, B.P. Quinn, R. Altemus, J.S. McCarthy, G.H. Mechtel, T.S. Ueng and R.R. Whitney, Phys. Rev. C 38 (1988) 800.
- [94] K.F. von Reden, C. Alcorn, S.A. Dytman, B. Lowry, B.P. Quinn, D.H. Beck, A.M. Bernstein, K.I. Blomqvist, G. Dodson, K.A. Dow, J. Flanz, G. Retzlaff, C.P. Sargent, W. Turchinetz, M. Farkhondeh, J.S. McCarthy, T.S. Ueng and R.R. Whitney, Phys. Rev. C 41 (1990) 1084.
- [95] A. Hotta, P.J. Ryan, H. Ogino, B. Parker, G.A. Peterson and R.P. Singhal, Phys. Rev. C 30 (1984) 87.
- [96] A. Zghiche, Ph.D. Thesis, Univ. de Paris Sud (1989).
- [97] L. Fetter and J.D. Walecka, Quantum Theory of Many-Particle Systems (McGraw-Hill, New York, 1971).
- [98] W.M. Alberico, M. Ericson and A. Molinari, Nucl. Phys. A 379 (1982) 429.
- [99] W.M. Alberico, M. Ericson and A. Molinari, Ann. Phys. (NY) 154 (1984) 356.
- [100] W.M. Alberico, A. Molinari, A. de Pace, M. Ericson and M.B. Johnson, Phys. Rev. C 34 (1986) 977.
- [101] W.M. Alberico, P. Czerski, M. Ericson and A. Molinari, Nucl. Phys. A 462 (1987) 269.
- [102] W.M. Alberico, R. Cenni and A. Molinari, Prog. Part. Nucl. Phys. 23 (1989) 171.
- [103] A. Dellafiore, F. Lenz and F.A. Brieva, Phys. Rev. C 31 (1985) 1088; F.A. Brieva and A. Dellafiore, Phys. Rev. C 36 (1987) 899.
- [104] M. Cavinato, D. Drechsel, E. Fein, M. Marangoni and A.M. Saruis, Nucl. Phys. A 423 (1984) 376; M. Cavinato, M. Marangoni and A.M. Saruis, Phys. Lett. B 235 (1990) 15.
- [105] S. Drodz, G. Cò, J. Wambach and J. Speth, Phys. Lett. B 185 (1987) 287; G. Cò, K.F. Quader, R.D. Smith and J. Wambach, Nucl. Phys. A 485 (1988) 61.
- [106] S. Fantoni and V.R. Pandharipande, Nucl. Phys. A 473 (1987) 234; R. Schiavilla, D.S. Lewart, V.R. Pandharipande, S.C. Pieper, R.B. Wiringa and S. Fantoni, Nucl. Phys. A 473 (1987) 267.
- [107] J.V. Noble, Phys. Rev. Lett. 46 (1981) 412.
- [108] L.S. Celenza, A. Rosenthal and C.M. Shakin, Phys. Rev. Lett. 53 (1984) 891; Phys. Rev. C 33 (1986) 1012.
- [109] M. Rho, Phys. Rev. Lett. 54 (1985) 767.
- [110] M. Ericson and M. Rosa-Clot, Z. Phys. A 324 (1986) 373.
- [111] P.J. Mulders, Nucl. Phys. A 459 (1986) 525.
- [112] M. Soyeur, G.E. Brown and M. Rho, Laboratoire National Saturne, preprint LNS/PH/91/14.
- [113] G. Do Dang and N. Van Giai, Phys. Rev. C 30 (1984) 731.
- [114] X. Song, J.P. Chen, P.K. Kabir and J.S. McCarthy, J. Phys. G 17 (1991) L75; X. Song, J.P. Chen and J.S. McCarthy, Z. Phys. A 341 (1992) 275.
- [115] C.J. Horowitz and J. Piekarewicz, Phys. Rev. Lett. 62 (1989) 391.
- [116] K. Wehrberger and F. Beck, Nucl. Phys. A 491 (1989) 587.
- [117] H. Kurosawa and T. Suzuki, Nucl. Phys. A 490 (1988) 571.
- [118] X. Ji, Phys. Lett. B 219 (1989) 143.
- [119] Y. Horikawa, F. Lenz and N.C. Mukhopadhyay, Phys. Rev. C 22 (1980) 1680.
- [120] C.R. Chinn, A. Picklesimer and J.W. Van Orden, Phys. Rev. C 40 (1989) 790, 1159; P.M. Boucher and J.W. Van Orden, Phys. Rev. C 43 (1991) 582.
- [121] F. Capuzzi, C. Giusti and F.D. Pacati, Nucl. Phys. A 524 (1991) 681.
- [122] S. Boffi and F. Capuzzi, Lett. Nuovo Cimento 25 (1979) 209; Nucl. Phys. A 351 (1981) 219.
- [123] T. de Forest, Jr., Nucl. Phys. A 163 (1971) 237.
- [124] F.G. Perey, in: Direct Interactions and Nuclear Reaction Mechanism, eds. E. Clementel and C. Villi (Gordon and Breach, New York, 1963) p. 125; F.G. Perey and B. Buck, Nucl. Phys. 32 (1962) 353.
- [125] L.R.B. Elton and A. Swift, Nucl. Phys. A 94 (1967) 52.
- [126] D.F. Jackson and I. Abdul Jalil, J. Phys. G 6 (1980) 481.
- [127] F. Capuzzi, C. Giusti and F.D. Pacati, in: 5th Workshop on Perspectives in Nuclear Physics at Intermediate Energies, eds. S. Boffi, C. Ciofi degli Atti and M.M. Giannini (World Scientific, Singapore, 1992) p. 237.
- [128] G. Orlandini and M. Traini, Rep. Prog. Phys. 54 (1991) 257.

- [129] R. Schiavilla, A. Fabrocini and V.R. Pandharipande, Nucl. Phys. A 473 (1987) 290; V.R. Pandharipande, in: Hadrons and Hadronic Matter, eds. D. Vautherin, F. Lenz and J.W. Negele (Plenum, New York, 1990) p. 293.
- [130] J.P. Chen, Z.E. Meziani, D. Beck, G. Boyd, L.M. Chinitz, D.B. Day, L.C. Dennis, G. Dodge, B.W. Filippone, K.L. Giovanetti, J. Jourdan, K.W. Kemper, T. Koh, W. Lorenzon, J.S. McCarthy, R.D. McKeown, R.G. Milner, R.C. Minehart, J. Morgenstern, J. Mougey, D.H. Potterveld, O.A. Rondon-Aramayo, R.M. Sealock, L.C. Smith, S.T. Thornton, R.C. Walker and C. Woodward, Phys. Rev. Lett. 66 (1991) 1283.
- [131] J.D. Bjorken, Phys. Rev. 179 (1969) 1547;  
J.D. Bjorken and E.A. Paschos, Phys. Rev. 185 (1969) 1975.
- [132] E.D. Bloom, D.H. Coward, H. DeStaeler, J. Drees, G. Miller, L.W. Mo, R.E. Taylor, M. Breidenbach, J.I. Friedman, G.C. Hartman and H.W. Kendall, Phys. Rev. Lett. 23 (1969) 930.
- [133] M. Breidenbach, J.I. Friedman, H.W. Kendall, E.D. Bloom, D.H. Coward, H. DeStaeler, J. Drees, L.W. Mo and R.E. Taylor, Phys. Rev. Lett. 23 (1969) 935.
- [134] G. Miller, E.D. Bloom, G. Buschhorn, D.H. Coward, H. DeStaeler, J. Drees, C.L. Jordan, L.W. Mo, R.E. Taylor, J.I. Friedman, G.C. Hartman, H.W. Kendall and R. Verdier, Phys. Rev. D 5 (1972) 528.
- [135] S.J. Wimpenny, Nucl. Phys. A 434 (1985) 3c.
- [136] C.G. Callan and D.J. Gross, Phys. Rev. Lett. 21 (1968) 311.
- [137] T. de Forest, Jr., Ann. Phys. (NY) 45 (1967) 365.
- [138] S. Boffi, C. Giusti and F.D. Pacati, Nucl. Phys. A 386 (1982) 599.
- [139] M. Gourdin, Nuovo Cimento 21 (1961) 1094.
- [140] D. Drechsel and H. Überall, Phys. Rev. 181 (1969) 1383.
- [141] F.A. Berends, A. Donnachie and D.L. Weaver, Nucl. Phys. B 4 (1967) 1, 54, 103.
- [142] R.A. Adelseck and B. Saghai, Phys. Rev. C 42 (1990) 108.
- [143] J. Cohen, Int. J. Mod. Phys. A 4 (1989) 1.
- [144] L. Tiator and D. Drechsel, Nucl. Phys. A 369 (1981) 208;  
D. Drechsel and L. Tiator, J. Phys. G 18 (1992) 449.
- [145] J.M. Laget, Can J. Phys. 62 (1984) 1046.
- [146] M. Cavinato, D. Drechsel, E. Fein, M. Marangoni and A.M. Saruis, Phys. Lett. B 127 (1983) 295; Nucl. Phys. A 444 (1985) 13.
- [147] J. Ryckebusch, K. Heyde, D. Van Neck and M. Waroquier, Phys. Lett. B 216 (1989) 252.
- [148] J. Ryckebusch, K. Heyde, D. Van Neck and M. Waroquier, Nucl. Phys. A 503 (1989) 694.
- [149] M. Cavinato, M. Marangoni and A.M. Saruis, Z. Phys. A 335 (1990) 401.
- [150] S. Boffi, F. Cannata, F. Capuzzi, C. Giusti and F.D. Pacati, Nucl. Phys. A 379 (1982) 509.
- [151] S. Boffi, in: From Nuclei to Particles, ed. A. Molinari (North-Holland, Amsterdam, 1981) p. 373.
- [152] P.O. Löwdin, Phys. Rev. 97 (1955) 1474;  
A.J. Coleman, Rev. Mod. Phys. 35 (1963) 668.
- [153] A.B. Migdal, Theory of Finite Fermi Systems and Applications to Atomic Nuclei (Interscience, New York, 1967).
- [154] J.M. Bang, F.G. Gareev, W.T. Pinkston and J.S. Vaagen, Phys. Rep. 125 (1985) 253.
- [155] C. Mahaux, P.F. Bortignon, R.A. Broglia and C.H. Dasso, Phys. Rep. 120 (1985) 1.
- [156] C. Mahaux and R. Sartor, Nucl. Phys. A 481 (1988) 381; A 493 (1989) 157; A 502 (1989) 525; A 503 (1989) 525.
- [157] C. Mahaux and R. Sartor, Single-particle motion in nuclei, in: Advances in Nuclear Physics, vol. 20, eds. J.W. Negele and E. Vogt (Plenum, New York, 1991) p. 1.
- [158] C. Ciofi degli Atti, E. Pace and G. Salmè, Phys. Rev. C 21 (1980) 805; Phys. Lett. B 141 (1984) 14.
- [159] Y. Akaishi, Nucl. Phys. A 416 (1984) 409c.
- [160] R. Schiavilla, V.R. Pandharipande and R. Wiringa, Nucl. Phys. A 449 (1986) 219.
- [161] A.E. Dieperink, T. de Forest Jr., I. Sick and R.A. Brandenburg, Phys. Lett. B 63 (1976) 261.
- [162] H. Meier-Hajduk, Ch. Hajduk, P.U. Sauer and W. Theis, Nucl. Phys. A 395 (1983) 332.
- [163] S. Ishikawa and T. Sasakawa, Few Body Systems 1 (1986) 143.
- [164] O. Benhar, A. Fabrocini and S. Fantoni, Nucl. Phys. A 497 (1989) 423c; A 505 (1989) 267; Phys. Rev. C 41 (1990) R24.
- [165] O. Benhar, A. Fabrocini and S. Fantoni, in: Modern Topics in Electron-Scattering, eds. B. Frois and I. Sick (World Scientific, Singapore, 1991) p. 160.
- [166] M.G.E. Brand, K. Allaart and W.H. Dickhoff, Nucl. Phys. A 509 (1990) 1;  
A. Ramos W.H. Dickhoff and A. Polls, Phys. Rev. C 43 (1991) 2239;  
B.E. Vonderfecht, W.H. Dickhoff, A. Polls and A. Ramos, Phys. Rev. 44 (1991) R1265.
- [167] W.H. Dickhoff, P.P. Domitrovich, K. Allaart, M.G.E. Brand, F.A. Muller, G.A. Rijsdijk, A. Polls and A. Ramos, in: Topical Workshop on Two-Nucleon Emission, eds. O. Benhar and A. Fabrocini (ETS Editrice, Pisa, 1991) p. 332;  
M.G.E. Brand, G.A. Rijsdijk, F.A. Muller, K. Allaart and W.H. Dickhoff, Nucl. Phys. A 531 (1991) 253.
- [168] D. Van Neck, M. Waroquier and J. Ryckebusch, Nucl. Phys. A 530 (1991) 347.
- [169] I.E. Lagaris and V.R. Pandharipande, Nucl. Phys. A 359 (1981) 331.
- [170] A.E.L. Dieperink and G.A. Miller, Phys. Rev. C 44 (1991) 866.

- [171] S. Boffi, Lett. Nuovo Cimento 1 (1971) 931;  
D.S. Koltun, Phys. Rev. Lett. 28 (1972) 182.
- [172] M.M. Giannini and G. Ricco, Ann. Phys. (NY) 102 (1976) 458.
- [173] J.R. Comfort and B.C. Karp, Phys. Rev. C 21 (1980) 2162.
- [174] A. Nadasen, P. Schwandt, P.P. Singh, W.W. Jacobs, A.D. Bacher, P.T. Debevec, M.D. Kaitchuk and J.T. Meek, Phys. Rev. C 23 (1981) 1023.
- [175] P. Schwandt, H.O. Mayer, W.W. Jacobs, A.D. Bacher, S.E. Vigdor and M.D. Kaitchuk, Phys. Rev. C 26 (1982) 55.
- [176] A.M. Lane, Phys. Rev. Lett. 8 (1962) 171.
- [177] J.J. Kelly, W. Bertozzi, T.N. Buti, J.M. Finn, F.W. Hersman, C. Hyde-Wright, M.V. Hynes, M.A. Kovash, B. Murdoch, B.E. Norum, B. Pugh, F.N. Rad, A.D. Bacher, G.T. Emery, C.C. Foster, W.P. Jones, D.W. Miller, B.L. Berman, W.G. Love, J.A. Carr and F. Petrovich, Phys. Rev. 39 (1989) 1222.
- [178] J.J. Kelly, Phys. Rev. C 39 (1989) 2120.
- [179] F. Capuzzi, Lecture Notes in Physics 55 (1976) 20.
- [180] H. Fiedeldey, Nucl. Phys. 77 (1966) 149.
- [181] W.E. Frahn and R.H. Lemme, Nuovo Cimento 5 (1957) 1564.
- [182] J. Mougey, M. Bemheim, A. Bussière, A. Gillebert, Pan Xuan Hö, M. Priou, D. Royer, I. Sick and G. Wagner, Nucl. Phys. A 262 (1976) 461.
- [183] K. Nakamura and N. Izutsu, Nucl. Phys. A 259 (1976) 301.
- [184] S. Boffi, C. Giusti, F.D. Pacati and S. Frullani, Nucl. Phys. A 319 (1979) 461.
- [185] A. Bernheim, A. Bussière, J. Mougey, D. Royer, D. Tarnowski, S. Turck-Chieze, S. Frullani, S. Boffi, C. Giusti, F.D. Pacati, G.P. Capitani, E. De Sanctis and G.J. Wagner, Nucl. Phys. A 375 (1982) 381.
- [186] S. Boffi, C. Giusti and F.D. Pacati, Nucl. Phys. A 336 (1980) 437.
- [187] S.R. Cotanch, Phys. Lett. B 76 (1978) 19.
- [188] S. Boffi, F. Capuzzi, C. Giusti and F.D. Pacati, Nucl. Phys. A 436 (1985) 438.
- [189] G. van der Steenhoven, H.P. Blok, M. Thies and P.J. Mulders, Phys. Lett. B 191 (1987) 227;  
G. van der Steenhoven, private communication.
- [190] C. Giusti and F.D. Pacati, Nucl. Phys. A 504 (1989) 685.
- [191] J.P. McDermott, Phys. Rev. Lett. 65 (1990) 1991.
- [192] Yahne Jin, D.S. Onley and L.E. Wright, Phys. Rev. C 45 (1992) 1311.
- [193] D.R. Yennie, F.L. Boos and D.G. Ravenhall, Phys. Rev. 137 (1965) B882.
- [194] F. Lenz and R. Rosenfelder, Nucl. Phys. A 176 (1971) 513;  
J. Knoll, Nucl. Phys. A 223 (1974) 462.
- [195] C. Giusti and F.D. Pacati, Nucl. Phys. A 473 (1987) 717; A 485 (1988) 461.
- [196] J. Heisenberg and H.P. Blok, Annu. Rev. Nucl. Part. Sci. 33 (1983) 569.
- [197] L.L. Frankfurt and M.I. Strikman, Phys. Lett. B 183 (1987) 254.
- [198] S. Boffi, C. Giusti and F.D. Pacati, Nucl. Phys. A 336 (1980) 416.
- [199] P.K.A. de Witt Huberts, J. Phys. G 16 (1990) 507; Prog. Part. Nucl. Phys. 24 (1989) 205.
- [200] V. Devanathan, Ann. Phys. (NY) 43 (1967) 74.
- [201] M.B. Leuschner et al., to be published.
- [202] G.J. Kramer, H.P. Blok, J.F.J. van den Brand, H.J. Bulten, R. Ent, E. Jans, J.B.J.M. Lanen, L. Lapikás, H. Nann, E.N.M. Quint, G. van der Steenhoven, P.K.A. de Witt Huberts and G.J. Wagner, Phys. Lett. B 227 (1989) 199.
- [203] J.W.A. den Herder, H.P. Blok, E. Jans, P.H.M. Keizer, L. Lapikás, E.N.M. Quint, G. van der Steenhoven and P.K.A. de Witt Huberts, Nucl. Phys. A 490 (1988) 507.
- [204] H.B.M. Raben, private communication
- [205] L. Lapikás, in: Proc. 6th Intern. Conf. on Nuclear Reaction Mechanisms, ed. E. Gadioli (Università di Milano, 1991) p. 610.
- [206] L. Lapikás, in 4th Workshop on Perspectives in Nuclear Physics at Intermediate Energies, eds. S. Boffi, C. Ciofi degli Atti and M.M. Giannini (World Scientific, Singapore, 1989) p. 419.
- [207] A.E.L. Dieperink and P.K.A. de Witt Huberts, Annu. Rev. Nucl. Part. Sci. 40 (1990) 239.
- [208] G. van der Steenhoven, Nucl. Phys. A 527 (1991) 17c.
- [209] S. Boffi and M. Radici, Phys. Lett. B 242 (1990) 151.
- [210] E.N.M. Quint, Ph.D. Thesis, Univ. of Amsterdam (1988).
- [211] H. Clement, P. Grabmayr, H. Roehm and G.J. Wagner, Phys. Lett. B 183 (1987) 127;  
P. Grabmayr, G.J. Wagner, H. Clement and H. Roehm, Nucl. Phys. A 494 (1989) 244;  
G.J. Wagner, Prog. Part. Nucl. Phys. 24 (1990) 17.
- [212] E.N.M. Quint, J.F.J. van den Brand, J.W.A. den Herder, E. Jans, P.H.M. Keizer L. Lapikás, G. van der Steenhoven, P.K.A. de Witt Huberts, S. Klein, P. Grabmayr, G.J. Wagner, H. Nann, B. Frois and D. Goutte, Phys. Rev. Lett. 57 (1986) 186.
- [213] E.N.M. Quint, B.M. Barnett, A.M. van den Berg, J.F.J. van den Brand, H. Clement, R. Ent, B. Frois, D. Goutte, P. Grabmayr, J.W.A. den Herder, E. Jans, G.J. Kramer, J.B.J.M. Lanen, L. Lapikás, H. Nann, G. van der Steenhoven, G.J. Wagner and P.K.A. de Witt Huberts, Phys. Rev. Lett. 58 (1987) 1088.

- [214] J.M. Cavedon, B. Frois, D. Goutte, M. Huet, Ph. Leconte, C.N. Papanicolas, X.H. Phan, S.K. Platchkov, S.E. Williamson, W. Boeglin and I. Sick, Phys. Rev. Lett. 49 (1982) 978.
- [215] I. Sick and P.K.A. de Witt Huberts, Comments Nucl. Part. Phys. 20 (1991) 177.
- [216] H.J. Bulten, private communication, and to be published.
- [217] S. Boffi and M. Radici, unpublished.
- [218] S. Boffi and M. Radici, Nucl. Phys. A 526 (1991) 602.
- [219] G. Bardin, J. Duclos, A. Magnon, B. Michel and J.C. Montret, Nucl. Phys. B 120 (1977) 45.
- [220] P. Brauel, T. Canzler, D. Cords, R. Felst, G. Grindhammer, M. Helm, W.-D. Kollman, H. Krehbiel and M. Schädlich, Z. Phys. C 3 (1979) 101.
- [221] T. Tamae, H. Kawahara, A. Tanaka, M. Nomura, K. Namai, M. Sugawara, Y. Kawazoe, H. Tsubota and H. Miyase, Phys. Rev. Lett. 59 (1987) 2919.
- [222] L. Chinitz, M. Bernheim, G.P. Capitani, A. Catarinella, J.F. Danel, E. De Sanctis, S. Frullani, F. Garibaldi, F. Ghio, M. Iodice, L. Lakehal-Ayat, J.M. LeGoff, J. LeRose, A. Magnon, C. Marchand, R. Minehart, J. Morgenstern, J. Mougey, S. Nanda, C. Perdrisat, R. Powers, V. Punjabi, A. Saha, P. Ulmer and P. Vernin, Phys. Rev. Lett. 67 (1991) 568, 1811 (E).
- [223] G. van der Steenhoven, private communication.
- [224] S. Boffi, M. Radici, J.J. Kelly and T.M. Payerle, Nucl. Phys. A 539 (1992) 597.
- [225] M. van der Schaer, H. Arenhövel, H.P. Blok, H.J. Bulten, E. Hummel, E. Jans, L. Lapikás, G. van der Steenhoven, J.A. Tjon, J. Wesseling and P.K.A. de Witt Huberts, Phys. Rev. Lett. 68 (1992) 776.
- [226] J. Morgenstern, Nucl. Phys. A 446 (1985) 315c.
- [227] G. van der Steenhoven, H.P. Blok, J.F.J. van den Brand, T. de Forest Jr., J.W.A. den Herder, E. Jans, P.H.M. Keizer, L. Lapikás, P.J. Mulders, E.N.M. Quint, P.K.A. de Witt Huberts, J. Mougey, S. Boffi, C. Giusti and F.D. Pacati, Phys. Rev. Lett. 57 (1986) 182.
- [228] G. van der Steenhoven, A.M. van den Berg, H.P. Blok, S. Boffi, J.F.J. van den Brand, R. Ent, T. de Forest Jr., C. Giusti, J.W.A. den Herder, E. Jans, G.J. Kramer, J.B.J.M. Lanen, L. Lapikás, J. Mougey, P.J. Mulders, F.D. Pacati, E.N.M. Quint and P.K.A. de Witt Huberts, Phys. Rev. Lett. 58 (1987) 1727.
- [229] D. Reffay-Pikeroen, M. Bernheim, S. Boffi, G.P. Capitani, E. De Sanctis, S. Frullani, F. Garibaldi, A. Gérard, C. Giusti, H. Jackson, A. Magnon, C. Marchand, J. Mougey, J. Morgenstern, F.D. Pacati, J. Picard, S. Turck-Chieze and P. Vernin, Phys. Rev. Lett. 60 (1988) 776.
- [230] P.E. Ulmer, H. Baghaei, W. Bertozi, K.I. Blomqvist, J.M. Finn, C.E. Hyde-Wright, N. Kalantar-Nayestanaki, S. Kowalski, R.W. Lourie, J. Nelson, W.W. Sapp, C.P. Sargent, L. Weinstein, B.H. Cottman, P.K. Teng, E.J. Winhold, M. Yamazaki, J.R. Calarco, F.W. Hersman, J.J. Kelly, M.E. Schulze and G. Audit, Phys. Rev. Lett. 59 (1987) 2259.
- [231] A. Magnon, M. Bernheim, M.K. Brussel, G.P. Capitani, E. De Sanctis, S. Frullani, F. Garibaldi, A. Gérard, H.E. Jackson, J.M. LeGoff, C. Marchand, Z.E. Meziani, J. Morgenstern, J. Picard, D. Reffay, S. Turck-Chieze, P. Vernin and A. Zghiche, Phys. Lett. B 222 (1989) 352.
- [232] H. Baghaei, W. Bertozi, K.I. Blomqvist, J.M. Finn, J. Flanz, C.E. Hyde-Wright, N. Kalantar-Nayestanaki, R.W. Lourie, J. Nelson, W.W. Sapp, C.P. Sargent, P.E. Ulmer, L. Weinstein, B.H. Cottman, P.K. Teng, E.J. Winhold, M. Yamazaki, J.R. Calarco, F.W. Hersman, C. Perdrisat, V. Punjabi, M. Epstein and D.J. Margaziotis, Phys. Rev. C 39 (1989) 177.
- [233] M. Jodice, S. Frullani, F. Garibaldi, F. Ghio, G.P. Capitani, E. De Sanctis, M. Bernheim, A. Gerard, A. Magnon, C. Marchand, J. Morgenstern, J. Picard, P. Vernin, A. Zghiche, J. Mougey and M. Brussel, in: 4th Workshop on Perspectives in Nuclear Physics at Intermediate Energies, eds. S. Boffi, C. Ciofi degli Atti and M.M. Giannini (World Scientific, Singapore, 1989) p. 402; Phys. Lett. B 282 (1992) 31.
- [234] J.B.J.M. Lanen H.P. Blok, E. Jans, L. Lapikás, G. van der Steenhoven and P.K.A. de Witt Huberts, Phys. Rev. Lett. 64 (1990) 2250.
- [235] T.W. Donnelly, J.W. Van Orden, T. de Forest Jr. and W.C. Hermans, Phys. Lett. B 136 (1978) 393; J.W. Van Orden and T.W. Donnelly, Ann. Phys. (NY) 131 (1981) 451.
- [236] R.W. Lourie, H. Baghaei, W. Bertozi, K.I. Blomqvist, J.M. Finn, C.E. Hyde-Wright, N. Kalantar-Nayestanaki, J. Nelson, S. Kowalski, C.P. Sargent, W.W. Sapp, P. Ulmer, J. Wiggins, B.H. Cottman, P.K. Teng, E.J. Winhold, M. Yamazaki, J.R. Calarco, F.W. Hersman, J.J. Kelly and M.E. Schulze, Phys. Rev. Lett. 56 (1986) 2364.
- [237] S. Boffi, in: Proc. Topical Workshop on Two-Nucleon Emission Reactions, eds. O. Benhar and A. Fabrocini (ETS, Pisa, 1991) p. 87.
- [238] S. Boffi and M.M. Giannini, Nucl. Phys. A 533 (1991) 441.
- [239] C. Giusti and F.D. Pacati, Nucl. Phys. A 535 (1991) 573; C. Giusti, F.D. Pacati and M. Radici, Nucl. Phys. A 546 (1992) 607.
- [240] E. Jans, in: 5th Workshop on Perspectives in Nuclear Physics at Intermediate Energies, eds. S. Boffi, C. Ciofi degli Atti and M.M. Giannini (World Scientific, Singapore, 1992) p. 287.
- [241] A. Zondervan, Ph.D. Thesis Vrije Univ. Amsterdam (1992).
- [242] T. Takaki, Phys. Rev. Lett. 62 (1989) 395; Phys. Rev. C 39 (1989) 359.
- [243] J.H. Koch, E.J. Moniz and N. Ohtsuka, Ann. Phys. (NY) 154 (1984) 99; J.H. Koch and N. Ohtsuka, Nucl. Phys. A 435 (1985) 765.
- [244] S. Homma, Nucl. Phys. A 446 (1985) 241c.
- [245] S. Homma, M. Kanazawa, K. Maruyama, Y. Murata, H. Okuno, A. Sasaki, and T. Taniguchi, Phys. Rev. C 27 (1983) 31.

- [246] S. Homma, M. Kanazawa, M. Koike, Y. Murata, H. Okuno, F. Soga, M. Sudo, M. Torikoshi, N. Yoshikawa, A. Sasaki and Y. Fujii, Phys. Rev. Lett. 53 (1984) 2536.
- [247] M. Kanazawa, S. Homma, M. Koike, Y. Murata, H. Okuno, F. Soga, N. Yoshikawa and A. Sasaki, Phys. Rev. C 35 (1987) 1828.
- [248] J.-M. Laget, Nucl. Phys. A 481 (1988) 765.
- [249] G.B. West, Phys. Rep. 18 (1975) 263.
- [250] P.D. Zimmerman, C.F. Williamson and Y. Kawazoe, Phys. Rev. C 19 (1979) 279.
- [251] I. Sick, D. Day and J.S. McCarthy, Phys. Rev. Lett. 45 (1980) 871.
- [252] P. Bosted, R.G. Arnold, S. Rock and Z. Szalata, Phys. Rev. Lett. 49 (1982) 1380.
- [253] B.D. Day, J.S. McCarthy, Z.E. Meziani, R. Minehart, R. Sealock, S.T. Thornton, J. Jourdan, I. Sick, B.W. Filippone, R.D. McKeown, R.G. Milner, D.H. Potterveld and Z. Szalata, Phys. Rev. Lett. 59 (1987) 427.
- [254] B.D. Day, J.S. McCarthy, T.W. Donnelly and I. Sick, Annu. Rev. Nucl. Part Sci. 40 (1990) 357.
- [255] E. Pace and G. Salmè, Phys. Lett. B 110 (1982) 411.
- [256] J.M. Finn, R.W. Lourie and B.H. Cottman, Phys. Rev. C 29 (1984) 2230.
- [257] R. Cenni, C. Ciofi degli Atti and G. Salmè, Phys. Rev. C 39 (1989) 1425.
- [258] C. Ciofi degli Atti, E. Pace and G. Salmè, Few-Body Systems, Suppl. no. 1 (1986) 281; Phys. Lett. B 177 (1987) 303; Phys. Rev. C 36 (1989) 1208; C 39 (1989) 259; Nucl. Phys. A 497 (1989) 349c.
- [259] C. Ciofi degli Atti, E. Pace and G. Salmè, Phys. Rev. C 43 (1991) 1155.
- [260] C. Ciofi degli Atti, S. Liuti and S. Simula, Phys. Rev. C 41 (1990) R2474.
- [261] S.A. Gurwitz and A.S. Rinat, Phys. Rev. C 35 (1987) 696;  
A.S. Rinat and R. Rosenfelder, Phys. Lett. B 193 (1987) 411;  
S.A. Gurwitz and A.S. Rinat, Phys. Lett. B 197 (1987) 6.
- [262] E.M.C. Collab., J.J. Aubert et al., Phys. Lett. B 123 (1983) 275.
- [263] S. Stein et al., Phys. Rev. D 12 (1975) 1884;  
A. Bodek et al., Phys. Rev. Lett. 50 (1983) 1431;  
R.G. Arnold et al., Phys. Rev. Lett. 52 (1984) 727.
- [264] A.C. Benvenuti et al., Phys. Lett. B 189 (1987) 483.
- [265] M. Arneodo et al., Nucl. Phys. B 333 (1990) 1.
- [266] S. Kullander, Nucl. Phys. A 518 (1990) 262.
- [267] P. Graström, E. Hagberg, S. Kullander and T. Lindqvist, Phys. Scr. 34 (1986) 495;  
J. Kwiecinski and B. Badelek, Phys. Lett. B 208 (1988) 508;  
P. Castorina and A. Donnachie, Phys. Lett. B 215 (1988) 589.
- [268] N.N. Nikolaev and B.G. Zakharov, Z. Phys. C 49 (1991) 607;  
V. Barone, M. Genovese, N.N. Nikolaev, E. Predazzi and B.G. Zakharov, Phys. Lett. B 268 (1992) 279; B 292 (1992) 181.
- [269] A. Bodek and J.L. Ritchie, Phys. Rev. D 23 (1981) 1070.
- [270] A. Krzywicki, Nucl. Phys. A 446 (1985) 135c; in: 3rd Workshop on Perspectives in Nuclear Physics at Intermediate Energies, eds. S. Boffi, C. Ciofi degli Atti and M.M. Giannini (World Scientific, Singapore, 1988) p. 159.
- [271] S.V. Akulinichev, S.A. Kulagin and G.M. Vagradov, Phys. Lett. B 158 (1985) 485; J. Phys. G 11 (1985) L245;  
S.V. Akulinichev, S. Shlomo, S.A. Kulagin and G.M. Vagradov, Phys. Rev. Lett. 55 (1985) 2239;  
S.V. Akulinichev and S. Shlomo, Phys. Rev. C 33 (1986) R 1551.
- [272] B.L. Birbrair, A.B. Gridnev, M.B. Zhalov, E.M. Levin and V.E. Starodubski, Phys. Lett. B 166 (1986) 119;  
B.L. Birbrair, E.M. Levin and A.G. Shubaev, Nucl. Phys. A 491 (1989) 618.
- [273] G.L. Li, K.F. Liu and G.E. Brown, Phys. Lett. B 213 (1988) 531.
- [274] R.L. Jaffe, in: Relativistic Dynamics and Quark–Nuclear Physics, eds. M.B. Johnson and A. Picklesimer (J. Wiley, New York, 1986) p. 537; Nucl. Phys. A 478 (1988) 3c.
- [275] C. Ciofi degli Atti and S. Liuti, Phys. Lett. B 225 (1989) 215; Phys. Rev. C 41 (1990) 1100.
- [276] C. Ciofi degli Atti and S. Liuti, Nucl. Phys. A 532 (1991) 241c; Phys. Rev. C 44 (1991) R1269.
- [277] F. Gross and S. Liuti, Phys. Rev. C 45 (1992) 1374.
- [278] M. Simonius, Lecture Notes in Physics 30 (1974) 38.
- [279] H. Arenhövel, W. Leidemann and E.L. Tomusiak, Z. Phys. A 331 (1988) 123;  
H. Arenhövel, Few Body Systems 4 (1988) 55;  
W. Leidemann, E.L. Tomusiak and H. Arenhövel, Phys. Rev. C 43 (1991) 1022.
- [280] C.E. Woodward, E.J. Beise, J.E. Belz, R.W. Carr, B.W. Filippone, W.B. Lorenzon, R.D. McKeown, B. Mueller, T.G. O'Neill, G. Dodson, K. Dow, M. Farkhondeh, S. Kowalski, K. Lee, N. Makins, R. Milner, A. Thompson, D. Tieger, J. van der Brand, A. Young, X. Yu and J.D. Zumbro, Phys. Rev. Lett. 65 (1990) 698;  
C.E. Jones-Woodward, E.J. Beise, J.E. Belz, R.W. Carr, B.W. Filippone, W.B. Lorenzon, R.D. McKeown, B. Mueller, T.G. O'Neill, G. Dodson, K. Dow, M. Farkhondeh, S. Kowalski, K. Lee, N. Makins, R. Milner, A. Thompson, D. Tieger, J.F.J. van der Brand, A. Young, X. Yu and J.D. Zumbro, Phys. Rev. C 44 (1991) R571.
- [281] A.K. Thompson, A.M. Bernstein, T.E. Chupp, D.J. DeAngelis, G.E. Dodge, G. Dodson, K.A. Dow, M. Farkhondeh, W. Fong, J.Y. Kim, R.A. Loveman, J.M. Richardson, H. Schmieden, D.R. Tieger, T.C. Yates, M.E. Wagshul and J.D. Zumbro, Phys. Rev. Lett. 68 (1992) 2901.

- [282] V. Dmitrasinovic, T.W. Donnelly and F. Gross, in: Research Program at CEBAF (III), RPAC III, ed. F. Gross (1988) p. 547.
- [283] Report of the CEBAF Out-of-Plane Task Force, in: Research Program at CEBAF (III), RPAC III, ed. F. Gross (1988) pp. 183–350.
- [284] J.D. Walecka, Nucl. Phys. A 285 (1977) 349.
- [285] P.Q. Huang and J.J. Sakurai, Annu. Rev. Nucl. Sci. 31 (1981) 375.
- [286] U. Amaldi, A. Böhm, L.S. Durkin, P. Langacker, A.K. Mann, W.J. Marciano, A. Sirlin and H.H. Williams, Phys. Rev. D 36 (1987) 1385.
- [287] T.W. Donnelly and R.D. Peccei, Phys. Rep. 50 (1979) 1.
- [288] T.W. Donnelly, M.J. Musolf, W.M. Alberico, M.B. Barbaro, A. De Pace and A. Molinari, Nucl. Phys. A 541 (1992) 525.
- [289] C.Y. Prescott, W.B. Atwood, R.L.A. Cottrell, H. DeStaebler, E.L. Garwin, A. Gonidec, R.H. Miller, L.S. Rochester, T. Sato, D.J. Sherden, C.K. Sinclair, S. Stein, R.E. Taylor, C. Young, J.E. Clendenin, V.W. Hughes, N. Sasao, K.P. Schüler, M.G. Borghini, K. Lübelsmeyer and W. Jentschke, Phys. Lett. B 84 (1979) 524.
- [290] W. Achenbach, D. Conrath, K.J. Dietz, W. Gasteyer, H.J. Gessinger, W. Hartmann, H.J. Kluge, H. Kessler, L. Koch, F. Neugebauer, E.W. Otten, E. Reichert, H.G. Andresen, A. Bornheimer, W. Heil, Th. Kettner, R. Neuhausen, B. Wagner, J. Ahrens, J. Jethwa and F.P. Schäfer, in: Physics with MAMI(A), eds. D. Drechsel and Th. Walcher (Mainz, 1988) p. 259.
- [291] P.A. Souder, R. Holmes, D.-H. Kim, K.S. Kumar, M.E. Schulze, K. Isakovitch, G.W. Dodson, K.A. Dow, M. Farkhondeh, S. Kowalski, M.S. Lubell, J. Bellanca, M. Goodman, S. Patch, R. Wilson, G.D. Cates, S. Dhawan, T.J. Gay, V.W. Hughes, A. Magnon, R. Michaels and H.R. Schaefer, Phys. Rev. Lett. 65 (1990) 694.
- [292] T.W. Donnelly, in: Perspectives of Nuclear Physics at Intermediate Energies, eds. S. Boffi, C. Ciofi degli Atti and M.M. Giannini (World Scientific, Singapore, 1983) p. 305.
- [293] S. Boffi, C. Giusti and F.D. Pacati, Nucl. Phys. A 476 (1988) 617.
- [294] C.E. Carlson, Phys. Rev. D 34 (1986) 2704.
- [295] A. Picklesimer and J.W. Van Orden, Phys. Rev. C 35 (1987) 266.
- [296] A. Bartl and W. Majerotto, Nucl. Phys. B 62 (1973) 267.
- [297] F. Gross, in: Report of the 1987 Summer Study Group (CEBAF, Newport News, VA, 1987) p. 183.
- [298] M. Simonius, Phys. Rev. Lett. 19 (1967) 279; in: Polarization Phenomena in Nuclear Reactions, eds. H.H. Barschall and W. Haeberli (Univ. of Wisconsin Press, Madison, 1971) p. 401.
- [299] J.D. Bjorken, Phys. Rev. 148 (1966) 1467.
- [300] A. Picklesimer and J.W. Van Orden, Phys. Rev. C 40 (1989) 290.
- [301] S. Boffi, C. Giusti, F.D. Pacati and M. Radici, in: Proc. CEBAF 1986 Summer Workshop, eds. F. Gross and R. Minehart (CEBAF, 1986) p. 133.
- [302] S. Boffi, C. Giusti, F.D. Pacati and M. Radici, Nucl. Phys. A 518 (1990) 639.
- [303] R.W. Lourie, Nucl. Phys. A 509 (1990) 653.
- [304] F.D. Pacati and M. Radici, Phys. Lett. B 257 (1991) 263.
- [305] S.K. Nanda, in: Research Program at CEBAF (III), RPAC III, ed. F. Gross (CEBAF, 1988) p. 83.
- [306] R. De Leo, S. Frullani, F. Garibaldi, F. Ghio, M. Jodice and G.M. Urcioli, preprint INFN-ISS 90/5 (INFN Sezione Sanità, Rome, 1990).
- [307] V. Bargmann, J. Michel and V.L. Telegdi, Phys. Rev. Lett. 2 (1959) 435.
- [308] R.W. Lourie, Phys. Rev. C 45 (1992) 540.
- [309] I.S. Barker, A. Donnachie and J.K. Storrow, Nucl. Phys. B 95 (1975) 347.